UNIVERSIDADE ESTADUAL DE CAMPINAS

INSTITUTO DE BIOLOGIA

ANDRÉ DA SILVA SANTIAGO

CARACTERIZAÇÃO DE DUAS PROTEÍNAS PERTENCENTES AO OPERON TOXINA-ANTITOXINA E DE UM FATOR DE TRANSCRIÇÃO DO TIPO LysR DE *XYLELLA FASTIDIOSA*

FUNCTIONAL CHARACTERIZATION OF TWO PROTEINS BELONGING TO TOXIN-ANTITOXIN OPERON AND A LysR-TYPE TRANSCRIPTION FACTOR FROM *XYLELLA FASTIDIOSA*

Campinas

2015

André da Silva Santiago

CARACTERIZAÇÃO DE DUAS PROTEÍNAS PERTENCENTES AO OPERON TOXINA-ANTITOXINA E DE UM FATOR DE TRANSCRIÇÃO DO TIPO LysR DE *XYLELLA FASTIDIOSA*

Tese apresentada ao Instituto de Biologia da Universidade Estadual de Campinas como parte dos requisitos exigidos para a obtenção de título de Doutor em Genética e Biologia Molecular na área de Genética Vegetal e Melhoramento

Thesis presented to the Biology Institute of the University of Campinas in a partial fulfillment of the requirements for the degree of Doctor in Genetics and Molecular Biology, in the area of Plant Genetics and Breeding

Aluno: André da Silva Santiago
Orientadora: Profª Drª Anete Pereira de Souza
Co-orientadores: Profª Drª Alessandra Alves de Souza
Dr. Clelton Aparecido dos Santos

Este exemplar corresponde à versão final da tese defendida pelo aluno André da Silva Santiago e orientado da profª. Drª. Anete Pereira de Souza

Campinas
2015

Agência(s) de fomento e nº(s) de processo(s): FAPESP, 2011/50268-4

Ficha catalográfica
Universidade Estadual de Campinas
Biblioteca do Instituto de Biologia
Mara Janaina de Oliveira - CRB 8/6972

Sa59c

Santiago, André da Silva, 1985-
Caracterização de duas proteínas pertencentes ao operon toxina-antitoxina e de um fator de transcrição do tipo LysR de *Xylella fastidiosa* / André da Silva Santiago. – Campinas, SP : [s.n.], 2015.

Orientador: Anete Pereira de Souza.
Coorientadores: Alessandra Alves de Souza e Clelton Aparecido dos Santos.
Tese (doutorado) – Universidade Estadual de Campinas, Instituto de Biologia.

1. *Xylella fastidiosa*. 2. Caracterização de proteínas. 3. Fatores de transcrição. I. Souza, Anete Pereira de,1962-. II. Souza, Alessandra Alves de. III. Santos, Clelton Aparecido dos,1984-. IV. Universidade Estadual de Campinas. Instituto de Biologia. V. Título.

Informações para Biblioteca Digital

Título em outro idioma: Functional characterization of two proteins belonging to toxin-antitoxin operon and a LysR-type transcription factor from *Xylella fastidiosa*
Palavras-chave em inglês:
Xylella fastidiosa
Protein characterization
Transcription factors
Área de concentração: Genética Vegetal e Melhoramento
Titulação: Doutor em Genética e Biologia Molecular
Banca examinadora:
Anete Pereira de Souza [Orientador]
Ljubica Tasic
Cristina Elisa Alvarez Martinez
Nelson Arno Wulff
Cleide Marques Ferreira
Data de defesa: 25-09-2015
Programa de Pós-Graduação: Genética e Biologia Molecular

FINANCIAMENTO DA PESQUISA E DA BOLSA

Fundação de Amparo à Pesquisa do Estado de São Paulo – FAPESP

Nº do Processo: 2001/07533-7
Nº do Processo: 2011/50268-4
Nº do Processo: 2012/51580-4

Agência: Coordenação de Aperfeiçoamento de Pessoal de Nível Superior (CAPES, Computational Biology Program).
Nº do processo: 23038.010030/2013-25, AUXPE 3380/2013

Campinas, 2015

Banca Examinadora

Profª. Drª. Anete Pereira de Souza (orientadora)

Profª. Drª. Ljubica Tasic

Profª. Drª. Cristina Elisa Alvarez Martinez

Prof. Dr. Nelson Arno Wulff

Profª. Drª. Luís Antônio Peroni

Profª. Drª. Sandra Martha Dias Gomes

Profª. Drª. Fabiana Fantinatti-Garboggini

Drª Cleide Marques Ferreira

AGRADECIMENTOS

Gostaria de agradecer primeiramente aos integrantes da comissão de orientação formada pela Profª. Dra. Anete Pereira de Souza por ter me aceitado no seu laboratório e me confiado este projeto de doutorado, Profª. Dra. Alessandra Alves de Souza e pelo Dr. Clelton Aparecido dos Santos que tanto me auxiliaram no projeto e na escrita dos artigos.

Durante os anos 2011 até meados 2015 tive a oportunidade de trocar experiências com pessoas empenhadas em fazer ciência e que também me ajudaram superar as dificuldades encontradas e sempre me motivaram na pré-banca – Profª. Drª. Fabiana Fantinatti-Garboggini e Profª. Drª. Anita Marsaioli, assim como aos membros titulares da banca de defesa Profª. Drª. Ljubica Tasic, Profª. Drª. Cristina Elisa Alvarez Matinez, Prof. Dr. Nelson Arno Wulff, Profª. Drª. Anita Marsaioli e aos suplentes Profª. Drª. Sandra Marta Dias Gomes, Profª. Drª. Fabiana Fantinatti-Garboggini e Profª. Drª. Cleide Marques Ferreira.

A todos os amigos do LAGM que sempre contribuíram para profissional e pessoalmente, Clelton Aparecido dos Santos, Juliano Sales Mendes, Marcelo Augusto Szymanski de Toledo, Lílian Luzia Beloti, Aline Crucello, Marianna Teixeira de Pinho Fávaro e Maria Augusta Crivelente Horta.

Ao professor que participou e teve grande influência desde a minha iniciação científica e sempre foi um exemplo para mim, Prof. Dr. Carlos Priminho Pirovani.

A todos do Centro de Biologia Molecular e Engenharia Genética CBMEG/ UNICAMP pelo companheirismo e ajuda.

À FAPESP pelo financiamento da pesquisa e pela bolsa de doutorado que me foi concedida referente aos projetos de auxílio e bolsa (2012/51580-4, 2001/07533-7 e 2011/50268-4), assim como a CAPES (Programa Biologia Computacional) e CNPq.

Por último e extremamente importantes, aos meus pais Sílvia Rejane Matos da Silva e Raimundo dos Reis Santiago que, mesmo morando muito longe, sempre estiveram presentes nesse caminho árduo.

RESUMO

Após sequenciamento do genoma da bactéria *Xylella fastidiosa* linhagem 9a5c, houve um grande aumento de informações relacionadas à fisiologia e patogenia deste microrganismo, porém muitas das proteínas identificadas na análise de seu genoma ainda não apresentam funções preditas. A caracterização de tais proteínas pode contribuir para o melhor conhecimento do processo de patogenicidade bacteriana. Sendo assim, este trabalho teve como objetivo caracterizar três proteínas, XfYcjZ (ORF *Xf*1480) a qual apresenta alta similaridade com membros da família de reguladores de transcrição do tipo LysR (LTTR) e das proteínas toxina (XfMqsR) e antitoxina (XfMqsA), as quais possuem similaridade com o sistema toxina-antitoxina MsqR/MqsA de *Escherichia coli*. Tais proteínas desempenham, entre outras funções, papel preponderante na regulação de genes envolvidos no metabolismo celular, divisão celular, *quorum sensing*, formação de biofilme, virulência e resposta ao estresse oxidativo. A caracterização estrutural destas proteínas baseou-se em dados provenientes de ensaios de dicroísmo circular (CD), cromatografia de filtração em gel e ultracentrifugação analítica. Já a caracterização funcional baseou-se na produção de anticorpos contra cada umas das proteínas estudadas, seguida de experimentos de imunodetecção durante as diferentes fases de formação do biofilme de *X. fastidiosa*. A proteína XfYcjZ-like apresentou-se na forma tetramérica em solução, sendo diferencialmente expressa nas fases de crescimento de *X. fastidiosa,* foi observado o seu papel na resposta ao estresse oxidativo, quando induzida por cobre II. Foi também demonstrado que a interação entre as proteínas toxina-antitoxina ocorre na razão molar 1:1, sendo o complexo mais termoestável, quando comparado as duas proteínas individualmente, dados estes obtidos por análise de desenovelmanto térmico por CD. Dados funcionais confirmaram a anotação das proteínas deste sistema, uma vez que a antitoxina possuiu domínio HTH na região N-terminal, o que lhe confere capacidade de se ligar ao promotor do operon; a toxina apresentou atividade de RNAse e também foi inibida pela antitoxina. Em adição, foi mostrado pela primeira vez que a antitoxina é secretada por meio de vesículas da membrana externa, o que é uma forte evidência que ela possa ter uma nova função em *X. fastidiosa*. Assim, esperamos que nossos resultados contribuam para o melhor entendimento do envolvimento dessas proteínas no ciclo de vida de *X. fastidiosa* e suas possíveis implicações para a patogenicidade bacteriana.

Palavras-chave: *Xylella fastidiosa*; caracterização de proteínas; sistema toxina-antitoxina; fator de transcrição LysR.

ABSTRACT

After the genome sequencing of the Xylella fastidiosa greater knowledge about the bacterial physiology and pathogenicity have become available, however many proteins still do not have predicted functions and are classified as hypothetical proteins. Characterization of these proteins can bring new insights about its role within bacteria physiology. Therefore, our work aimed to characterize three proteins termed XfYcjZ (orf Xf1480), which possesses high identity with the LysR-type transcriptional regulator (LTTR) family; XfMqsR (orf Xf2162) and XfMqsA (orf Xf2163) which possess identity with the toxin-antitoxin operon MqsR and MqsA from Escherichia coli. These genes were reported to be involved in cell cycle, quorum sensing, biofilm formation, virulence and oxidative stress response. The functional characterization of these proteins was based on circular dichroism (CD), analytical size-exclusion chromatography, analytical ultracentrifugation and western blottings, which demonstrated the protein XfYcjZ is present in tetrameric form in solution and is globular, as shown by size exclusion chromatography and analytical ultracentrifugation. Our analyses also showed that XfYcjZ is differentially induced in the X. fastidiosa growth phases as well as its expression changed to cupper-induced oxidative stress, which is a indicative that XfYcjZ is involved in oxidative stress. The characterization of the orfs Xf2162 and Xf2163 was based on the cloning, expression and purification of the heterologous proteins and they were analysed as for the capacity of interaction between the proteins XfMqsR and XfMqsA and between XfMqsA and promoter of the operon. We have shown that XfMqsA is present as a dimer and the XfMqsR in monomer in solution and the interaction occurs in molar ratio 1:1 and the complex XfMqsA and XfMqsR is thermodynamically favorable and more stable that the isolated proteins. XfMqsR possesses RNAse activity and XfMqsA was able to inhibit it in fluorimetric assay. Moreover, it was demonstrated by MS/MS and western blotting that the XfMqsA is secreted by X. fastidiosa via outer membrane vesicles. We hope these results can contribute to better understand the involvement of these proteins in the X. fastidiosa lifecycle and the possible involvement in its pathogenicity.

Keywords: *Xylella fastidiosa*; protein characterization; toxin-antitoxin system; LysR-type transcription factor

SUMÁRIO

Apresentação da Tese

Esta tese teve como objetivo caracterizar três proteínas da bactéria *Xylella fastidiosa* estirpe 9a5c, a qual é um importante fitopatógeno que causa grandes perdas econômicas na citricultura brasileira. A *X. fastidiosa* apresenta crescimento lento (fastidioso), possuindo capacidade de formação de biofilme no interior do xilema da planta, o que ocasiona em estágio avançado da infecção, déficit hídrico e morte das plantas suscetíveis, a qual podemos destacar a laranja doce (*Citrus sinensis*). Dentre as espécies de bactérias fitopatogênicas mais estudadas atualmente, a *X. fastidiosa* se encontra na oitava posição, dado os elevados prejuízos que a doença resultante (CVC ou amarelinho) vem causando à citricultura mundial.

Devido a sua importância, esse projeto foi elaborado de forma a estudar três proteínas de *X. fastidiosa* potencialmente envolvidas na patogenicidade, as quais foram identificadas como um fator de transcrição do tipo LysR (Xf1480) e duas proteínas pertencentes ao operon toxina-antitoxina (XfMqsR e XfMqsA). Os resultados obtidos durante o período de doutoramento estão apresentados nesta tese no formato de dois artigos científicos, sendo que um deles já foi publicado e outro foi submetido a uma revista científica internacional.

O Capítulo 1 aborda a clonagem, expressão e purificação do fator de transcrição LysR. As análises foram feitas com base em homologia de sequência e propriedades hidrodinâmicas da proteína heteróloga, tais como ultracentrifugação analítica e cromatografia de filtração em gel. Também foi realizada a detecção da proteína nas fases de crescimento de *X. fastidiosa* e seu possível envolvimento na resposta a íons de cobre II. O artigo referente à esses dados foi intitulado "Characterization of the LysR-type transcriptional regulator YcjZ-like from *Xylella fastidiosa* overexpressed in *Escherichia coli*", e publicado no periódico Protein Expression and Purification (doi: 10.1016/j.pep.2015.05.003).

O Capítulo 2 está disposto em forma de manuscrito e descreve a clonagem, expressão e purificação da toxina (Xf2162) e da antitoxina (Xf2163) de *X. fastidiosa,* assim como a capacidade de interação entre as duas e a constante de interação calculada por calorimetria isotérmica. Além disso, também foi demonstrada, por *western blotting*, a detecção das duas proteínas durante as fases de crescimento de *Xylella fastidiosa,* assim como a presença da antitoxina dentro das vesículas da membrana externa, que foi detectada por espectrometria de massas e *western blotting*. Tais dados foram submetidos à publicação em

periódico internacional intitulado "*Xylella fastidiosa* secretes the antitoxin of a toxin-antitoxin system homologous to MsqR/MsqA from *Escherichia coli*"..

Por último, as atividades realizadas provenientes do trabalho de colaboração com outros projetos em andamento no grupo se encontram no anexo, na forma de um artigo publicado na *Biochemistry and Biophysics Acta*, em 2013, e intitulado "Small-angle X-ray scattering and *in silico* modeling approaches for the accurate functional annotation of an LysR-type transcriptional regulator".

1. INTRODUÇÃO

A citricultura possui grande importância na participação do Produto Interno Bruto (PIB) no estado de São Paulo, maior produtor nacional de laranja. O estado voltou-se para a produção de laranja no início da década de 1960 e tal atividade contribuiu muito para que o Brasil se tornasse o maior exportador de suco concentrado de laranja do mundo. Somente o estado de São Paulo correspondeu a 72% da produção nacional em 2013 (http://www.ibge.gov.br/home/estatistica/indicadores/agropecuaria/lspa/estProdAgr_201309.pdf).

Entretanto, várias doenças acometem as plantações de laranja, dentre as quais podemos destacar a clorose variegada de citros (CVC), causada pela bactéria *Xylella fastidiosa* (Bové; Ayres, 2007) o cancro cítrico, causado pela espécie *Xanthomonas citri* subsp. *citri* (Li; Wang, 2014) e a doença chamada greening ou (Huanglongbing/HLB) (Lee *et al.*, 2015), causada pela bactéria *Candidatus liberibacter asiaticus* e *Candidatus liberibacter americanos* (http://www.fundecitrus.com.br).

Dentre as doenças apresentadas, a CVC é uma das mais estudadas (Mansfield *et al.*, 2012). A bactéria *X. fastidiosa* tem a capacidade de colonizar os vasos xilemáticos de plantas susceptíveis, além de poder crescer na forma de biofilme dentro dos vasos xilemáticos de plantas infectadas, o que a torna resistente a vários compostos antimicrobianos usados na agricultura, assim como aqueles usados pela planta em resposta à infecção (Almeida *et al.*, 2008). A formação de biofilme também é importante para a sobrevivência em ambientes turbulentos e com escassez de nutrientes, como o xilema e o aparelho bucal de insetos (Mansfield *et al*., 2012).

Dentre as estirpes estudadas por Doddapaneni e colaboradores (2006), as quatro estirpes de *X. fastidiosa* (9a5c, Ann 1, Dixon e Temecula-I) apresentam 76,2% do genoma conservado. A quantidade de genes exclusivos para cada estirpe foi: 241 genes para *X. fastidiosa* estipe 9a5c (de um total de 2678 genes), 96 genes para a estirpe Dixon (total de 2622 genes), 145 para a estirpe Ann I (total de 2815 genes) e 10 para a estirpe Temecula-I (total de 2034 genes).

Além disso, foi demonstrado que a estirpe *X. fastidiosa* 9a5c possui a capacidade de responder ao tratamento com substâncias que causam estresse oxidativo e antibióticos, tais como íons de cobre II e tetraciclina, respectivamente, modulando a expressão de algumas *orfs* (Muranaka *et al.*, 2012). Dentre as ORFs que sofreram alteração no perfil de expressão, encontram-se as *orfs* Xf1480, Xf2162 e Xf2163, as quais possuem, respectivamente,

identidade com um fator de transcrição LysR, uma toxina com atividade de RNAse e uma antitoxina com domínio hélice-volta-hélice (HTH).

De acordo o banco de dados do LNCC (http://www.xylella.lncc.br/), o genoma de cinco estirpes, Dixon, Temecula, Ann-1, M12 e M23. A *Xylella fastidiosa* estirpe Dixon é a causadora da escaldadura da folha e amendoeira (almond leaf scorch) em amendoeiras suscetíveis, *Prunus dulcis* (Lin *et al*. 2015) . A *Xylella fastidiosa* estirpe Temecula é a causadora da doença de Pierce em videiras, *Vitis vinífera* (Lin *et al*. 2015). A estirpe Ann-1 acomete a planta conhecida como oleandro, (*Nerium oleander* L.), utilizada com a finalidade de ornamentação(Lin *et al*. 2015). As outras duas estirpes são a M12 e a M23 (Chen *et al*. 2010). A duas causam escaldadura em folhas de amendoeiras, mas a M23 também causa a doença de Pierce.

A comparação dessas cinco estirpes quanto à presença das *orfs* em estudo demonstrou que todas elas possuem o gene homólogo a *orf Xf1480* da estirpe 9a5c, compartilhando 27% de identidade entre elas. Quanto ao operon toxina-antitoxina *Xf2162* e *Xf2163*, os genes homólogos foram encontrados nas estirpes Temecula e M23, enquanto as estirpes Dixon, Ann-1 e M12 não apresentam nenhuma dessas *orfs*.

A formação de biofilme é tida como o principal mecanismo de patogenicidade para essa espécie bacteriana. A sua formação ocorre através de associação célula-célula, as quais são envolvidas por uma camada externa de substâncias poliméricas compostas de polissacarídeos, DNA e proteínas. Tal estrutura funciona como uma barreira e confere resistência à entrada de compostos nocivos para as células (Limoli; Jones; Wozniak, 2015). No processo de formação do biofilme, a comunicação célula-célula, também conhecida como *quorum sensing*, tem crucial importância na diferenciação celular. A comunicação celular vai regular genes específicos que facilitam a atividade em grupo, tais como produção de proteínas, toxinas extracelulares e deposição do EPS (Toyofuku *et al.,* 2015). A camada externa de substâncias poliméricas também influencia a comunicação célula-célula, pelo fato de reter produtos metabólicos e moléculas de sinalização (Drescher *et al* 2014).

Visto que as *orfs* Xf1480, Xf2162 e Xf2163 foram induzidas em tratamentos prévios com íons de cobre II e tetraciclina (Muranaka *et al*., 2012), nós formulamos a hipótese de que elas poderiam de alguma forma estar envolvidas na patogenicidade de *X. fastidiosa*. Dessa forma, com o intuito de melhor entender a possível ligação dessas *orfs* com o metabolismo bacteriano, tais alvos foram clonados e as proteínas correlatas foram expressas em sistema de expressão heteróloga. Dessa forma, foi possível que as funções das proteínas

fossem investigadas, utilizando-se de um conjunto de ensaios bioquímicos e biofísicos para a sua caracterização.

2. REVISÃO BIBLIOGRÁFICA

2.1 – Clorose Variegada do Citrus e *Xylella fastidiosa*

A Clorose Variegada dos Citros (CVC) é uma doença de grande importância econômica, cujo agente causal é o fitopatógeno *X. fastidiosa* (Hartung *et al.*, 1994), uma bactéria Gram-negativa hospedeira do xilema da planta. *X. fastidiosa* possui capacidade de formar biofilme, aderindo milhares de células no xilema e assim, ocluindo os vasos xilemáticos. À medida que a bactéria vai se espalhando pela planta, mais vasos xilemáticos vão sendo obstruídos.

A doença é transmitida por 12 espécies de vetores comumente chamados de cigarrinha e pertencentes à família Cicadellidae. As cigarrinhas adquirem a bactéria quando se alimentam de plantas contaminadas e podem abriga-las por tempo indeterminado. Dessa forma o controle dos vetores é de extrema importância para evitar o alastramento da doença. Estudos epidemiológicos estimam que, a partir de uma árvore infectada, a CVC foi capaz de atingir 90% de uma plantação de 20 hectares em 12 anos, no norte de São Paulo (Gottwald *et al.*, 1993). Inicialmente, os sintomas apresentados são pequenos pontos amarelados na face adaxial da folha, seguido de necrose à medida que a doença avança; tal sintoma assemelha-se à deficiência de zinco. As folhas também ficam com aspecto de murchas, devido ao desequilíbrio hídrico, assim como os frutos ficam menores (Fig. 1) (Muranaka *et al.* 2013).

Os métodos atualmente utilizados para controle da doença são: obtenção de plantas sadias em viveiros certificados pela Secretaria de Agricultura do Estado de São Paulo; poda dos galhos que apresentarem os sintomas da doença em estágio inicial e controle dos insetos vetores da bactéria (http://www.fundecitrus.com.br/doencas/cvc/9)

Diante de toda a importância da doença, a *X. fastidiosa* foi o primeiro fitopatógeno a ter o seu genoma sequenciado (Simpson *et al*., 2000). Nas anotações das *orfs* presentes no genoma da bactéria, ainda existem várias delas com função não identificada. Desta forma, a caracterização funcional de proteínas produzidas por *orfs* não identificadas previamente, ajudará no entendimento da biologia e da fitopatogenicidade da *X. fastidiosa.*

É possível atribuir o mecanismo de patogenicidade de *X. fastidiosa* à disfunção do sistema de condução de água e sais minerais da planta por oclusão e ao desequilíbrio de reguladores de crescimento (Hopkins, 1989). Tal conjunto de alterações provoca necrose e

abscisão foliar, redução no crescimento vegetal, declínio do vigor e, finalmente, morte da planta infectada em estágios avançados da doença.

As fases de desenvolvimento do biofilme microbiano já foram estabelecidas compreendendo a: I – fase de adesão inicial, caracterizada pela adesão de algumas células ou grupos de células a superfície a ser colonizada; II – fase de adesão irreversível devido à produção de EPS, o que contribui para uma adesão mais estável; III – início da maturação, quando se inicia a fase de estruturação e arquitetura do biofilme; IV – biofilme maduro, quando a densidade celular atinge seu maior grau e a arquitetura do biofilme é altamente complexa, e V – fase de dispersão, na qual alguns grupos de células se destacam do biofilme maduro para colonizarem outras partes do hospedeiro (Fig. 2) (Sauer *et al*., 2002).

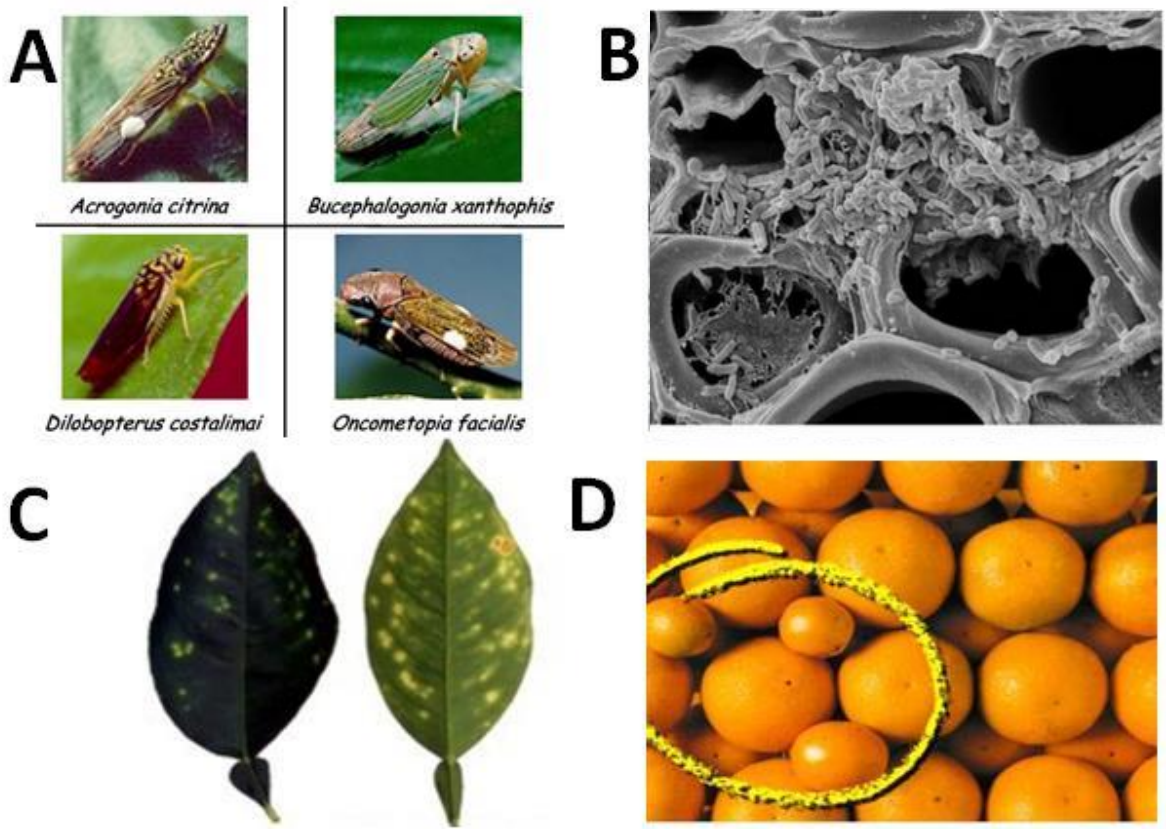

Figura 1 – (A) Espécies de cigarrinha que são capazes de transmitir *X. fastidiosa*. (B) Eletromicrografia do xilema de uma planta em estágio avançado de infecção. (C) Manchas amareladas em folhas de plantas doentes, semelhantes à deficiência por zinco. (D) Comparação entre frutos provenientes de plantas infectadas por *X. fastidiosa* (frutos menores) e frutos derivados de uma planta sadia (frutos maiores). Adaptado de Manual técnico de CVC – Fundecitrus (A, C e D) e (B) Mansfield *et al.*, (2012).

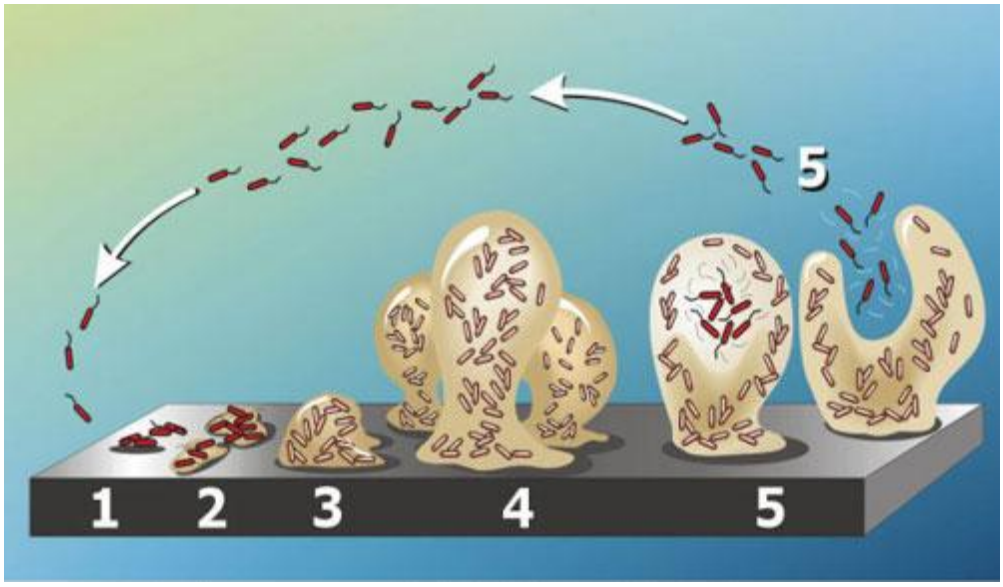

Figura 2 – Fases de desenvolvimento do biofilme microbiano. Fase 1: adesão inicial de células a superfície, corresponde ao 3º dia do crescimento *in vitro*. Fase 2: produção de EPS resultando na adesão firme e irreversível a superfície, 5º dia. Fase 3: desenvolvimento inicial da arquitetura do biofilme, 10º dia. Fase 4: maturação da arquitetura do biofilme, 20º dia. Fase 5: dispersão de células do biofilme, 30º dia. Adaptado de Sauer *et al*. (2002).

X. fastidiosa, além de causar doença em citros, também ataca diversos hospedeiros como: alfafa e videira (Goheen *et al.*, 1973); pessegueiro (Hopkins *et al.*, 1973), (Nyland *et al.*, 1973), amendoeira (Mircetich *et al.*, 1976); ameixeira (Hopkins, 1989); e cafeeiros (Paradela Filho *et al.*, 1997).

A formação do biofilme é uma das principais características de patogenicidade para algumas bactérias. O biofilme é formado através da associação entre células envoltas por uma camada de material secretado, constituído por substâncias poliméricas extracelulares, do inglês EPS – *extracelullar polymeric substances*, que protege as bactérias de substâncias nocivas (Cruz; Cobine; De La Fuente, 2012; Janissen *et al.*, 2015). A constituição exata ainda permanece incerta, mas sabe-se que essa estrutura é formada por polissacarídeos, fragmentos de DNA, proteínas e peptídeos, e chegam a constituir até 90% da massa do biofilme (Yonezawa; Osaki; Kamiya, 2015).

Como característico de bactérias Gram-negativas, *X. fastidiosa* é capaz de produzir vesículas da membrana externa (Ionescu *et al*., 2014). Tais nanoestruturas possuem entre 10 e 300 nm, possuem bicamada lipídica proveniente da membrana citoplasmática e da membrana externa e envolve o conteúdo presente no periplasma bacteriano (Haurat; Elhenawy; Feldman, 2015). As vesículas da membrana externa surgem como protuberâncias

da membrana externa formada por lipopolissacarídeo e contendo proteínas e fragmentos de DNA (Fig. 3) (Kuehn; Kesty, 2005).

Várias evidências parecem colaborar com a hipótese de que a liberação das vesículas está baseado em alterações na estrutura de peptidoglicano, pois foi relatado que em linhagens de *Porphyromonas gingivalis* mutante para amidase, uma enzima que catalisa a hidrólise de ligações amida do peptidoglicano, leva a uma produção maior de vesículas da membrana externa. O comportamento oposto também foi visto, ou seja, a indução da produção de amidase leva a diminuição da quantidade de vesículas liberadas (Kim *et al.*, 2015). A possível justificativa para isso é que a mutação para a amidase leva ao acúmulo de substâncias relacionadas à composição da parede celular, estimulando a produção de vesículas (Hayashi; Hamada; Kuramitsu, 2002).

Diversas suposições têm sido feitas a respeito da função das vesículas (Ellis; Kuehn, 2010; Schertzer; Whiteley, 2013, Kuipers *et al*., 2015). Dentre as hipóteses geradas, as vesículas podem auxiliar na dispersão de *X. fastidiosa* através da sua ligação com a parede dos vasos xilemáticos, dessa forma reduziria o contato da própria célula com as paredes das células e ela teria capacidade de colonizar mais eficientemente a planta (Ionescu *et al*., 2014). Funções adicionais têm sido especuladas quando a capacidade de ativar o resposta de defesa das plantas por carregar elicitores e fatores de virulência que ativam as resposta de hipersensibilidade das plantas (Ellis; Kuehn, 2010), assim como ajuda na colonização da bactéria em determinado ambiente (Ionescu *et al*., 2014; Kuipers *et al*., 2015; Olsen; Amano, 2015).

De acordo com Ionescu e colaboradores (2015), a produção de vesículas estaria associada ao aumento da capacidade de dispersão das bactérias dentro da planta, pois as vesículas se fixariam nos locais disponíveis do xilema, impedindo que as bactérias se fixassem nesses mesmos lugares (Fig 4).

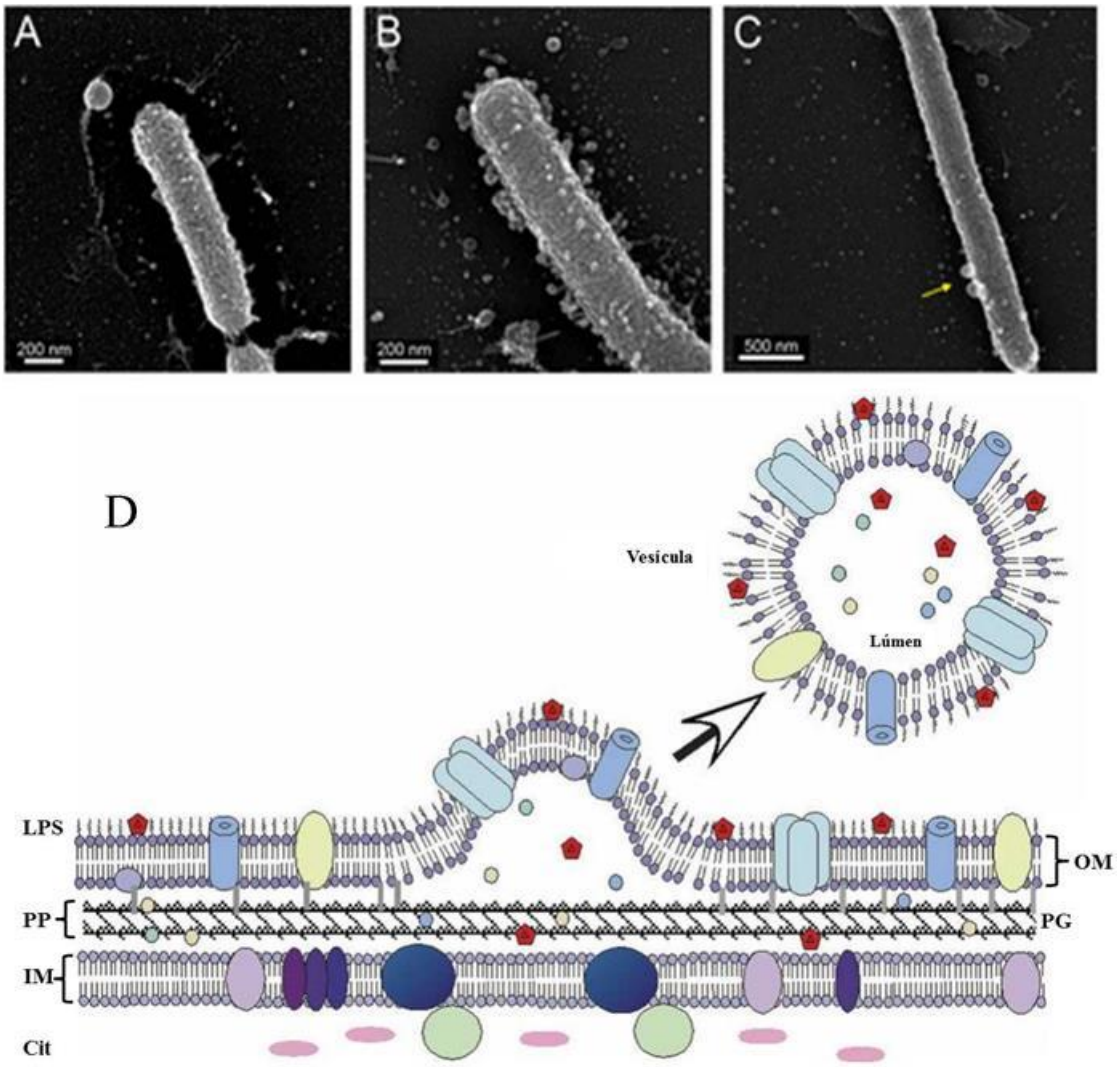

Figura 3 – (A-C) Eletromicrografia de células e vesículas da membrana externa de *X. fastidiosa.* (D) Modelo para a formação da vesícula da membrana externa. Ao destacar-se carrega o material presente no periplasma bacteriano (PP) e é envolto também pela membrana externa (OM) composta de lipopolissacarídeos (LPS), mas não possui fragmentos de peptidoglicano (PG). Os outros compartimentos celulares referidos na figura são a membrana interna (IM) e o citoplasma (Cit). Adaptado de Ionescu *et al*., 2014 (A, B e C) e de Kuehn 2005 (D).

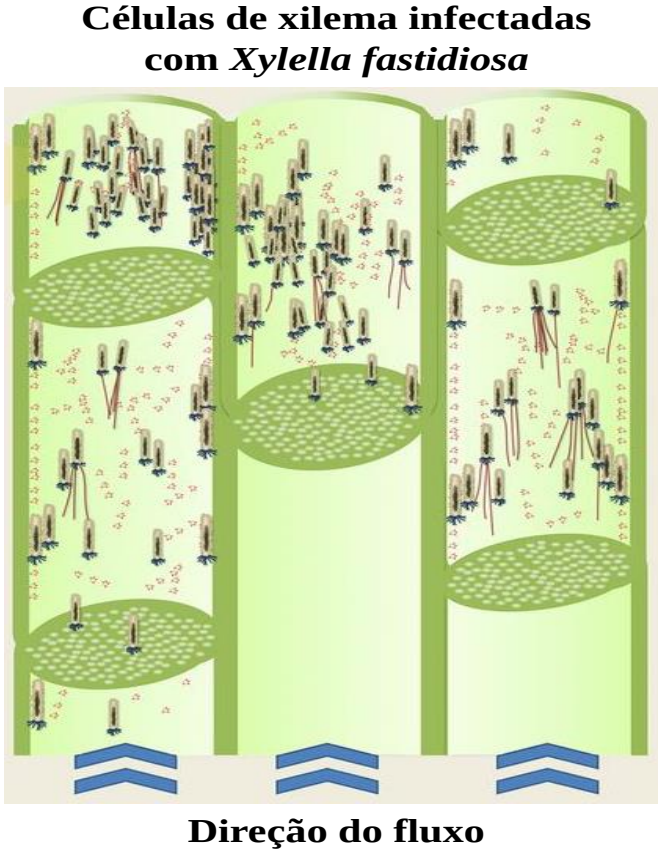

Figura 4 – Interação das vesículas da membrana externa (pequenos círculos vermelhos) com a parede dos elementos de vaso reduziria a capacidade de interação das células com a parede, facilitando a dispersão e consequentemente a patogenicidade (Ionescu *et al.,* 2014)

A seguir é apresentada uma descrição das principais características das proteínas que foram alvo de estudo desta tese, as quais estão envolvidas na biologia e fitopatogeniciade da *X. fastidiosa*.

2.2. Reguladores Transcricionais da Família LysR

Os reguladores transcricionais do tipo LysR (LTTR) são a família mais bem caracterizada do grupo de reguladores transcricionais. Eles são altamente conservados e abundantes entre as bactérias, com ortólogos funcionais identificados em *Archaea* e organismos eucariotos (Perez-Rueda; Collado-Vides, 2001; Sun; Klein, 2004; Stec *et al.*, 2006.

A família LTTR foi primeiramente documentada por (Henikoff *et al.*, 1988), que concluiram que havia pelo menos nove proteínas reguladoras transcricionais funcionais que

apresentam similaridade de sequência aminoacídica com reguladores transcricionais de *E. coli*, *Salmonella enterica* serovar Typhimurium, *Rhizobium* spp. e *Enterobacter cloacae*.

Originalmente as proteínas LTTRs foram descritos como ativadores transcricionais de um único gene divergente transcrito, que exibia autorregulação negativa (Lindquist *et al.*, 1989 Parsek *et al.*, 1994). Contudo, trabalhos posteriores consideraram as LTTRs como reguladoras transcricionais globais, atuando como ativadores ou repressores de um único gene ou operon (Hernandez-Lucas *et al.*, 2008).

Um fator muito importante para que as LTTRs realizem suas funções é a presença e atuação dos coindutores que podem variar de uma proteína a um íon. Geralmente, esses coindutores, participam de uma alça de *feedback*, na qual o produto ou composto intermediário de uma dada via metabólica ou de biossíntese (geralmente ativada por um LTTR) atua como a molécula co-indutora necessária para a ativação ou repressão transcricional (Celis, 1999; Van Keulen et al., 2003; Picossi et al., 2007). Os sítios de ligação para os coindutores apresentam baixa similaridade entre os fatores de transcrição LysR e situam-se na extremidade C-terminal nos domínio denominados RD1 e RD2, siglas provenientes do inglês “regulatory domains” (Maddocks; Oyston, 2008).

A conservação das LTTRs no genoma das bactérias implica que elas têm evoluído desempenhando um papel regulador importante sobre os genes. Esta regulação é exercida por meio de diversas funções semelhantes, cujos produtos podem estar envolvidos no metabolismo, na divisão celular, *quorum sensing*, virulência, motilidade, fixação de nitrogênio, respostas ao estresse oxidativo, produção e secreção de toxina (Maddocks; Oyston, 2008).

Apesar do tamanho da família das proteínas LTTR e as diversas funções que os LTTRs desempenham, importantes regiões estruturais permanecem altamente conservadas. As proteínas LTTRs possuem cerca de 330 aminoácidos, sendo a região C terminal um domínio de ligação ao cofator e a região N-terminal uma sequência HTH (Fig. 5), que fornece um meio de ligação com o DNA. A sequência HTH está presente em grande parte dos LTTRs e aproximadamente em 95% de todas as proteínas de ligação a DNA em procariotos (Maddocks; Oyston, 2008).

Figura 5 – Representação de um fator de transcrição LysR de *Vibrio cholerae*, AphB (PDB ID: 3SZP; Acesso NCBI: AAD45271), com destaque para a sua região N-terminal conservada (em azul e em vermelho) e o seu domínio de ligação ao DNA hélice-volta-hélice (HTH) em azul. Figura gerada utilizando a ferramenta Pymol (Version 1.7.4 Schrödinger, LLC).

2.3. Sistema Toxina-Antitoxina

Os sistemas toxina-antitoxinas (TA) são ubíquos nos cromossomos bacterianos e seu papel na fisiologia bacteriana ainda é controverso. Várias hipóteses têm sido debatidas acerca das suas funções, sendo comprovada sua participação na formação de células persistentes (bactérias que são resistentes a antibióticos sem que tenha ocorrido mutação), controle do crescimento, regulação gênica e morte celular programada. No genoma, os sistemas toxina-antitoxina, geralmente, consistem de dois genes localizados em um operon e que codifica para duas proteínas: uma toxina estável, responsável por interromper um processo celular essencial, e uma antitoxina que pode se ligar à toxina e formar um complexo para neutralizar sua atividade (Fig. 6) (Wang *et al.*, 2011).

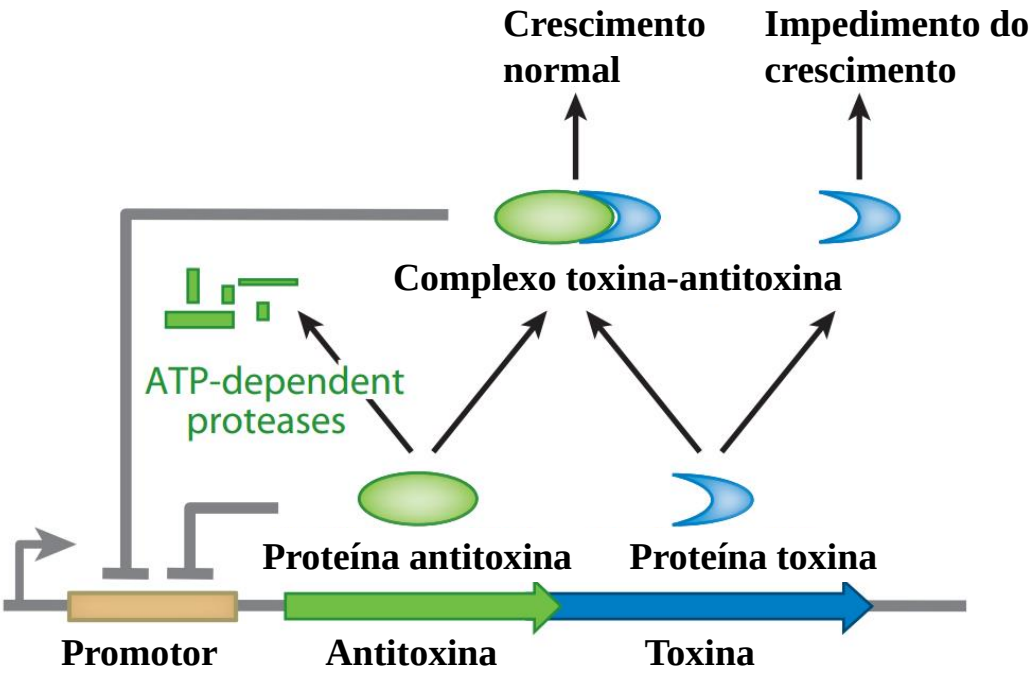

Figura 6 – Modo de ação do sistema toxina - antitoxina do tipo II. As proteínas são transcritas no mesmo operon e a antitoxina é suscetível à ação de proteases, resultando em toxinas livres. Fonte: Alterado de Yamaguchi, Y.; Park, J. H.; Inouye, M. (2011).

Em *X. fastidiosa* estipe 9a5c, o operon toxina-antitoxina está delimitado por duas *orfs* que codificam proteínas relacionadas à montagem do fago, GPV e GPW, (Fig. 7). A

mesma disposição de *orfs* é encontrada na *X. fastidiosa* estirpe Temecula e, de acordo com os autores, pode indicar que a aquisição desses genes provavelmente tenha acontecido por transferência horizontal (Lee *et al.*, 2014).

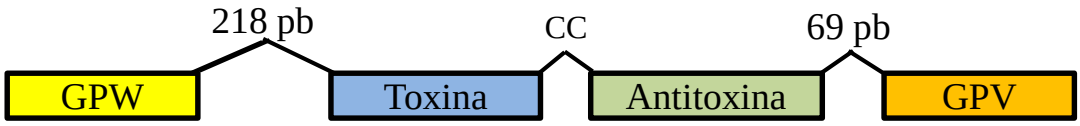

Figura 7 – Disposição dos genes para toxina e antitoxina em *X. fastidiosa* estirpe 9a5c. O operon está delimitado por genes relacionados a formação de fagos GPW e GPV. A toxina e antitoxina estão separadas por dois pb e possuem uma região promotora *upstream* à toxina com 218 pb.

Inicialmente, os sistemas TA foram descobertos em plasmídeos, mas posteriormente foram encontrados nos cromossomos de diversas espécies de eubactérias e arqueobactérias (Yamaguchi, *et al*. 2011). Os sistemas TA são classificados em cinco grupos, detalhados a seguir. No grupo I, a regulação do gene da toxina é realizada por um RNA antissenso transcrito a partir de uma *orf* próxima ao gene da toxina, o qual age formando um dúplex de RNA com o RNA da toxina, impedindo assim a tradução da proteína correspondente à toxina (Gerdes; Wagner, 2007; Schuster; Bertram, 2013). O grupo II é caracterizado por um operon contendo os dois genes separados por aproximadamente um ou dois pares de bases. A toxina e a antitoxina formam um complexo estável, bloqueando a ação da toxina. Na maioria dos casos, o gene que codifica para a antitoxina se encontra antes do gene da toxina, de modo que ela seja produzida antes da toxina (Yamaguchi; Inouye, 2009). No grupo III, o RNA da antitoxina forma um complexo com a proteína tóxica, resultando na neutralização da sua toxicidade. Esse sistema se diferencia do grupo I, pelo fato do RNA da antitoxina não funcionar como um RNA antissenso para inibir a tradução da toxina (Schuster; Bertram, 2013). No tipo IV, a antitoxina protege o alvo da ação da toxina (Masuda *et al*., 2012) e no tipo V, a antitoxina possui atividade de RNAse específica para o RNA da toxina (Wang *et al*., 2012).

Levando em consideração os mecanismos envolvidos no funcionamento do operon toxina-antitoxina do tipo II, sabe-se que a antitoxina regula a atividade da toxina ligando-se a ela e formando o complexo proteína-proteína (Brown *et al*. 2013), acarretando na inibição da atividade de ribonuclease da toxina (Wang *et al*., 2011; Brown *et al*., 2011). Entretanto, a meia-vida dessas proteínas no meio intracelular é diferente: a toxina tende a ser estável enquanto a antitoxina é suscetível à degradação pela ação da Lon protease (Wang;

Wood, 2011). Essas diferenças podem resultar em um acúmulo de toxinas livre (Franch, *et al*. 1997; Cook *et al*. 2013). Além disso, a antitoxina possui capacidade para regular genes relacionados a estresse, além do próprio promotor do operon toxina-antitoxina (Wang; Wood, 2011).

Estudos envolvendo análise da expressão gênica demonstraram que o sistema toxina-antitoxina está envolvido com resposta a estresse (Wang, *et al*., 2011; Kwan *et al*.; 2014) e patogenicidade, uma vez que esse sistema influencia na formação de células persistentes e formação de biofilme em *E. coli* (Wang; Wood, 2011) e em *X. fastidiosa* estirpe Temecula (Lee; *et al*. 2014). Essa influência se deve à regulação do fator sigma σS da RNA polimerase (*rpoS*) pela antitoxina. Quando a antitoxina é degradada, o *rpoS* é induzido, levando a um aumento da concentração de di-GMP (diguanilato cíclico monofosfato), favorecendo a adesão celular e a formação de biofilme. Já quando a antitoxina está ligada, as células tendem a permanecer na fase planctônica (Wang; Wood; 2012; Lord, *et al*., 2014; Yamaguchi, *et al*, 2009). Porém, quando analisamos o genoma da *X. fastidiosa* estirpe 9a5c, percebemos que ela não possui o gene *rpoS*. A proteína com maior similaridade é o fator sigma RpoH, a qual apresenta 25% de identidade com a proteína RpoS. A diferença entre eles é que o gene para o fator sigma *rpoH* está relacionado com estresse promovido por temperatura, enquanto a *rpoS* está relacionada com fase estacionária.

Em *E. coli,* a antitoxina também está relacionada com a regulação negativa do gene *cspD*, o qual codifica para uma chaperona *cold shock protein* (Fig. 8A) que possui capacidade de inibir a replicação de DNA (Wang; Wood, 2011). Essa proteína apresenta 57% de identidade com a Xf2034, que também codifica para uma *cold shock protein*, e provavelmente é um dos genes regulados pela proteína XfMqsA, uma vez que, quando a sua região promotora é analisada, a seguinte sequência foi encontrada ACCT(N_3)C<u>AAA</u>TT na posição -12, onde os nucleotídeos sublinhados representam as variações de sequência (Fig. 8B).

Como demonstrado por Kim *et al.,* (2010) e Wang *et al*., (2011), a proteína MqsA de *E. coli* é capaz de se ligar ao promotor do gene *cspD* e reprimir a sua transcrição. Em casos de estresses, a antitoxina é degradada pela Lon protease, reativando a transcrição do gene *cspD*, o qual inibe o crescimento celular, por inibir a replicação de DNA. Tal fato contribui para a formação de células persistentes.

Em várias bactérias Gram-negativas, a indução de chaperonas relacionadas ao choque térmico está associada ao aumento na concentração de RpoH; entretanto os

mecanismos moleculares que controlam o equilíbrio de chaperonas e RpoH ainda não são totalmente conhecidos (El-Samad *et al*., 2005).

Do ponto de vista biotecnológico, o interesse na exploração do sistema TA em humanos tem emergido principalmente para a supressão da replicação do vírus HIV. A construção de um vetor viral contendo o gene para a toxina MazF de *E. coli*, sob regulação do promotor HIV-1 LTR, posteriormente inserido em linfócitos T auxiliar CD4+. Após infecção desses linfócitos pelo HIV-1 a toxina foi produzida, acarretando em inibição da replicação viral sem afetar o crescimento da célula humana (Chono *et al*., 2011).

A

```
Xf2034_X.fastidiosa MQSGTVKWFSDQKGFGFISPDDGTPEVFAHYSGINSKGFRSLHEGQRVTYDVTQGPKGPQ 60
cspD_E.coli         MEKGTVKWFNNAKGFGFICPEGGGEDIFAHYSTIQMDGYRTLKAGQSVQFDVHQGPKGNH 60
                    *:.******.: ******.*:.*  ::***** *: .*:*:*: ** * :** ***** :
Xf2034_X.fastidiosa ASNITPI------- 67
cspD_E.coli         ASVIVPVEVEAAVA 74
                    ** *.*:
```

B

```
                  -12          -23
    GGTGATGCGAGACCTTTGCAAATTGAAATGAGTAGTGTACGTCCCCTAGCGCACAGACTG
  1 ---------+---------+---------+---------+---------+---------+ 60
    CCACTACGCTCTGGAAACGTTTAACTTTACTCATCACATGCAGGGGATCGCGTGTCTGAC

    AGTATGCAAAGCTTGTGTCCGAATGACAATCACTCTCGCGCAACTTTACTAAT
 61 ---------+---------+---------+---------+---------+--- 113
    TCATACGTTTCGAACACAGGCTTACTGTTAGTGAGAGCGCGTTGAAATGATTA
```

Figura 8 – (A) Alinhamento da proteína codificada pela *orf Xf2034* com a sua homóloga em *E. coli*, realizado utilizando a ferramenta ClustalW. A similaridade é de 57% entre as proteínas. (B) Análise da região promotora da *orf Xf2034* com a presença de um possível *motif* de interação com a proteína XfMqsA (-12 a -23). Os nucleotídeos sublinhados são referentes às modificações de sequência quando comparadas ao motif presente no promotor do operon XfMqsA-XfMqsR.

Recentemente, um sistema toxina antitoxina de *X. fastidiosa* estirpe Temecula (Lee *et al*., 2014), foi caracterizado no qual foi demonstrado a influência da toxina para formação de biofilme. No referido estudo foi demonstrado que o mutante *X. fastidiosa* estirpe Temecula ΔMqsA (antitoxina), apresentaram maior capacidade de formação de biofilme, pois a toxina se encontra livre dentro da célula.

O operon toxina antitoxina funciona de modo equilibrado, onde qualquer desequilíbrio pode levar ao excesso de toxina livre, podendo ser benéfico ou maléfico para a bactéria. Este sitema poderá sinalizar a formação de células persistentes e/ou biofilme nos casos em que haja excesso de toxina. Por outro lado, o crescimento normal será recuperando quando antitoxina for produzida, levando a inibição da toxina e aumento da motilidade (Lee *et*

al., 2014; Barrios 2006). Entretanto, a caracterização dessas proteínas *in vitro* não foi até o momento relatado para *X. fastidiosa* estirpe 9a5c.

3. OBJETIVO

Realizar a caracterização funcional e bioquímica do fator de transcrição codificado pela *orf Xf1480* (XfYcjZ) e do sistema toxina-antitoxina codificado pelas *orfs Xf2162* e *Xf2163* (proteínas XfMqsR e XfMqsA), a fim de verificar o envolvimento destas proteínas na patogenicidade de *X. fastidiosa.*

3.1 – OBJETIVOS ESPECÍFICOS

- Clonar as *orfs Xf1480* (XfYcjZ), *Xf2162* (XfMqsR) e *Xf2163* (XfMqsA) expressar e purificar as proteínas produzidas por elas;
- Analisar o enovelamento secundário das proteínas recombinantes expressas e purificadas por meio de dicroísmo circular;
- Realizar a caracterização hidrodinâmica das proteínas purificadas por meio de cromatografia de exclusão por massa molecular e ultracentrifugação analítica;
- Caracterizar termodinamicamente a interação entre as proteínas XfMqsR e XfMqsA;
- Analisar a interação com promotores por meio de ensaio de retardamento da mobilidade eletroforética (EMSA - Electrophoretic Mobility Shift Assay) utilizando a proteína XfYcjZ e seu próprio promotor, bem como a proteína XfMqsA com o promotor do operon.
- Realizar teste de atividade RNAse com a proteína XfMqsR e sua inibição com a proteína XfMqsA;
- Avaliar estabilidade térmica do complexo XfMqsR/XfMqsA e compará-la com as proteínas individualmente.
- Avaliar o perfil de expressão das proteínas por *western blotting* durantes as fases de desenvolvimento de *X. fastidiosa* por meio de anticorpos policlonais contra as proteínas alvo;
- Avaliar a presença das proteínas XfMqsA e XfMqsR no secretoma de *X. fastidiosa*.

4 – RESULTADOS E DISCUSSÃO

Os resultados e discussão foram organizados em duas partes:

(I) Na Parte 1 é apresentado o manuscrito intitulado “Characterization of the LysR-type transcriptional regulator YcjZ-like from *Xylella fastidiosa* overexpressed in *Escherichia coli*”, publicado no periódico *Protein Expression and Purification*, o qual apresenta todos os resultados obtido para a proteína XfYcjZ.

(II) A segunda parte dos resultados é apresentada na forma de um manuscrito, o qual contém todos os resultados obtidos na caracterização funcional das proteínas do sistema toxina-antitoxina, o qual se encontra submetido à revista *Molecular Plant Pathology*.

4.1. ARTIGO 1

"Characterization of the LysR-type transcriptional regulator YcjZ-like from *Xylella fastidiosa* overexpressed in *Escherichia coli*"

Autores: André S. Santiago, Clelton A. Santos, Marcelo A.S. Toledo, Juliano S. Mendes, Lilian L. Beloti, Alessandra A. Souza, Anete P. Souza

Publicado na Revista *Protein Expression and Purification*
Volume 113 (2), páginas 72–78, Maio, 2015

Protein Expression and Purification 113 (2015) 72–78

Contents lists available at ScienceDirect

Protein Expression and Purification

journal homepage: www.elsevier.com/locate/yprep

Characterization of the LysR-type transcriptional regulator YcjZ-like from *Xylella fastidiosa* overexpressed in *Escherichia coli*

André S. Santiago [a], Clelton A. Santos [a], Juliano S. Mendes [a], Marcelo A.S. Toledo [a], Lilian L. Beloti [a], Alessandra A. Souza [b], Anete P. Souza [a,c,*]

[a] Centro de Biologia Molecular e Engenharia Genética (CBMEG), Universidade Estadual de Campinas, Campinas, SP, Brazil
[b] Centro APTA Citros Sylvio Moreira/IAC, Rodovia Anhanguera Km 158, Cordeirópolis, SP, Brazil
[c] Departamento de Biologia Vegetal, Instituto de Biologia (IB), Universidade Estadual de Campinas, Campinas, SP, Brazil

ARTICLE INFO

Article history:
Received 27 January 2015
and in revised form 4 May 2015
Available online 12 May 2015

Keywords:
Xylella fastidiosa
Biofilm
YcjZ
Transcriptional regulator

ABSTRACT

The *Xylella fastidiosa* 9a5c strain is a xylem-limited phytopathogen that is the causal agent of citrus variegated chlorosis (CVC). This bacterium is able to form a biofilm and occlude the xylem vessels of susceptible plants, which leads to significant agricultural and economic losses. Biofilms are associated with bacterial pathogenicity because they are very resistant to antibiotics and other metal-based chemicals that are used in agriculture. The *X. fastidiosa* YcjZ-like (XfYcjZ-like) protein belongs to the LysR-type transcriptional regulator (LTTR) family and is involved in various cellular functions that range from quorum sensing to bacterial survival. In the present study, we report the cloning, expression and purification of XfYcjZ-like, which was overexpressed in *Escherichia coli*. The secondary folding of the recombinant and purified protein was assessed by circular dichroism, which revealed that XfYcjZ-like contains a typical α/β fold. An initial hydrodynamic characterization showed that XfYcjZ-like is a globular tetramer in solution. In addition, using a polyclonal antibody against XfYcjZ-like, we assessed the expression profile of this protein during the different developmental phases of *X. fastidiosa* in *in vitro* cultivated biofilm cells and demonstrated that XfYcjZ-like is upregulated in planktonic cells in response to a copper shock treatment. Finally, the ability of XfYcjZ-like to interact with its own predicted promoter was confirmed *in vitro*, which is a typical feature of LysR. Taken together, our findings indicated that the XfYcjZ-like protein is involved in both the organization of the architecture and the maturation of the bacterial biofilm and that it is responsive to oxidative stress.

Introduction

Xylella fastidiosa is a gram-negative, xylem-limited bacterium whose full genome is available [1]. The *X. fastidiosa* 9a5c strain is the causal agent of citrus variegated chlorosis (CVC), which is also known as "*amarelinho*" in Brazil. This bacterium is able to form a biofilm structure inside the xylem vessels of susceptible plants, which results in hydric impairment, a decrease in nutrients and, ultimately, plant death during the later stages of disease. Therefore, this bacterium is associated with great economic losses in São Paulo, which is the highest producer of concentrated orange juice in Brazil [2]. To prevent the *X. fastidiosa* from spreading in the field, copper-based chemicals are used [3], which cause bacterial oxidative stress, among other effects [4–6]; however, living organisms have a large repertoire of responses to stress conditions, including modulation of the gene expression profile and increased production of transcriptional regulators, which allow them to protect themselves and to adapt and survive under these conditions [7].

LysR-type proteins are members of the largest family of transcription regulators (LTTRs)[1] in prokaryotes and are highly conserved in the bacteria kingdom [8,9]. The proteins in this family are involved in numerous cellular functions, including oxidative stress responses [10], cell wall shape [11], quorum sensing [12], efflux pumps, secretion, motility [13], nitrogen fixation [14], virulence [15], cell division [16], metabolism and environmental recog-

* Corresponding author at: Centro de Biologia Molecular e Engenharia Genética (CBMEG), Universidade Estadual de Campinas, CP 6010, 13083-875 Campinas, São Paulo, Brazil. Tel./fax: +55 19 3521 1089.
E-mail address: anete@unicamp.br (A.P. Souza).

[1] *Abbreviations used:* LTTR, LysR-type transcriptional regulators; XfYcjZ-like, YcjZ of *X. fastidiosa*; HTH, helix-turn-helix; SEC, size-exclusion chromatography; AUC, analytical ultracentrifugation; CD, circular dichroism; EMSA, electrophoresis mobility shift assay.

http://dx.doi.org/10.1016/j.pep.2015.05.003
1046-5928/

nition [17]. Initially, LTTRs were classified as repressors [18,19]; however, as previously reported, they can also act as activators, depending on the circumstances and the signaling molecules [20]. LTTRs share a high degree of conservation in the helix-turn-helix (HTH) domain at the N-terminus, which is directly involved in DNA binding, whereas the C-terminus, which possesses the regulatory domains (RD) 1 and 2 that are co-inducer binding sites [21–23], exhibits low amino acid conservation.

In the present study, we report the initial functional and hydrodynamic characterization of a LysR-type transcriptional regulator called YcjZ-like from *X. fastidiosa* strain 9a5c (XfYcjZ-like). Recombinant XfYcjZ-like was overexpressed in an *Escherichia coli* host and purified by two-step chromatography. An initial structural analysis confirmed the secondary and tertiary structures of the recombinant and purified protein. We used a polyclonal antibody against XfYcjZ-like to confirm the expression profile of this protein during the biofilm growth of *X. fastidiosa* and demonstrated that XfYcjZ-like was able to respond to a copper shock treatment because it was upregulated in planktonic cells. In addition, the interaction of XfYcjZ-like with its own predicted promoter was analyzed *in vitro*. Our results provide new information regarding the involvement of the XfYcjZ-like transcription regulator in bacterial pathogenicity.

Materials and methods

Bacterial strain, amplification, plasmid and cloning

The coding sequence of XfYcjZ-like (975 pb; NCBI Reference Sequence: WP_010894223.1) was amplified from *X. fastidiosa* 9a5c genomic DNA by PCR using specific primers designed with a *Nde*I restriction site in the forward primer (5′-GGCCATATGGCCAG ACGCAAC-3′) and an *Xho*I site in the reverse primer (5′-CACGCTCGAGTTGGCGATGG-3′). The PCR program used for *xfycjZ*-like amplification included a denaturation step at 94 °C for 120 s, followed by an annealing step at 56 °C for 45 s and a final step at 72 °C for 90 s. This cycle was repeated 30 times. After PCR amplification, the amplicon was inserted into the pET28a vector using standard molecular biology methods [24], which added a His_6-tag to the N-terminus. The recombinant vector that was generated was subjected to DNA sequencing to confirm that the cloned sequence did not contain any base substitutions.

Amino acid sequence alignment and protein structure prediction

The amino acid sequence alignment between XfYcjZ-like and the *E. coli* YcjZ protein (EcYcjZ; GenBank ID EOQ56594.1) was analyzed using the ClustalW2 server (http://www.ebi.ac.uk/Tools/msa/clustalw2/). Structural modeling prediction of XfYcjZ-like was performed using the I-TASSER server (http://zhanglab.ccmb.med.umich.edu/I-TASSER/) [25].

XfYcjZ-like expression and purification

Positive colonies, carrying the pET28:*xfycjZ*-like construct, were grown in a pre-inoculated 10 mL of Luria–Bertani (LB) broth containing 30 μg mL^{-1} kanamycin at 37 °C and 250 rpm for 12 h and were then transferred to 1 L of LB broth and grown at the same conditions until an OD_{600} of 0.9 was reached. The cultures were then induced with 5.6 mmol L^{-1} lactose for 12 h at 22 °C. The cells were collected by centrifugation at 8000 rpm, 8 °C.

To perform protein extraction, the cells were resuspended in 50 mmol mL^{-1} phosphate buffer, pH 7.8, 300 mmol mL^{-1} NaCl and 10 mmol mL^{-1} β-mercaptoethanol (buffer A) and sonicated using the Ultrasonic Homogenizer 4710 series instrument (Cole-Parmer instrument Co., Chicago, IL, USA) set at 70% duty cycle, with 1 min on and 5 min off on ice.

For recombinant protein purification, the cell lysate was clarified by centrifugation at 16,000×*g* for 45 min at 5 °C and loaded on a column with Ni-NTA agarose superflow (Qiagen; Hilden, Germany) and eluted with an imidazole gradient, from 0 until 500 mmol L^{-1} in buffer A. Subsequently, the purity was estimated by running the proteins on a 12% sodium dodecyl sulfate polyacrylamide gel electrophoresis (SDS–PAGE) gel, which was stained using Coomassie Brilliant Blue R-250 (USB, Cleveland, OH, USA).

Analytical size-exclusion chromatography (SEC)

Analytical size-exclusion chromatography (SEC) experiments were performed on an AKTA FPLC system using a Superdex 200 10/300 GL prepacked column (GE Healthcare – Pittsburgh, PA, USA) that was previously equilibrated with buffer A. Aliquots of 500 μL of protein (approximately 25 μmol L^{-1}) were loaded onto the column at a flow rate of 0.5 mL min^{-1}, and the elution profile was monitored by the absorbance at 280 nm. To estimate the Stokes radius (R_s) of the recombinant XfYcjZ-like protein, a mix of protein standards with known R_s, including carbonic anhydrase (Mw = 29 kDa, 23.9 Å), ovalbumin (Mw = 44 kDa, 30.5 Å), conalbumin (Mw = 75 kDa, 36.4 Å), aldolase (Mw = 158 kDa, 48.1 Å) and ferritin (Mw = 440 kDa, 61 Å) were used to calibrate the column. All of the protein standards (GE Healthcare) were prepared at a concentration of 3 mg mL^{-1} in buffer A. The void volume of the column was determined using blue dextran (GE Healthcare). The elution profiles obtained for the recombinant XfYcjZ-like and standard protein were converted to the partition coefficient Kav using the following formula:

$$\mathrm{Kav} = \frac{\mathrm{Ve} - V_0}{\mathrm{Vt} - V_0}$$

where Ve is the elution volume of the protein, V_0 is the void volume of the column and Vt is the total column volume (24 mL). The XfYcjZ-like R_s was calculated by the adjusted linear fitting of the R_s of the standard proteins plotted against the $-(\log \mathrm{Kav})^{1/2}$. The experimental R_s obtained from the SEC analysis was used to estimate the frictional ratio (f/f_0) as the ratio of the experimental R_s to the radius of a sphere of the same molecular mass.

Measurement of circular dichroism

Circular dichroism (CD) spectra of the purified His_6-tagged XfYcjZ-like protein were measured using a Jasco J-810 Spectropolarimeter dichrograph (Japan Spectroscopic, Tokyo, Japan). The far-UV CD spectra were generated at 25 °C from a 13.6 μmol L^{-1} solution in 10 mmol L^{-1} sodium phosphate buffer at pH 7.8. The assays were carried out using a quartz cuvette with a 2 mm path length. Ten measurements within the 260–190 nm range at a rate of 20 nm min^{-1} were recorded. The deconvolution of the CD spectrum was performed using the DICRHOWEB server (http://dichroweb.cryst.bbk.ac.uk/).

Analytical ultracentrifugation measurements

Sedimentation velocity experiments of the XfYcjZ-like protein were carried out at concentrations ranging from 0.2 to 0.7 mg mL^{-1} in buffer A using a Beckman Optima XL-A analytical ultracentrifuge. Data acquisition during analytical ultracentrifugation (AUC) was performed at 280 nm, 20 °C, and 35,000 rpm using an AN-50Ti rotor. The AUC data analyses were performed with SedFit software (Version 12.1). The experimental *s*-value was calculated for the standard sedimentation coefficient at a concentration of 0 mg mL^{-1} of protein ($s^0_{20,w}$) to prevent interferences

derived from the buffer density, viscosity and temperature [26] by using the linear fitting of the curve of the $s_{20,w}$-value as a function of the protein concentration. The buffer viscosity (η = 1.0513 × 10^{-2} poise), buffer density (ρ = 1.0163 g mL^{-1}) and partial-specific XfYcjZ-like volume (Vbar: XfYcjZ-like = 0.733194 mL g^{-1}) used for the analysis were estimated by the Sednterp server (http://sednterp.unh.edu/). The R_s, MMpred, $s^0_{20,w}$ and f/f_0 for XfYcjZ-like were obtained from the AUC data analyses by SedFit.

Electrophoretic mobility shift assay (EMSA)

The XfYcjZ-like promoter identified in the *X. fastidiosa* 9a5c genome (NCBI Reference Sequence: NC_002488.3) was cloned, and its recognition and interaction with the recombinant purified XfYcjZ-like protein were analyzed by EMSA. The cloned region comprised a 262 bp DNA fragment that was upstream of the open reading frame (ORF) that encodes XfYcjZ-like and was cloned with the following specific primers: 5′-TTCGAGGGCGAACGGGAGGC-3′ and 5′-TGCGTCTGGCCATGGCGC-3′, forward and reverse, respectively. For the EMSA, the DNA fragment was incubated with the XfYcjZ-like protein in its tetrameric form at the following DNA:protein molar ratios: 1:0, 1:1, 1:2, 1:4, 1:8, 1:16, 1:32, 1:64 and 1:100 using the promoter at 11.76 nmol mL^{-1} in 10 mmol L^{-1} phosphate buffer, 150 mmol L^{-1} NaCl. Then, the mix was resolved by agarose electrophoresis using a 1.5% agarose gel run at 40 V for 3 h. Subsequently, the gel was stained with ethidium bromide and analyzed using the Kodak Electrophoresis Documentation and Analysis System (EDAS).

Western blotting analysis

Polyclonal antibodies against XfYcjZ-like were produced by Rheabiotech (Campinas, SP, Brazil) and used in the XfYcjZ-like immunodetection assays. To conduct copper shock, the bacteria were treated with a sublethal concentration of 1 mM $CuSO_4$ for 24 h prior to the collection day, and the control cells were collected during the days mentioned below. The total protein (approximately 5 μg) from *X. fastidiosa* 9a5c after 3, 5, 10, 15, 20 and 30 days of development was extracted according to [27] and loaded on a 12% SDS–PAGE gel. After separation, the proteins were transferred in triplicate to a nitrocellulose membrane using a Trans-Blot SD Semi-Dry Transfer Cell (Bio-Rad). The membranes were blocked with casein for 12 h and washed 3 times for 10 min with Tris-buffered saline and 0.1% tween 20 (TTBS) (NaCl 0.137 mmol L^{-1}, KCl 0.025 mmol L^{-1}, Tris 0.025 mmol L^{-1}, pH 7.5). The membrane was incubated with the primary antibody (anti-XfYcjZ-like) in a 1–4000 dilution for 6 h, washed under the same conditions as described previously and then incubated with alkaline phosphatase-conjugated anti-rabbit IgG (Santa Cruz Biotechnology Inc.; USA) for 4 h, followed by another set of washes with TTBS and incubation with the revelation buffer (Tris 100 mmol L^{-1}, NaCl 100 mmol L^{-1}, $MgCl_2$ 5 mmol L^{-1}, pH 9.0) with nitro blue tetrazolium/5-bromo-4-chloro-3-indolyl phosphate (NBT/BCIP; Sigma, USA), following the manufacturer's instructions.

Results and discussion

Alignment of XfYcjZ-like with its E. coli homolog and structural prediction analysis

XfYcjZ-like (324 amino acid residues) in the *X. fastidiosa* 9a5c genome was annotated as a LTTR protein that is involved in bacterial pathogenicity [1]. The alignment of the XfYcjZ-like amino sequence with that of *E. coli* YcjZ (Fig. 1A) showed a high degree of identity (approximately 58%), hence the name XfYcjZ-like. The LTTRs are described as being well conserved among bacteria [21,28], and this protein family encompasses approximately 800 members that have been identified based on their amino acid sequence identity [9]. In the XfYcjZ-like N-terminal domain that contains the HTH motif involved in DNA-binding, the identity with the homologous EcYcjZ region is even greater, reaching 65%; however, notable differences are observed between the C-terminal domains. XfYcjZ-like contains 27 C-terminal amino acid residues that are not present in the homologous *E. coli* protein. Because the LTTR C-terminal domain is described as containing co-inducer binding sites [21–23], this observation suggests that different co-inducers than those that act in *E. coli* can modulate the activity of XfYcjZ-like.

To obtain information about the predicted structure of XfYcjZ-like, we used the I-TASSER server to generate a putative model of its protein structure (Fig. 1B). Although no YcjZ homolog structure is available in the Protein Data Bank (PDB; http://www.rcsb.org), the predicted model of XfYcjZ-like showed a TM-score of 0.884 for the structural alignment between the query structure (XfYcjZ-like) and the known structure of AphB, a LTTR family gene activator from *Vibrio cholerae* (PDB code 3SZP) [29]. The TM-score is a proposed scale for measuring the structural similarity between two structures [30]; thus, the TM-score value obtained in this study indicates that the predicted XfYcjZ-like model contains the correct topology. The predicted XfYcjZ-like model showed an N-terminal DNA-binding domain in a typical HTH fold that was composed of three α-helices (α1–α3) followed by two β-strands (β1 and β2), whereas the C-terminal domain showed a typical α/β fold (Fig. 1B). Therefore, although we show only a putative model for XfYcjZ-like, it presents features similar to those of another LTTR protein whose structure is available [21,29].

Recombinant XfYcjZ-like was overexpressed and obtained in a soluble form with a dominant α-helical structure

In this study, XfYcjZ-like was cloned, and the recombinant protein was overexpressed in *E. coli* and purified using chromatographic methods. After the affinity chromatography step, a band of approximately 38.5 kDa, which corresponds to the size of the amino acid sequence of XfYcjZ-like plus the N-terminal His_6-tag added by the pET28a vector, was observed on a 12% SDS–PAGE gel (Fig. 2A). The recombinant protein was mostly present in the soluble fraction and resulted in a yield of 4 mg of purified protein per liter of bacterial culture. The purified XfYcjZ-like fraction remained stable in solution and showed no protein degradation for several days. The secondary structure of the recombinant and purified XfYcjZ-like was evaluated by CD (Fig. 2B). The CD analysis of the recombinant protein revealed that XfYcjZ-like has a typical spectrum for a protein that is rich in α-helical structures and is approximately 36.7% α-helix structure, 15% β-sheet and 38% random coil. The CD spectrum deconvolution matched the modeling analysis and strengthens the structural prediction of XfYcjZ-like by I-TASSER (Fig. 1B), in which the N-terminal α-helix rich DNA-binding HTH motif was observed.

Hydrodynamic characterization of XfYcjZ-like

We employed analytical SEC and AUC to evaluate the characteristics of the recombinant, purified XfYcjZ-like protein in solution. Table 1 summarizes the results obtained from the hydrodynamic characterization of XfYcjZ-like. XfYcjZ-like was eluted as a unique peak during the analytical SEC experiments (Fig. 3A), with a retention profile corresponding to an apparent molecular mass (MM_{app}) of 159 ± 4 kDa and R_s of 44.4 ± 1 Å (Fig. 3B). By comparing the predicted hydrodynamic data from the amino acid sequence of

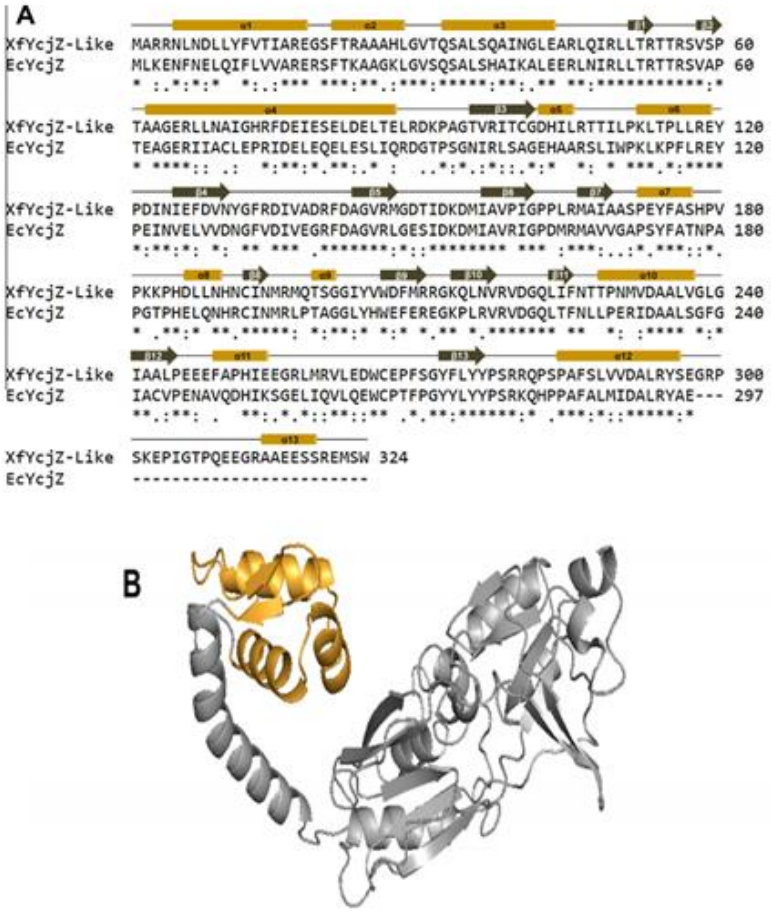

Fig. 1. XfYcjZ-like sequence alignment analysis and protein structure prediction. (A) The amino acid sequences of XfYcjZ-like (NCBI Reference Sequence: WP_010894223.1) and the *E. coli* YcjZ protein (EcYcjZ; GenBank ID EOQ56594.1), were aligned using the ClustalW2 server (http://www.ebi.ac.uk/Tools/msa/clustalw2/), which revealed high identity (58%). Conservation between identical amino acid residues is indicated by an asterisk, residues with strongly similar properties are shown by a double dot and weakly similar properties are represented by a single dot. (B) Structural modeling prediction of XfYcjZ-like. The N-terminal DNA-binding motif (residues 1–60) is highlighted in gold in the model with the best C-score. The modeling prediction was performed using the I-TASSER server (http://zhanglab.ccmb.med.umich.edu/I-TASSER/). (For interpretation of the references to color in this figure legend, the reader is referred to the web version of this article.)

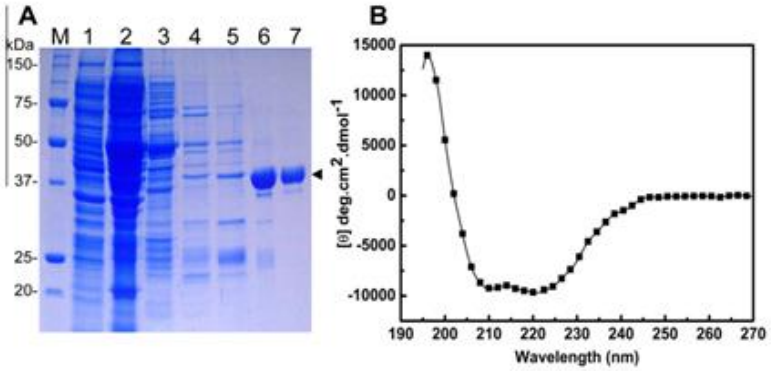

Fig. 2. XfYcjZ-like protein purification and secondary structural analysis. (A) SDS–PAGE 12% gel showing XfYcjZ-like protein purification. M: molecular mass markers; lane 1, cell lysate before protein induction; lane 2, cell lysate after protein induction; lanes 3–6, proteins eluted using an imidazole gradient (20, 50, 75 and 100 mmol L^{-1}, respectively); lane 7, protein after size exclusion chromatography. The recombinant purified XfYcjZ-like is indicated by a black left-pointing triangle. The protein purification-yielded proteins with a purity greater than 95%. (B) Circular dichroism spectra of XfYcjZ-like. The CD results suggested that XfYcjZ-like is rich in α-helical structures.

XfYcjZ-like with the experimental SEC data (Table 1 and Fig. 3A and B), the recombinant purified XfYcjZ-like is possibly a tetramer in solution and shows an f/f_0 value of 1.25. This result is expected for a protein with a globular shape. From the AUC data analysis, our findings indicate that XfYcjZ-like sediments as a single species with $s^0_{20,w}$ and an experimental molecular mass (MM_{exp})

Table 1
Hydrodynamic properties of recombinant purified XfYcjZ-like protein.

Technique	Property
Predicted hydrodynamic data[a]	Monomer = R_0 22.4 Å, MM_{pred} 38.5 kDa Dimer = R_0 28.2 Å, MM_{pred} 77.1 kDa Tetramer = R_0 35.5 Å, MM_{pred} 154.2 kDa
SEC	R_s 44.4 ± 1 Å MM_{app} 159 ± 4 kDa f/f_0[b] 1.25
AUC	$s^0_{20,w}$ (S) 6.65 ± 0.02 f/f_0[c] 1.36 ± 0.1 MM_{exp} 151 ± 2 kDa R_s 46 ± 2 Å

[a] Predicted from the amino acid sequence using the Sednterp server (http://sednterp.unh.edu/).
[b] From the ratio of R_s obtained from SEC analyses by R_0 of the tetramer predicted data.
[c] Obtained from SedFit analysis.

of 6.65 ± 0.02 S and 151 ± 2 kDa, respectively, which suggests that it behaves as a tetramer in solution (Fig. 3C and D; Table 1). The AUC sedimentation velocity data also indicated that XfYcjZ-like exhibited an f/f_0 of 1.36 ± 0.1 and R_s of 46 ± 2, suggesting that it has a globular shape. The AUC data corroborated the analytical SEC results and confirmed the tetrameric state of XfYcjZ-like in solution.

The oligomeric states of the LTTR proteins in solution have been described as dimers and tetramers, although octameric forms have also been observed [10,13,29,31]. The tetrameric state is reported as the most common oligomeric form of the LTTR proteins because this conformation correctly positions the HTH domain to facilitate protein:DNA interactions, although the tetramer must undergo a conformational change for DNA binding to occur [29].

Interaction with its promoter

The ability of recombinant XfYcjZ-like to interact with DNA was investigated by EMSA. We initially searched for the predicted promoter of the *xfycjZ*-like gene in the *X. fastidiosa* genome [1]. A 262 bp DNA sequence upstream of *xfycjZ*-like contains all of the regulatory regions required for a promoter (Fig. 4A) and was used for the protein:DNA binding experiments. The LTTRs recognize specific pseudopalindromic DNA sequences, e.g., ATC-N_9-GAT [32] and T-N_{11}-A [33], that permit protein:DNA interactions and subsequent gene regulation. The predicted *xfycjZ*-like promoter contains five T-N_{11}-A DNA sequences: −12 to −24; −37 to −49, −59 to −71, −87 to −99 and −102 to −114 (Fig. 4A).

Our results showed that the recombinant and purified XfYcjZ-like protein was able to interact *in vitro* with its cis-regulatory element at a molar ratio as low as 1:2 (DNA:protein) and showed a 96% interaction rate at a 1:16 ratio, which led to a shift in the mobility of the DNA fragment (Fig. 4B). We therefore concluded that recombinant XfYcjZ-like was produced in an active and folded state.

XfYcjZ-like immunoblotting during X. fastidiosa growth

Polyclonal antibodies against XfYcjZ-like were used to assess the protein expression profile during different phases of *X. fastidiosa* biofilm growth and in associated planktonic cells. XfYcjZ-like was differentially expressed during biofilm formation and planktonic growth of *X. fastidiosa*. XfYcjZ-like was strongly detected until 15 days of planktonic growth, whereas in the biofilm cells, higher levels of protein expression were detected at 5 and 20 days (Fig. 5A). The *X. fastidiosa* biofilm developmental process was described previously [27]. On the 5th day, microcolony formation

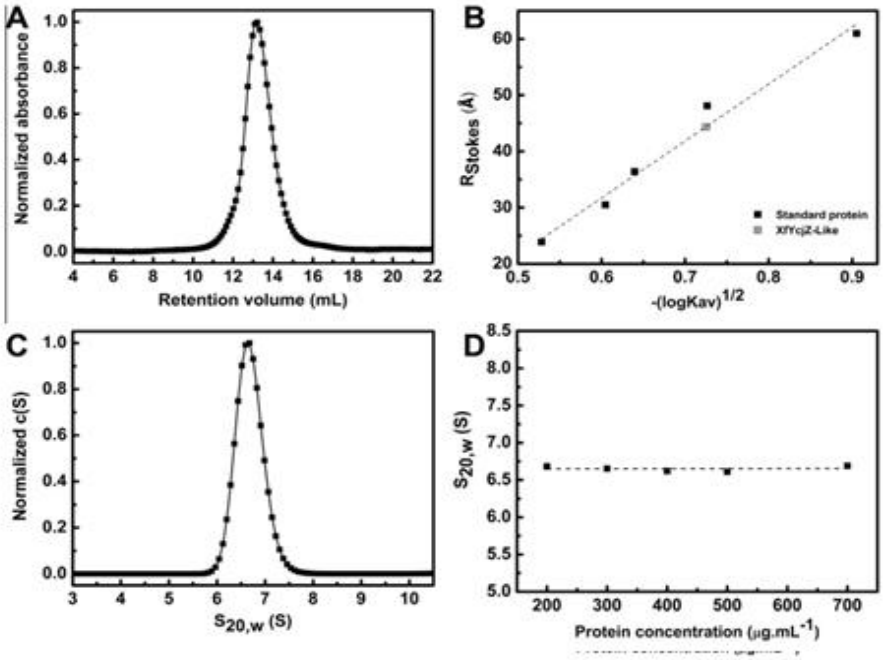

Fig. 3. Hydrodynamic properties of XfYcjZ-like. (A) Chromatogram of the analytical SEC experiments for recombinant, purified XfYcjZ-like protein. (B) The linear fitting of the Stokes radius (R_s) of the standard proteins (black square), carbonic anhydrase (Mw = 29 kDa, 23.9 Å), ovalbumin (Mw = 44 kDa, 30.5 Å), conalbumin (Mw = 75 kDa, 36.4 Å), aldolase (Mw = 158 kDa, 48.1 Å) and ferritin (Mw = 440 kDa, 61 Å) as a function of the values of $-(\log Kav)^{1/2}$ were used to estimate the R_s of the XfYcjZ-like as 44.4 ± 1 Å (open square). (C) Sedimentation velocity AUC experiments of XfYcjZ-like using a range of concentrations from 200 to 700 µg mL^{-1} in buffer (C). Panel C shows the c(S) distribution of XfYcjZ-like at 700 µg mL^{-1}. The sedimentation profiles show that one species predominated. (D) Dependence of XfYcjZ-like $s_{20,w}$ (S) as a function of protein concentration, which allowed us to obtain $s^0_{20,w}$ (S) of 6.65 ± 0.02. The hydrodynamic analyses indicated that XfYcjZ-like is a tetramer in solution.

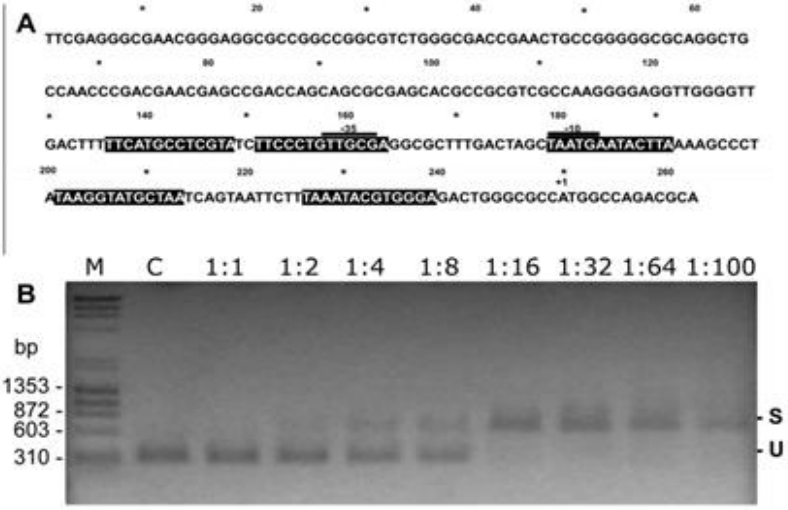

Fig. 4. XfYcjZ-like interacts with its own predicted promoter. (A) DNA sequence (262 bp) used in the EMSA analysis. The proposed -10 box and -35 box of the predicted *xfycjZ*-like promoter ($P_{xfycjZ\text{-}like}$) are indicated. +1 indicates the *xfycjZ*-like start codon. The LTTR predicted binding sites ($T\text{-}N_{11}\text{-}A$) are highlighted in black. (B) Interaction of XfYcjZ-like with its own putative $P_{xfycjZ\text{-}like}$. M, molecular weight marker; C, control reaction with the DNA fragment in the absence of protein; 1:1, 1:2, 1:4, 1:8, 1:12, 1:16, 1:32, 1:64 and 1:100 gradient of molar ratios of DNA:protein, considering the tetrameric form of XfYcjZ-like. The shifted bands (S) and unbound DNA fragment (U) are indicated on the right.

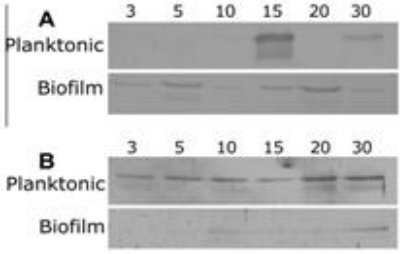

Fig. 5. Immunodetection of XfYcjZ-like during the *X. fastidiosa* planktonic and biofilm growth modes. (A) Detection of XfYcjZ-like during normal bacterial growth. (B) Detection of XfYcjZ-like after oxidative stress conditions were induced by a copper treatment. The numbers 3, 5, 10, 15, 20 and 30 correspond to the different days during biofilm growth. The associated planktonic cells were also collected. The total protein samples from each day were extracted, normalized using BCA quantification, and evaluated by Western blot using polyclonal antibodies against XfYcjZ-like.

is initiated; on the 15th day, the architecture of the biofilm begins to organize; and biofilm maturation occurs on the 20th day. Thus, XfYcjZ-like is involved in the development of the biofilm architecture and its maturation. These results are consistent with the involvement of the LTTRs in quorum sensing [34] and bacterial pathogenicity [35].

Interestingly, after a copper treatment, the detection of XfYcjZ-like in the planktonic cells was more pronounced (Fig. 5B), with it being detected on all of the days analyzed. Muranaka et al. [36] showed by microarray analysis that the ORF that encodes XfYcjZ-like was upregulated after oxidative stress was induced by copper treatment. Thus, our direct immunodetection findings confirmed that XfYcjZ-like is involved in the response to oxidative stress and can play a role in metal detoxification or metal homeostasis, as previously reported for *Enterococcus faecalis*, in which several LysR proteins were activated by copper [37]. Additionally, HbrL, which also belongs to the LTTR family of transcriptional regulators, in *Rhodobacter capsulatus* is responsive to iron [38].

The low response to copper during the different biofilm phases was intriguing (Fig. 5B). This result may have occurred because the *X. fastidiosa* biofilm is primarily composed of dead cells [39]. In this instance, a polysaccharide-rich gel layer is formed around the biofilm, which makes the biofilm less sensitive to environmental changes [40].

Conclusion

The LysR family participates in a myriad of cell functions, which range from cell division to bacterial pathogenicity. In this study, we attempted to understand the role of XfYcjZ-like during the developmental process of *X. fastidiosa* biofilm formation and during the response to copper. The formation of biofilms is considered the main pathogenicity mechanism of *X. fastidiosa*; therefore, understanding how this structure is formed can lead to the development of alternatives for controlling this phytopathogen. Our findings showed that XfYcjZ-like was upregulated by copper shock in planktonic cells and was involved in the organization of the architecture and maturation of biofilms and, consequently, in bacterial pathogenicity.

We hope to contribute to future studies focusing on the role that LTTRs, such as XfYcjZ-like, play in the modulation of gene expression, particularly during the phases in which the plant–bacteria interaction allows the bacteria (e.g., *X. fastidiosa*) to effectively colonize a susceptible plant, thus causing a specific disease.

Acknowledgments

This study was supported by Grants from the Fundação de Amparo à Pesquisa do Estado de São Paulo – Brazil (FAPESP, Process 2012/51580-4 and 2001/07533-7) and Coordenação de Aperfeiçoamento de Pessoal de Nível Superior (CAPES, Computational Biology Program). A.S.S. is the recipient of a Ph.D. fellowship from FAPESP (Process 2011/50268-4), CAS is the recipient of a Post-Doctoral fellowship, and A.P.S. is the recipient of a Research fellowship, both from the Conselho Nacional de

Desenvolvimento Científico e Tecnológico (CNPq). We gratefully acknowledge the Laboratório de Espectroscopia e Calorimetria (LEC), Laboratório Nacional de Biociências – LNBio (Campinas, Brazil), for their support of the CD and AUC studies.

References

[1] A.J. Simpson, F.C. Reinach, P. Arruda, F.A. Abreu, M. Acencio, R. Alvarenga, L.M. Alves, J.E. Araya, G.S. Baia, C.S. Baptista, M.H. Barros, E.D. Bonaccorsi, S. Bordin, J.M. Bove, M.R. Briones, M.R. Bueno, A.A. Camargo, L.E. Camargo, D.M. Carraro, H. Carrer, N.B. Colauto, C. Colombo, F.F. Costa, M.C. Costa, C.M. Costa-Neto, L.L. Coutinho, M. Cristofani, E. Dias-Neto, C. Docena, H. El-Dorry, A.P. Facincani, A.J. Ferreira, V.C. Ferreira, J.A. Ferro, J.S. Fraga, S.C. Franca, M.C. Franco, M. Frohme, L.R. Furlan, M. Garnier, G.H. Goldman, M.H. Goldman, S.L. Gomes, A. Gruber, P.L. Ho, J.D. Hoheisel, M.L. Junqueira, E.L. Kemper, J.P. Kitajima, J.E. Krieger, E.E. Kuramae, F. Laigret, M.R. Lambais, L.C. Leite, E.G. Lemos, M.V. Lemos, S.A. Lopes, C.R. Lopes, J.A. Machado, M.A. Machado, A.M. Madeira, H.M. Madeira, C.L. Marino, M.V. Marques, E.A. Martins, E.M. Martins, A.Y. Matsukuma, C.F. Menck, E.C. Miracca, C.Y. Miyaki, C.B. Monteiro-Vitorello, D.H. Moon, M.A. Nagai, A.L. Nascimento, L.E. Netto, A. Nhani Jr., F.G. Nobrega, L.R. Nunes, M.A. Oliveira, M.C. de Oliveira, R.C. de Oliveira, D.A. Palmieri, A. Paris, B.R. Peixoto, G.A. Pereira, H.A. Pereira Jr., J.B. Pesquero, R.B. Quaggio, P.G. Roberto, V. Rodrigues, M.R.A.J. de, V.E. de Rosa Jr., R.G. de Sa, R.V. Santelli, H.E. Sawasaki, A.C. da Silva, A.M. da Silva, F.R. da Silva, W.A. da Silva Jr., J.F. da Silveira, M.L. Silvestri, W.J. Siqueira, A.A. de Souza, A.P. de Souza, M.F. Terenzi, D. Truffi, S.M. Tsai, M.H. Tsuhako, H. Vallada, M.A. Van Sluys, S. Verjovski-Almeida, A.L. Vettore, M.A. Zago, M. Zatz, J. Meidanis, J.C. Setubal, The genome sequence of the plant pathogen *Xylella fastidiosa*. The *Xylella fastidiosa* consortium of the organization for nucleotide sequencing and analysis, Nature 406 (2000) 151–159.

[2] C.M. Rodrigues, A.A. de Souza, M.A. Takita, L.T. Kishi, M.A. Machado, RNA-Seq analysis of *Citrus reticulata* in the early stages of *Xylella fastidiosa* infection reveals auxin-related genes as a defense response, BMC Genomics 14 (2013) 676.

[3] M.W. LeChevallier, C.D. Cawthon, R.G. Lee, Inactivation of biofilm bacteria, Appl. Environ. Microbiol. 54 (1988) 2492–2499.

[4] J. Baker, S. Sitthisak, M. Sengupta, M. Johnson, R.K. Jayaswal, J.A. Morrissey, Copper stress induces a global stress response in *Staphylococcus aureus* and represses sae and agr expression and biofilm formation, Appl. Environ. Microbiol. (2010) 150–160.

[5] S. Chillappagari, A. Seubert, H. Trip, O.P. Kuipers, M.A. Marahiel, M. Miethke, Copper stress affects iron homeostasis by destabilizing iron–sulfur cluster formation in *Bacillus subtilis*, J. Bacteriol. 192 (2010) 2512–2524.

[6] P. Sornchuer, P. Namchaiw, J. Kerdwong, N. Charoenlap, S. Mongkolsuk, P. Vattanaviboon, Copper chloride induces antioxidant gene expression but reduces ability to mediate H_2O_2 toxicity in *Xanthomonas campestris*, Microbiology (Reading, England) 160 (2014) 458–466.

[7] E. Cabiscol, J. Tamarit, J. Ros, Oxidative stress in bacteria and protein damage by reactive oxygen species, Int. Microbiol. 3 (2000) 3–8.

[8] M.A. Schell, Molecular biology of the LysR family of transcriptional regulators, Annu. Rev. Microbiol. 47 (1993) 597–626.

[9] S.E. Maddocks, P.C. Oyston, Structure and function of the LysR-type transcriptional regulator (LTTR) family proteins, Microbiology (Reading, England) 154 (2008) 3609–3623.

[10] M.A. Toledo, D.R. Schneider, A.R. Azzoni, M.T. Favaro, A.C. Pelloso, C.A. Santos, A.M. Saraiva, A.P. Souza, Characterization of an oxidative stress response regulator, homologous to *Escherichia coli* OxyR, from the phytopathogen *Xylella fastidiosa*, Protein Expr. Purif. 75 (2011) 204–210.

[11] T. Shimada, K. Yamazaki, A. Ishihama, Novel regulator PgrR for switch control of peptidoglycan recycling in *Escherichia coli*, Genes Cells 18 (2013) 123–134.

[12] E.P. O'Grady, D.T. Nguyen, L. Weisskopf, L. Eberl, P.A. Sokol, The *Burkholderia cenocepacia* LysR-type transcriptional regulator ShvR influences expression of quorum-sensing, protease, type II secretion, and afc genes, J. Bacteriol. 193 (2011) 163–176.

[13] B.J. Habdas, J. Smart, J.B. Kaper, V. Sperandio, The LysR-type transcriptional regulator QseD alters type three secretion in enterohaemorrhagic *Escherichia coli* and motility in K-12 *Escherichia coli*, J. Bacteriol. 192 (2010) 3699–3712.

[14] H.R. Schlaman, B.J. Lugtenberg, R.J. Okker, The NodD protein does not bind to the promoters of inducible nodulation genes in extracts of bacteroids of *Rhizobium leguminosarum* biovar *viciae*, J. Bacteriol. 174 (1992) 6109–6116.

[15] K.A. Matthias, R.F. Rest, Control of pili and sialyltransferase expression in *Neisseria gonorrhoeae* is mediated by the transcriptional regulator CrgA, Mol. Microbiol. 91 (2014) 1120–1135.

[16] Z. Lu, M. Takeuchi, T. Sato, The LysR-type transcriptional regulator YofA controls cell division through the regulation of expression of ftsW in *Bacillus subtilis*, J. Bacteriol. 189 (2007) 5642–5651.

[17] M. Takao, H. Yen, T. Tobe, LeuO enhances butyrate-induced virulence expression through a positive regulatory loop in enterohaemorrhagic *Escherichia coli*, Mol. Microbiol. 93 (2014) 1302–1313.

[18] S. Lindquist, F. Lindberg, S. Normark, Binding of the *Citrobacter freundii* AmpR regulator to a single DNA site provides both autoregulation and activation of the inducible ampC beta-lactamase gene, J. Bacteriol. 171 (1989) 3746–3753.

[19] K. Vercammen, Q. Wei, D. Charlier, A. Dotsch, S. Haussler, S. Schulz, F. Salvi, G. Gadda, J. Spain, M. Levin Rybtke, T. Tolker-Nielsen, J. Dingemans, L. Ye, P. Cornelis, *Pseudomonas aeruginosa* LysR PA4203 regulator NmoR acts as a repressor of the PA4202 nmoA gene encoding a nitronate monooxygenase, J. Bacteriol. (2014).

[20] T. Kakuda, T. Hirota, T. Takeuchi, H. Hagiuda, S. Miyazaki, S. Takai, VirS, an OmpR/PhoB subfamily response regulator, is required for activation of vapA gene expression in *Rhodococcus equi*, BMC Microbiol. 14 (2014) 243.

[21] E. Stec, M. Witkowska-Zimny, M.M. Hryniewicz, P. Neumann, A.J. Wilkinson, A.M. Brzozowski, C.S. Verma, J. Zaim, S. Wysocki, G.D. Bujacz, Structural basis of the sulphate starvation response in *E. coli*: crystal structure and mutational analysis of the cofactor-binding domain of the Cbl transcriptional regulator, J. Mol. Biol. 364 (2006) 309–322.

[22] W.M. Zhang, J.J. Zhang, X. Jiang, H. Chao, N.Y. Zhou, Transcriptional activation of multiple operons involved in *para*-nitrophenol degradation by *Pseudomonas* sp. strain WBC-3, Appl. Environ. Microbiol. 81 (2015) 220–230.

[23] O. Porrua, M. Garcia-Jaramillo, E. Santero, F. Govantes, The LysR-type regulator AtzR binding site: DNA sequences involved in activation, repression and cyanuric acid-dependent repositioning, Mol. Microbiol. 66 (2007) 410–427.

[24] J. Sambrook, D.W. Russell, Molecular Cloning: A Laboratory Manual, third ed., Cold Spring Harbor Laboratory Press, Cold Spring Harbor, NY, 2001.

[25] A. Roy, A. Kucukural, Y. Zhang, I-TASSER: a unified platform for automated protein structure and function prediction, Nat. Protoc. 5 (2010) 725–738.

[26] P. Schuck, M.A. Perugini, N.R. Gonzales, G.J. Howlett, D. Schubert, Size-distribution analysis of proteins by analytical ultracentrifugation: strategies and application to model systems, Biophys. J. 82 (2002) 1096–1111.

[27] R. Caserta, M.A. Takita, M.L. Targon, L.K. Rosselli-Murai, A.P. de Souza, L. Peroni, D.R. Stach-Machado, A. Andrade, C.A. Labate, E.W. Kitajima, M.A. Machado, A.A. de Souza, Expression of *Xylella fastidiosa* fimbrial and afimbrial proteins during biofilm formation, Appl. Environ. Microbiol. 76 (2010) 4250–4259.

[28] E. Perez-Rueda, J. Collado-Vides, Common history at the origin of the position-function correlation in transcriptional regulators in archaea and bacteria, J. Mol. Evol. 53 (2001) 172–179.

[29] J.L. Taylor, R.S. De Silva, G. Kovacikova, W. Lin, R.K. Taylor, K. Skorupski, F.J. Kull, The crystal structure of AphB, a virulence gene activator from *Vibrio cholerae*, reveals residues that influence its response to oxygen and pH, Mol. Microbiol. 83 (2012) 457–470.

[30] Y. Zhang, J. Skolnick, Scoring function for automated assessment of protein structure template quality, Proteins 57 (2004) 702–710.

[31] G. Vadlamani, M.D. Thomas, T.R. Patel, L.J. Donald, T.M. Reeve, J. Stetefeld, K.G. Standing, D.J. Vocadlo, B.L. Mark, The beta-lactamase gene regulator AmpR is a tetramer that recognizes and binds the D-Ala-D-Ala Motif of its repressor UDP-MurNAc-pentapeptide, J. Biol. Chem. (2014).

[32] K. Goethals, M. Van Montagu, M. Holsters, Conserved motifs in a divergent nod box of *Azorhizobium caulinodans* ORS571 reveal a common structure in promoters regulated by LysR-type proteins, Proc. Natl. Acad. Sci. USA 89 (1992) 1646–1650.

[33] M.R. Parsek, R.W. Ye, P. Pun, A.M. Chakrabarty, Critical nucleotides in the interaction of a LysR-type regulator with its target promoter region. catBC promoter activation by CatR, J. Biol. Chem. 269 (1994) 11279–11284.

[34] A. Ilangovan, M. Fletcher, G. Rampioni, C. Pustelny, K. Rumbaugh, S. Heeb, M. Camara, A. Truman, S.R. Chhabra, J. Emsley, P. Williams, Structural basis for native agonist and synthetic inhibitor recognition by the *Pseudomonas aeruginosa* quorum sensing regulator PqsR (MvfR), PLoS Pathog. 9 (2013) e1003508.

[35] C. Tam, O. Demke, T. Hermanas, A. Mitchell, A.P. Hendrickx, O. Schneewind, YfbA, a *Yersinia pestis* regulator required for colonization and biofilm formation in the gut of cat fleas, J. Bacteriol. 196 (2014) 1165–1173.

[36] L.S. Muranaka, M.A. Takita, J.C. Olivato, L.T. Kishi, A.A. de Souza, Global expression profile of biofilm resistance to antimicrobial compounds in the plant-pathogenic bacterium *Xylella fastidiosa* reveals evidence of persister cells, J. Bacteriol. 194 (2012) 4561–4569.

[37] M. Latorre, J. Galloway-Pena, J.H. Roh, M. Budinich, A. Reyes-Jara, B.E. Murray, A. Maass, M. Gonzalez, *Enterococcus faecalis* reconfigures its transcriptional regulatory network activation at different copper levels, Metallomics 6 (2014) 572–581.

[38] S. Zappa, C.E. Bauer, The LysR-type transcription factor HbrL is a global regulator of iron homeostasis and porphyrin synthesis in *Rhodobacter capsulatus*, Mol. Microbiol. 90 (2013) 1277–1292.

[39] S. Chatterjee, R.P. Almeida, S. Lindow, Living in two worlds: the plant and insect lifestyles of *Xylella fastidiosa*, Annu. Rev. Phytopathol. 46 (2008) 243–271.

[40] P.A. Cobine, L.F. Cruz, F. Navarrete, D. Duncan, M. Tygart, L. De La Fuente, *Xylella fastidiosa* differentially accumulates mineral elements in biofilm and planktonic cells, PLoS One 8 (2013) e54936.

Parte 2. Resultados e discussão referentes às proteínas Toxina-antitoxina

O conjunto de dados referentes às ORFs XfMqsR e XfMqsA foram compilados em forma de artigo e submetido ao periódico Molecular Plant Pathology, intitulado *"Xylella fastidiosa secretes the antitoxin of a toxin-antitoxin system homologous to MsqR/MsqA from Escherichia coli."* com número de registro MPP-AO-15-159, apresentado a seguir.

4.2. ARTIGO 2

"*Xylella fastidiosa* secretes the antitoxin of a toxin-antitoxin system homologous to MsqR/MsqA from *Escherichia coli*"

Autores: André da Silva Santiago, Juliano Sales Mendes, Clelton Aparecido dos Santos, Marcelo Augusto Szymanski de Toledo, Lílian Luzia Beloti, Aline Crucello, Maria Augusta Crivelente Horta, Marianna Teixeira de Pinho Favaro, Alessandra Alves de Souza, Anete Pereira de Souza.

Manuscrito submetido na Revista *Molecular Plant Pathology*

Junho/2015

Xylella fastidiosa secretes the antitoxin of a toxin-antitoxin system homologous to MsqR/MsqA from *Escherichia coli*

André da Silva Santiago[1], Juliano Sales Mendes[1], Clelton Aparecido dos Santos[1], Marcelo Augusto Szymanski de Toledo[1], Lílian Luzia Beloti[1], Aline Crucello[1], Maria Augusta Crivelente Horta[1], Marianna Teixeira de Pinho Favaro, Alessandra Alves de Souza[2], Anete Pereira de Souza[1]

[1]Centro de Biologia Molecular e Engenharia Genética – Instituto de Biologia – Unicamp

[2]Instituto Agronômico de Campinas IAC – APTA-Citrus

To whom correspondence should be addressed: Anete P. de Souza, Centro de Biologia Molecular e Engenharia Genética, Unicamp. Avenida Cândido Rondon, 400, Cidade Universitária/Unicamp,

Caixa Postal 6010, CEP 13083-875

Tel: +55 19 3521-1089

E-mail: anete@unicamp.br

Running head: The toxin-antitoxin system from *Xylella fastidiosa*

Keywords: Toxin-antitoxin system; *Xylella fastidiosa* strain 9a5c; Biofilm, Outer Membrane Vesicles; protein interaction.

ABSTRACT

The mechanisms involved in biofilm formation remain unknown. Therefore, elucidating how some bacteria form biofilms is a major barrier to understanding the progression of diseases caused by biofilm-producing bacteria. Several investigations found that the toxin-antitoxin operon is related to biofilm formation. This operon is composed of a toxin with RNAse activity and its cognate antitoxin, which is able to inhibit toxin activity. In this study, we report the characterization of a toxin-antitoxin system from *Xylella fastidiosa* that is homologous to MqsR-MqsA of *Escherichia coli.* Using a kit to detect RNAses, we demonstrated that XfMqsR has the capacity to degrade RNA and is inhibited by XfMqsA. Using size-exclusion chromatography, the interaction between these heterologous proteins was demonstrated to occur at a 1:1 ratio; moreover, denaturing circular dichroism revealed that the complex is more thermoresistant than either isolated protein. Calorimetry showed a high affinity between these proteins, with a K_d of 0.785±0.241 nmol.L^{-1}. We also demonstrated that these proteins are differentially expressed during the planktonic and biofilm phases. In addition, our findings showed that the antitoxin is secreted into the extracellular medium via outer membrane vesicle formation. This is the first report of the secretion of this antitoxin.

1. INTRODUCTION

Genes encoding the toxin-antitoxin (TA) operon are widespread among bacteria and archaea (Gerdes, 2012). This operon can be present in plasmids or chromosomes, and its genes are co-expressed under the regulation of the same promoter, which is negatively autoregulated by the antitoxin via its DNA-binding domain (Hayes and Kedzierska, 2014). Physiologically, the TA operon is involved in post-segregational killing, which can induce the death of cells that fail to inherit a plasmid (Brzozowska, and Zielenkiewicz 2013; Park *et al*., 2013) and the formation of persister cells, which confer antibiotic tolerance to bacterial populations lacking genetic mutations and biofilm formation (Gerdes, 2012; Germain *et al*., 2015).

TA systems were initially discovered in plasmids but were later encountered in the chromosomes of myriad species of bacteria and archaea (Yamaguchi *et al*., 2011). These operons are classified according to the mode of action of the antitoxins, which can be a protein or RNA and which are classified into five groups (Gerdes and Wagner, 2007; Wang *et al*., 2012; Brantl and Jahn, 2015). The proteins in this study belong to type II, which is the

most common type. In Type II systems, the proteins consist of a stable toxin and a labile antitoxin and the respective genes are separated by two nucleotides and are regulated by the same promoter.

The antitoxin regulates the activity of the toxin via the formation of a toxin-antitoxin complex (Brown *et al*., 2013). The complex inhibits the ribonuclease activity of the toxin and allows the cell to recover its normal growth rate (Wang *et al*., 2011; Brown *et al*., 2011). However, the half-lives of these proteins are different: the toxin tends to be stable, but the antitoxin is susceptible degradation by the Lon protease (Wang and Wood, 2011). This differential regulation can result in increased accumulation of free toxins following antitoxin degradation (Franch *et al*., 1997; Cook *et al*., 2013). Moreover, the antitoxin possesses the capacity to regulate not only the TA operon but also detoxification-related genes (Wang *et al*., 2011).

Gene expression studies have revealed that the TA operon is involved in the stress response (Wang *et al*., 2011; Kwan *et al*., 2014) and pathogenicity because the persister cell generation and biofilm formation are influenced by TA system expression in *E. coli* (Wang and Wood, 2011) and in the *Xylella fastidiosa* strain Temecula (Lee *et al*., 2014). This influence is due to the regulation of the RNA polymerase sigma factor σ^S by the antitoxin. When the antitoxin is degraded by the Lon proteases, *rpoS* and c-di-GMP are induced, leading to cell adhesion and biofilm formation. When the antitoxin is bound to the *rpoS* promoter, the cells are biased towards the planktonic phase (high motility) (Wang and Wood, 2011; Lord *et al*., 2014; Yamaguchi *et al*., 2009).

These factors are a matter of concern related to the yield of several crops and to human diseases. Biofilms are involved in the pathogenicity of several species because they confer resistance to antibiotics and other chemicals used to control the bacterial population (Kouzel *et al*., 2015; Ruhl *et al*., 2014) (e.g., *X. fastidiosa* (Caserta *et al*., 2013; Janissen *et al*., 2015), *Neisseria meningitides* (Arenas *et al*., 2015); *Streptococcus pneumonia* (Domenech *et al*., 2015) *Salmonella enterica* O'Leary *et al*., 2015) and *Peseudomonas syringae* (Chowdhury; Jagannadham, 2013).

This study focuses on *X. fastidiosa*, a Gram-negative, fastidious, xylem-limited bacterium (Simpson *et al*. 2000) the database for this species is available at http://www.xylella.lncc.br/xf-webbie/final/main.html#. In Brazil, *Xylella fastidiosa* strain 9a5c is the causal agent of the citrus variegated chlorosis, which affects many crops (Muranaka *et al*., 2012). The pathogenicity of *X. fastidiosa* is related to its capacity to develop a biofilm in the xylem vessels, resulting in hydric deficiency, hindrance of nutrient transport

and death in the later stages of infection (Rodrigues *et al*., 2013). It was demonstrated that two TA systems from the *X. fastidiosa* strain Temecula play an important role in increasing biofilm mass and persister cell formation (Lee *et al*., 2014).

Another important feature related to Gram-negative bacteria is their capacity to produce outer membrane vesicles (OMV), which are 20 to 300 nm in diameter (Ionescu *et al*., 2014; Schertzer and Whiteley, 2013, Kuipers *et al*., 2015; Ellis and Kuehn, 2010). Recently, it was reported that *X. fastidiosa* is able to produce and release OMVs, leading to the hypothesis that OMV secretion is related to the capacity of *X. fastidiosa* to spread throughout the plant xylem (Ionescu *et al*., 2014). OMVs have been reported to carry virulence factors and toxins (Ellis and Kuehn, 2010; Altindis and Mekalanos, 2014), however, their role in pathogenicity is not completely understood (Schertzer and Whiteley, 2013; Kuehn and Kesty, 2005). OMVs are involved in the modulation of immune responses, the secretion of antibacterial compounds, the facilitation of bacterial spreading and protection from the environment surrounding the cell by preventing other cells from colonizing the same site (Ionescu *et al*., 2014; Kuipers *et al*., 2015; Olsen and Amano, 2015).

This work aimed to characterize the *orfs Xf2162* and *Xf2163* of *X. fastidiosa* strain 9a5c, which were classified in the *X. fastidiosa* database as a hypothetical protein and an HTH-type transcriptional regulator, respectively, and also identified as XF2490 and XF2491 according to the previous genome annotation. Using tools for sequence prediction, we identified these proteins based on homology. Then, functional and biochemical approaches were applied to characterize a type II XfMqsR/XfMqsA system. This work focused on XfMqsA, which was found to display a novel subcellular localization; this result suggests that XfMqsA performs an extracellular function.

2. EXPERIMENTAL PROCEDURES

2.1 Cloning, expression and purification–

The ORFs Xf2162 (303 bp; NCBI nº. AAF85288.1) and Xf2163 (402 bp; NCBI nº. AAF85289.1) were amplified from the genomic DNA of *X. fastidiosa* using the following specific primers: XfMqsA: forward, CAAGGACATATGACCATGAGATGTCC, and reverse, ACGGCTCGAGACTCTTCACTTCG; XfMqsR: forward, ATGGCATATGGAGAAAGGCAC, and reverse, GGACATCTCGAGGTCATAACTCC. The forward primer contained an *Nde*I restriction site, and the reverse primer contained a

*Xho*I restriction site. After digestion, XfMqsA was cloned into pET29a, and the toxin was cloned into pET28a; then, they were inserted into competent C43 (DE3) cells.

Protein expression was induced via the addition of lactose at a final concentration of 5.6 mmol.L^{-1} after the OD_{600} reached 0.6 for XfMqsA and 1.0 for XfMqsR, and the cells were grown at 37ºC with shaking at 250 rpm. Then, the temperature was reduced to 25ºC, and the cells were grown with shaking at 250 rpm for 12 h. The cells were centrifuged, and the pellet was stored at -20ºC.

To accomplish protein purification via affinity chromatography using a nickel-nitrilotriacetic acid (Ni-NTA) column, the pellet was suspended in phosphate buffer (25 mmol.L^{-1} sodium phosphate (pH 7.8), 150 mmol.L^{-1} NaCl, and 20 mmol.L^{-1} β-mercaptoethanol). The cells were disrupted via sonication for 8 cycles of 1 min of sonication and 5 min of rest (Cole Parmer Ultrasonic Homogenizer 4710). The supernatant was loaded by gravity in the Ni-NTA resin column, and the protein was eluted using an imidazole gradient as follows: the toxin and antitoxin were eluted with imidazole at concentrations of 50 mmol.L^{-1} and 100 mmol.L^{-1}, respectively. Both proteins were separated from contaminants using a Superdex 200 10/300 (GE Healthcare) gel filtration column as described below.

2.2 – Analytical size-exclusion chromatography –

Analytical size-exclusion chromatography was used to determine the oligomeric conformations of both proteins. A Superdex 200 10/300 pre-packed column (GE LifeScience) was used at a flow rate of 0.4 mL/min. After equilibration with sodium phosphate buffer, 7 μmol.L^{-1} of each protein was applied and detected using a UV-VIS flow cell at 280 nm. To obtain the XfMqsR-XfMqsA complex, the proteins were mixed at concentrations of 7 μmol.L^{-1} each and incubated for 12 h at 25ºC; then, they were applied at a 1:1 ratio under the same conditions described above.

2.3 – Circular dichroism and thermal unfolding –

The fractions corresponding to the proteins were dialyzed in sodium phosphate buffer (10 mmol.L^{-1} sodium phosphate (pH 7.8) and 1 mmol.L^{-1} tris(2-carboxyethyl)phosphine (TCEP). The far-UV circular dichroism (CD) spectra of recombinant XfMqsR and XfMqsA were measured using a JASCO J-810 spectropolarimeter (dichrograph; Japan Spectroscopic; Japan). The assays were performed in a quartz cuvette with a path length of 1 mm, and 10 measurements were recorded at 222 nm at a rate of 50 nm.min^{-1} at 25°C for the toxin and the antitoxin at concentrations of 21 and 20 μmol.L^{-1}, respectively.

Each protein was unfolded separately at a concentration of 10 μmol.L^{-1} to obtain the melting temperature (Tm). Then, the proteins were mixed and incubated for 12 hours at 25°C to enable their interaction. Both proteins were subjected to the same experimental conditions. The temperature was adjusted from 20ºC to up to 90°C, with an increase of 1°C per minute, followed by a decrease of 1°C per minute until the temperature reached 20°C.

2.4 – Isothermal calorimetry – ITC

The heterologous proteins obtained via affinity chromatography in the Ni-NTA column and via size exclusion chromatography were dialyzed in sodium phosphate buffer (25 mmol.L^{-1} sodium phosphate (pH 7.8), 150 mmol.L^{-1} NaCl, and 0.3 mmol.L^{-1} TCEP) for 16 hours at 25ºC.

An Auto iTC 200 calorimeter (MicroCal, Northampton, MA, USA) was used to determine the binding constant and heat of the interaction. XfMqsR was used as the titrant at a concentration of 100 μmol.L^{-1}, and XfMqsA was used as the titrand in the cell at a concentration of 10 μmol.L^{-1}. Thirty-three injections containing 1 μL of XfMqsR were titrated at 25°C under 1000 rpm with 300 s intervals between each injection.

The obtained heat signals from the raw ITC data were integrated using Origin software (MicroCal, Inc.). The heat from the reference buffer and the titrant, which is the heat due to the diffusion of the protein in the buffer, was subtracted to calculate the corrected heat release. A single-site binding isotherm model was used to match the data and to assess the dissociation affinity (K_d), enthalpy (ΔH), entropy (ΔS), and the binding stoichiometry (N).

2.5 – Electrophoretic mobility shift assay (EMSA) –

Two DNA fragments from the region upstream of the promoter were tested. This region consisted of 216 bp and was divided into two fragments. The first was 113 bp in length and was amplified using the primers AGCTTGGGGGGACTCACC and CCTGAGACGACGTTATCAGAACC (forward and reverse, respectively), and the second was 126 bp in length and was amplified using the primers GGTTCTGATAACGTCGTTCTCAGG and CTCCATGCACCATTTTAACTTATTAGG (forward and reverse, respectively). The latter sequence corresponds to position -210 to -97, and the former sequence corresponds to the region from position -120 to the initial ATG. To assess the interaction between XfMqsA and these DNA fragments, 100 ng of each fragment were mixed with increasing concentrations of XfMqsA in its dimeric form at the following

ratios of DNA:XfMqsA: 1:0; 1:1; 1:2; 1:5; 1:10; 1:20 and 1:50. The mixtures were incubated for 2 hours at 25ºC and then applied to a 2% agarose gel at 40 V for 4 hours.

2.6 – RNase activity essay –

The RNAseAlert Kit (Invitrogen, Carlsbad, CA, USA) was used to investigate whether XfMqsR possesses RNAse activity. The reactions were performed in a 96-well flat-bottom plates in a total volume of 50 µL. A total of 5 µmol.L-1 of each heterologous protein were mixed with 5 µL of fluorescent substrate and 5 µL of 10X RNaseAlert lab test buffer. After adding the protein, the plate was immediately placed in the fluorometer (2300 EnSpire Multimode Plate Reader, Perkin-Elmer). The reactions were monitored for 200 min using excitation/emission wavelengths of 490/520 nm. The proteins were solubilized in buffer containing 25 mmol.L^{-1} (pH 7.8) phosphate and 150 mmol.L^{-1} NaCl. RNAse A was used as a positive control according to the manufacturer's instructions.

Additionally, RNAse activity was visualized in an agarose gel. Increasing concentrations of XfMqsR were mixed with 800 ng of total RNA from *X. fastidiosa* and incubated for 30 min at 25°C; then, the RNA was applied to a 1% denaturing agarose gel at 80 V for 2 h.

2.7 – Protein expression based on Western blot

X. fastidiosa cells were inoculated in 50 mL of periwinkle wilt GelRite or PWG broth (0.4% w/v phytone peptone, 0.1% w/v trypticase peptone, 7.35 mM KH_2PO_4, 6.89 mM K_2HPO_4, 1.62 mM $MgSO_4$, 0.001% w/v hemin chloride, 0.002% g/L phenol red, and 0.4% w/v glutamine, pH 6.8) at an initial OD_{600} of 0.3, at 150 rpm and 25°C. The cells were collected 3, 5, 10, 15, 20 or 30 days after inoculation. Total protein samples were extracted via sonication in buffer (50 mmol.L^{-1} sodium phosphate, 300 mmol.L^{-1} NaCl, 0.2% Tween-20, 20 mmol.L^{-1} β-mercaptoethanol and 3 mmol.L^{-1} EDTA). We used the Ultrasonic Homogenizer 4710 Series (Cole Parmer) set at a potency of 70% for four rounds of sonication of 20 sec each.

The extracts were quantified using the Pierce BCA Protein Assay Kit (Rockford, IL, USA) according to the manufacturer's instructions. Then, 5 µg of total protein were applied to a 13.5% SDS-PAGE gel. After migration, the proteins were transferred to a nitrocellulose membrane using a Trans-Blot SD Semi-Dry apparatus (Bio-Rad) with constant voltage of 25 V for 20 min. Then, the membrane was blocked with 5% BSA for 8 h in TTBS buffer (0.1% Tween-20, 136 mmol.L^{-1} NaCl, 2.6 mmol.L^{-1} KCl, and 25 mmol.L^{-1} Tris, pH

7.5). The solution was replaced with primary antibody obtained from serum from a rabbit immunized with the heterologous protein (1:4000 for the toxin and 1:1000 for the antitoxin), and the membrane was incubated overnight. Then, the secondary antibody (peroxidase-conjugated anti-rabbit IgG, 1:20,000) was applied for 4 h. Subsequently, the membrane was incubated in electrochemiluminescence (ECL) detection reagent (1:1 ratio of A:B; GE Healthcare), wrapped in thin plastic and placed in the BAS 2325 Cassette (Fujifilm). Hyperfilm ECL (GE Healthcare) was allowed to absorb the chemiluminescence for 30 sec in a dark room prior to insertion of the film into the RP X-OMAT M6B developer (Kodak).

The band intensities were calculated using the GS-800 calibrated densitometer (Bio-Rad). The X-ray films were scanned under a green filter at 600 dpi. Quantity One 4.6.3 software (Bio-Rad) was utilized to quantify the Western blots.

2.8 – Detection of XfMqsA in the culture supernatant

X. fastidiosa was inoculated in 50 mL of PWG broth. The cells were collected on days 3, 5 10, 20 and 30 based on previous studies of biofilm development (Caserta *et al*., 2010). The media were centrifuged at 4000 rpm to precipitate the cells. Then, the supernatants were filtered with 0.22 μm membranes to completely remove the bacteria. The supernatant was lyophilized and suspended in 4 mL of water. An aliquot of 1 mL was treated with 100 $mmol.L^{-1}$ dithiothreitol for 1 h and 300 $mmol.L^{-1}$ iodoacetamide for 30 minutes. Then, 75 ng of trypsin was added to accomplish digestion *in solution*.

The peptides were chromatographically separated in a nanoAcquity UPLC (WATERS) in two columns in line with a Q-TOF-Micro mass spectrometer (Micromass). The first column (referred to as the trapping column) was 5 μm x 180 μm x 20 mm, and the second column was 1.7 μm x 100 μm x 100 mm; the samples were eluted at a flow rate of 0.6 μL/min for 50 min. An acetonitrile gradient was set up as follows: initial elution with 1% v/v acetonitrile for 1 min, increasing from 1% to 50% until 40 min, increasing from 50 to 85% until 45 min, maintaining at 85% for 2 min and then decreasing to 1% until completion at 50 min.

The peptides were ionized at 3000 V and fragmented using collision energy ranging from 20 to 95 eV according to the m/z and the size of the peptides, considering a charge state ranging from 2+ to 4+.

The spectra for the fragmentation patterns were analyzed using ProteinLynx Global Server 2.4 software (WATERS). The peptide sequences were compared with the

SwissProt database for tryptic digestion considering missed cleavage at up to one site and a maximal error of 30 ppm.

2.9 – OMV sedimentation and protein extraction

Vesicle separation was accomplished based on the method of Voegel (Voegel *et al* 2010). The bacteria were centrifuged; then, the supernatant was recovered and filtered with a 0.22 μm membrane. The supernatant was centrifuged at 100,000 x g for 4 hours (L8-80M Ultracentrifuge, Beckman) and the pellet was washed twice with water, centrifugued at 100,000 g for 2 hours to remove extracellular proteins. The precipitate was treated with lysozyme for 10 minutes, suspended in 150 μL of Laemmli buffer (0.1% β-mercaptoethanol, 0.0005% Bromophenol blue, 10% glycerol, 2% SDS, and 63 mmol.L^{-1} Tris-HCl, pH 6.8) and then sonicated 3 times for 5 seconds each using the Cole Parmer 4710 series ultrasonic homogenizer. The extract was subjected to SDS-PAGE and Western blot as described above using polyclonal antibodies against XfMqsA and XfMqsR.

3. RESULTS

3.1 – Identification of the proteins based on sequence similarity –

Initially, the XfMqsR and XfMqsA sequences were annotated as a conserved hypothetical protein and an HTH-type transcription regulator, respectively. Based on comparative analysis using the annotated proteins and alignment tools, we identified the proteins as components of a TA system homologous to a TA system in *E. coli* for which a structure determined by X-ray crystallography was available. The toxin shared up to 61% sequence similarity (Fig. 1A), and the antitoxin shared 42% sequence similarity (Fig. 1B).

Sequence alignment analysis using the primary sequences based on the models of the MqsR/MqsA system from *E.* coli showed that the XfMqsA sequence possesses two domains: a putative zinc-finger at the N-terminal CXXC (residues 3-6 and 37-40) and a well-conserved C-terminal XRE-HTH DNA-binding motif domain that encompasses domains α2,

α3, α4 and α5 (residues 74-127). These N- and C-terminal domains displayed 28% and 59% similarity with *E. coli*, respectively (Fig. 1B).

The most similar residues to XfMqsR were located in the β-sheet regions. Although RNAse activity was detected, the primary sequence did not display similarity to the RNAse domain. No domains in the toxin were predicted to be involved in RNAse activity or protein interaction.

3.2 – Cloning, expression and purification

After the analysis of the ORF sequences, XfMqsR was cloned into pET28a, and XfMqsA was cloned into pET29a. The former clone produced a 13.2 kDa His-tagged protein with a pI of 8.7, and the latter clone produced a 15.94 kDa His-tagged protein with a pI of 6.74. Positive colonies containing the respective inserts were selected, and the induced recombinant proteins were produced with stable conformations based on size-exclusion chromatography (Fig. 2A). The insertion of the His-tag into the C-terminal end of XfMqsA proceeding from the pET29a was critical for the suitable conformation of the N-terminus because when the protein was cloned into pET28a, including the His tag at the N-terminus disturbed the suitable conformation of the region containing the zinc finger, resulting in protein aggregation and precipitation as observed by size-exclusion chromatography (data not shown).

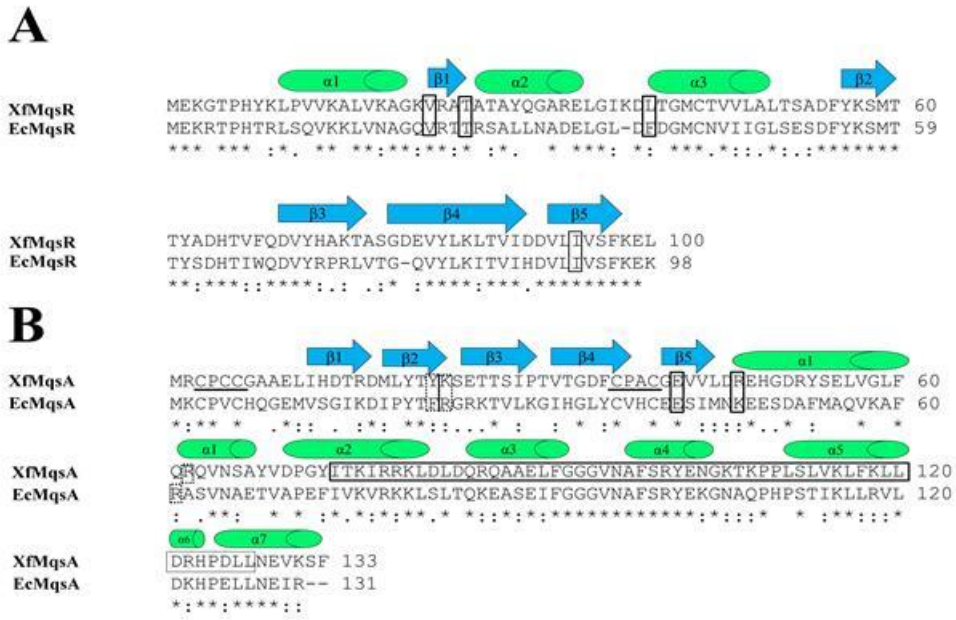

Fig. 1. Sequence alignment analysis and protein structure prediction of XfMqsR and XfMqsA. (A) The amino acid sequences of XfMqsR (NCBI Reference Sequence AAF85288.1) and the E. coli protein MqsR (GenBank ID Q46865.1) were aligned using the ClustalW2 server (http://www.ebi.ac.uk/Tools/msa/clustalw2/), revealing high identity (61%). Conservation between identical amino acid residues is indicated by an asterisk; residues with strongly similar properties are shown by a double-dot; and weakly similar properties are represented by a single dot. The residues involved in the protein-protein interaction that corresponded to *E. coli* protein residues are boxed. (B) The amino acid sequences of XfMqsA (NCBI Reference Sequence AAF85289.1) and the E. coli protein MqsA (GenBank ID CAQ33360.1) were aligned using the ClustalW2 server (http://www.ebi.ac.uk/Tools/msa/clustalw2/), revealing high identity (42%). Conservation between identical amino acid residues is indicated by an asterisk; residues with strongly similar properties are shown by a double-dot; and weakly similar properties are represented by a single dot. The two zinc finger motifs are underlined. The residues involved in the interaction with XfMqsR that corresponded to *E. coli* protein residues are placed in a dotted box. The residues involed in promoter recognition that corresponded to the *E. coli* protein and the HTH are placed in a solid box.

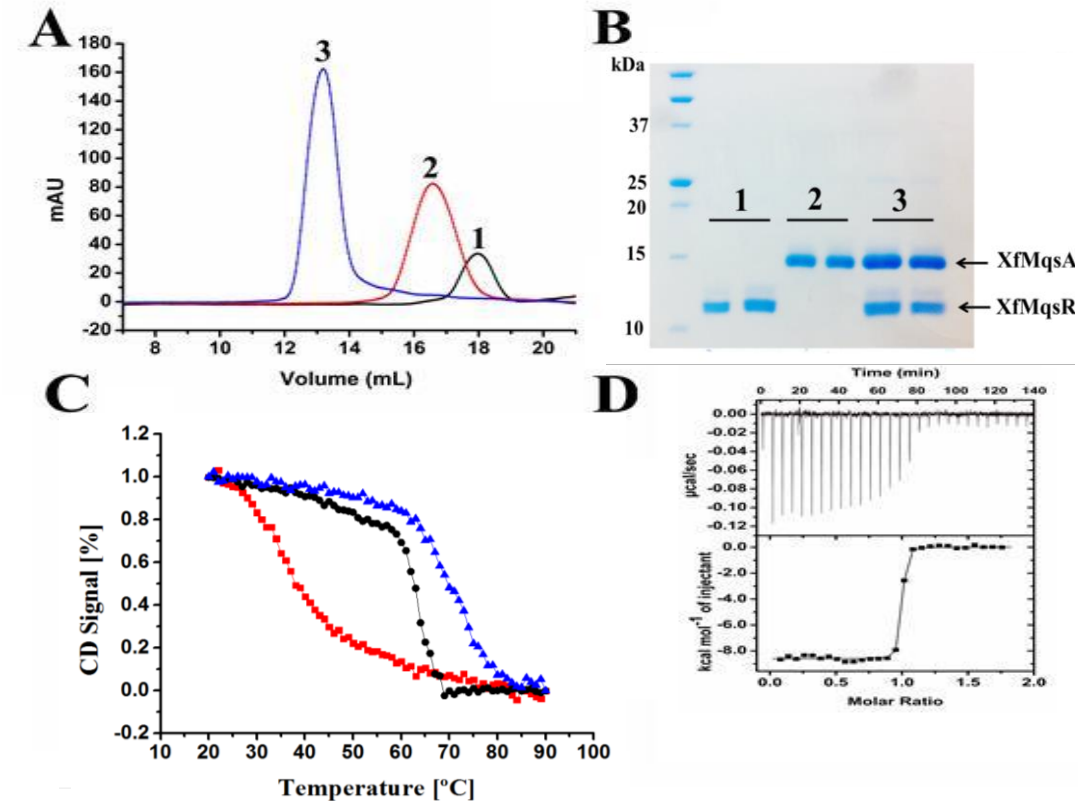

Fig. 2. Hydrodynamic properties of the interaction between XfMqsR and XfMqsA. (A) Chromatogram of the analytical size-exclusion chromatography experiments for the recombinant purified toxin and antitoxin.The toxin and the antitoxin are represented by the black and red lines, respectively, and the complex is represented by the blue line. (B) SDS-PAGE (15%) of the fractions eluted during the analytical size-exclusion chromatography experiment. XfMqsR was 13.1 kDa, and XfMqsA was 15.94 kDa. (C) Analysis of complex thermostability. The spectra at 222 nm represent the losses of protein structure with increasing temperature. The Tms obtained were 37ºC for the antitoxin, 62.5°C for the toxin and 70ºC for the complex. (D) Determination of the dissociation constant (Kd) of the interaction based on ITC. The characteristics of the interaction curve revealed a high-affinity thermodynamically favorable interaction at a protein molar ratio of 1:1; for this interaction, ΔH was -8609±36.51, and ΔS was 11.8 cal/mol/deg.

Both proteins were purified by the same two methods (affinity chromatography using the Ni-NTA column and size-exclusion chromatography) to remove undesirable proteins, resulting in high purity solutions. The proteins were present in the soluble phase and formed secondary structures based on circular dichroism (data not shown).

The purification of XfMqsA and XfMqsR resulted in yields of 10 mg/L and 0.4 mg/L, respectively. The low production per liter of XfMqsR may have occurred due to its RNAse activity, which results in slower cell growth to reach the desired OD_{600}. Our hypothesis is that the basal level of XfMqsR expression can delay the cell growth That was the reason why the cells were induced at high $O.D._{600}$. Therefore, a high amount of this protein inside the cells may be detrimental to further protein production.

3.3 – Interactions of these proteins based on size-exclusion chromatography

To confirm the formation of a stable complex *in vitro*, the heterologous proteins, which eluted as unique peaks via size-exclusion chromatography, were mixed at a 1:1 ratio (7 $\mu mol.L^{-1}$ each). This mixture was injected into the same pre-packed column. The detection of a fraction representing the complex demonstrated that the proteins were completely bound at a 1:1 ratio following incubation for 12 h, as no peak that represented the isolated proteins was observed (Fig. 2A). The peaks corresponding to the XfMqsA, XfMqsR and the complex eluted at retention volumes of 13.5 mL, 16 mL and 18 mL. When fitted to the calibration curve generated using protein standards, the apparent molecular weights obtained were 31.6 kDa for XfMqsA and 16.9 kDa for XfMqsR, which corresponded to dimeric and monomeric forms, respectively (data not shown). The proteins eluted at the peaks were separated via 15% SDS-PAGE (Fig. 2B), and the results confirmed that both XfMqsA and XfMqsR were present in the complex.

3.4 – Thermal stability analysis based on circular dichroism

Both proteins displayed absorption of polarized light at 222 nm, which was the wavelength chosen for the analysis of unfolding due to increasing temperature. XfMqsA showed a Tm of 37.8ºC and displayed a high capacity to recover its secondary structure, as approximately 86% of the protein that unfolded at 90 ºC was able to restore its α-helix structure when the temperature returned to 20ºC. XfMqsR displayed a high Tm (62.5ºC), but was not able to recover any of its secondary structure after unfolding at 90ºC. Surprisingly, the complex showed high thermostability, displaying a higher Tm (70.5ºC) than either protein alone, and was able to recover 50% of its secondary structure (Fig. 2C).

3.5 – Isothermal titration calorimetry (ITC)

After subtracting the heat provided by the buffer, we obtained the specific heat of the interaction at the molar ratio involved in complex formation. The interaction was characterized by strong binding due to a pronounced slope, revealing a nanomolar affinity (Fig. 5). After fitting, the ITC experiment revealed a dissociation constant of 0.785±0.241 $nmol.L^{-1}$ and a 1:1 stoichiometry. We found that ΔH was -8609±36.51 and that ΔS was 11.8 cal/mol/deg, indicating that complex formation is thermodynamically favorable (Fig. 2D).

3.6 – Shift assay

As demonstrated by the sequence comparison, XfMqsA possesses a XRE-HTH DNA-binding domain located between residues 74 and 127, which indicates its possible capacity for transcriptional regulation. Therefore, we investigated its ability to interact with its own promoter using an EMSA. The antitoxin has been documented to possess a regulatory capacity for its own promoter and for genes involved in oxidative stress (Hayes and Kedzierska, 2014; Brown *et al*., 2013). A DNA fragment was chosen as a negative control; this fragment was located farther from the initial ATG and encompassed positions -210 to -97 (Fig. 3A). The putative promoter consists of the region from position -120 to the initial ATG and encompasses putative motifs and regulatory sites (Fig. 3C). The absence of a nonspecific interaction was confirmed because there was no shift in the migration of the fragment (Fig. 3B). In contrast, the 126 bp fragment, which corresponds to the region closer to the initial ATG, was shifted following the addition of increasing amounts of protein. A weak interaction was observed at 1:2 and 1:5 DNA:protein molar ratios, and these interactions may be the result of a specific interaction. However, the greater shift with increasing molar ratios may have occurred due to nonspecific interactions between XfMqsA and other nucleotides outside the recognition motif (Fig. 3D).

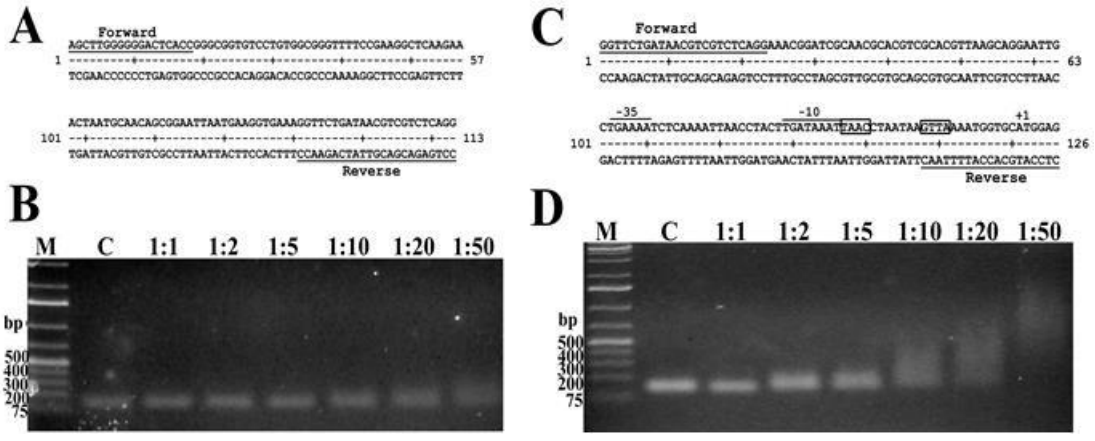

Fig. 3. Shift assay of the fragment correspondening to the negative control and the likely promoter. (A) Sequence of the 113 bp fragment that includes nucleotides -210 to -97. (B) Shift assay with increasing concentrations of antitoxin. (C) Sequence of the 126 bp fragment that includes nucleotides -120 to the initial ATG. (D) Shift assay with increasing concentrations of antitoxin.

3.7 – RNAse activity assay

After we confirmed the interaction between these proteins, quantitative analysis was applied to measure RNAse activity. To this end, the purified heterologous proteins were assessed using the RNAse Alert Kit. XfMqsR showed RNAse activity, but its activity was less than that of the positive control, RNAse A, because XfMqsR is sequence-specific and because RNAse A cleaves the phosphodiester bond between the 5'-ribose of a nucleotide and the phosphate group attached to the 3'-ribose of an adjacent pyrimidine nucleotide. XfMqsA was able to inhibit the XfMqsR activity, as the relative fluorescence released when both proteins were present was lower than that emitted in the presence of XfMqsR alone. There was no RNAse contamination, as no fluorescence was released from the negative control (Fig. 4A). The RNAse activity was also visualized in an agarose gel, in which the bands corresponding to the 23S, 16S and small RNAs (sRNA) were completely digested by XfMqsR (Fig. 4B).

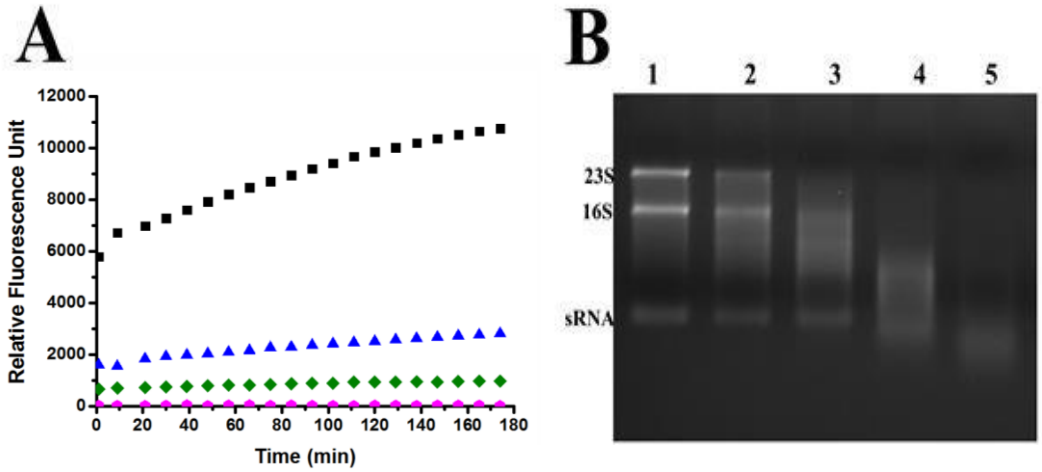

Fig. 4. Assessment of the RNAse activity of the toxin. (A)Fluorimetric measurement of toxin activity and its inibition by the antitoxin. The pink line represents the negative control, and the green line represents toxin inhibition by the antitoxin. The blue line represents toxin activity, and the black line represents the activity of the positive control RNAse A. (B) Visualization of digested RNA in a 1% denaturing agarose gel in the presence of increasing concentrations of XfMqsR. Lane 1, 800 ng of total RNA without XfMqsR. Lane 2, 800 ng of total RNA with 1 μmol.L^{-1} XfMqsR. Lane 3, 800 ng of total RNA with 2 μmol.L^{-1} XfMqsR. Lane 4, 800 ng of total RNA with 5 μmol.L^{-1} XfMqsR; Lane 5, 800 ng of total RNA with 10 μmol.L^{-1} XfMqsR.

3.8 – TA system protein expression levels are altered during X. fastidiosa *growth*

After confirmation of their capacity to interact and form a complex, we analyzed the expression profiles of XfMqsR and XfMqsA during the growth phases of *X. fastidiosa* strain 9a5c via western blot using polyclonal antibodies. The cells in both the planktonic and biofilm phases were analyzed because cells in these two phases were previously demonstrated to exhibit different expression patterns associated with *X. fastidiosa* development (Muranaka *et al.* 2012).

Alterations in the levels of these proteins were observed during the planktonic phase, detected as a variation on the 10th day: the antitoxin level was undetectable, whereas the toxin was detected. On the 15th day, the antitoxin level was very low, and the toxin was detected at an approximately 4-fold increased concentration. During the biofilm phase, reduced levels of the toxin and the antitoxin were detected on day 5 (Fig. 5). In fact, the lowest levels of toxin and antitoxin expression were detected on the 5th day, and the difference in protein expression was not significant at the other time points.

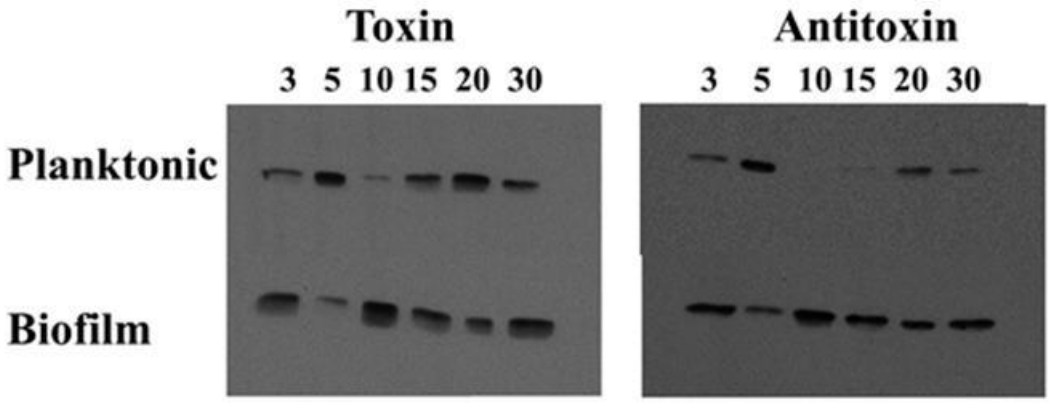

Fig. 5. Immunodetection of the toxin and the antitoxin in *X. fastidiosa* during the planktonic and biofilm growth phases. The expression of both proteins was evaluated on the 3rd, 5th, 10th, 15th, 20th and 30th days, which represent the phases of *X. fastidiosa* growth. The cells were collected, and the planktonic and biofilm phases were separated. The total proteins were quantified using the BCA method, and the Western blots were peformed using polyclonal antibodies.

3.9 – Detection of XfMqsA via MS/MS and Western blot

To examine the possibility that XfMqsR and XfMqsA are secreted into the extracellular medium, we investigated extracellular proteins and proteins inside OMVs. After isolating the OMVs via ultracentrifugation, the assessment was performed using MS/MS. One intriguing result was the presence of four peptides from the OMVs set that matched to Xf2163, which corresponds to the antitoxin from strain 9a5c. The peptide sequences are provided in Table 1. To confirm the presence of the antitoxin in OMVs, the fraction corresponding to the extracellular proteins and OMVs was subjected to SDS-PAGE. The band corresponding to XfMqsA (15 kDa) was identified via Western blot on the 10th, 20th and 30th days (Fig. 6A) but was not detected in the extracellular medium (Fig. 6B). Moreover, no band corresponding to XfMqsR was detected in either the OMVs or the extracellular media (Fig. 6C and 6D).

Table 1. Peptides identified by MS/MS that matched to antitoxin from *Xylella fastidiosa*.

Peptides	*m/z*	Mass Weight (Da)	Charge
CPCCGAAELIHDTR	553.9035	1658.6963	+2
YSELVGLFQR	606.3224	1210.6346	+2
QVNSAYVDPGYITK	777.8915	1553.7726	+2
KLDLDQR	444.2489	886.4872	+2
XfMqsA sequence MRCPCCGAAELIHDTRDMLYTYKSETTSIPTVTGDFCPACGEVVLDREHGDRYSELV GLFQRQVNSAYVDPGYITKIRRKLDLDQRQAAELFGGGVNAFSRYENGKTKPPLSLV KLFKLLDRHPDLLNEVKSF			

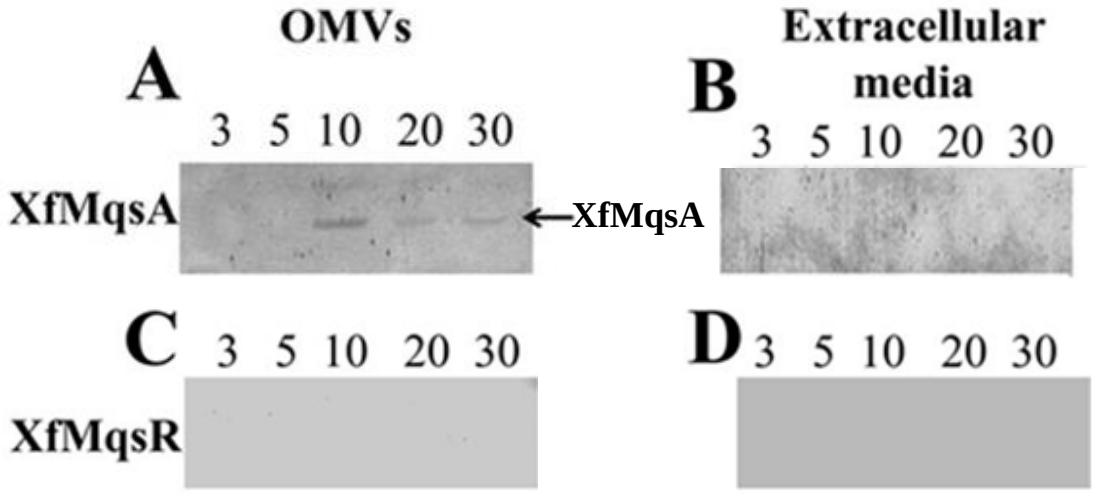

Fig. 6. Immunodetection of XfMqsA and XfMqsR in outer membrane vesicles from *X. fastidiosa* strain 9a5c. (A) The expression of XfMqsA within vesicles from the 3rd, 5th, 10th, 20th and 30th days was evaluated using a polyclonal anti-XfMqsA antibody. The extracellular media were passed through a 0.22 μm filter, and the pellets were collected for Western blot using a polyclonal antibody against XfMqsA. (B) Western blot of the extracellular media for XfMqsA. (C) The expression of XfMqsR within the vesicles from the 3rd, 5th, 10th, 20th and 30th days was evaluated using a polyclonal anti-XfMqsR antibody. The extracellular media were passed through a 0.22 μm filter, and the pellets were collected for Western blot using a polyclonal antibody against XfMqsR. (D) Western blot of the extracellular media for XfMqsR.

4 - DISCUSSION

Studies on the TA system have raised many inquiries regarding its functions. TA systems are widely distributed in bacteria and archaea (Park *et al*., 2013). Bacterial pathogenicity has been proposed to be directly proportional to the number of TA systems in the genome compared with the genomes of non-epidemic-related species (Georgiades and Raoult, 2011). Several studies have demonstrated the participation of the TA system in biofilm formation (Fasani and Savageau, 2013, van Acker *et al*., 2014; Wen *et al*., 2014). Our work provides a detailed characterization of a TA system from *X. fastidiosa* strain 9a5c and indicates the presence of XfMqsA within OMVs, which has not previously been reported.

The ORFs identified in this study were classified as a hypothetical protein (XfMqsR) and an HTH-type transcriptional regulator (XfMqsA) in the *X. fastidiosa* database. Our result demonstrated that XfMqsR and XfMqsA are homologous to MqsR and MqsA from *E. coli*, respectively. The formation of the TA complex was thermodynamically favorable and displayed a high dissociation constant. XfMqsA was able to hinder the RNA activity of its

cognate protein, and both proteins were differentially expressed at high levels during the biofilm phase. Moreover, XfMqsA was detected inside OMVs, as confirmed by Western blot.

Although the XfMqsR amino acid sequence did not include any detectable domains, it displayed activity that was similar to its *E. coli* homolog. This activity was primarily localized to the β-sheet regions and involved RNAse activity, although the primary sequence did not display similarity to other RNAse domains. In *E. coli,* MqsR specifically cleaves mRNAs, primarily at 5′-G▲CU and G▲CC sites (Wang *et al*., 2012; Christensen-Dalsgaard *et al*., 2010).

Although XfMqsA exhibits lower similarity than the toxin, XfMqsA possesses conserved domains related to its interaction with its promoter and the toxin. The residues Asn97 and Arg101, which are conserved in *E. coli* and *X. fastidiosa* (Fig. 1B), are involved in promoter recognition. Additionally, the residues containing the HTH-domain share 59% similarity with the corresponding region in *E. coli*. According to previous report (Brown *et al*., 2011), the antitoxin recognizes a palindromic region (TAACCT(N_3)AGGTTA); here, we identified a very similar palindrome (TAACCT(N3)AAGTTA) located between positions -24 and -9 that may serve as the antitoxin anchoring site. The conserved residues Asn97 and Arg101 are responsible for the recognition of eight nucleotides: 5’ TAAC 3’ in the forward strand and 5 ‘AGGT 3’ in the reverse strand (Wang and Wood, 2011).

Regarding to the interactions of the antitoxin with DNA, the antitoxin can regulate operon expression as well as the expression of genes related to oxidative stress (Wang and Wood, 2011; Kwan *et al*., 2014). An analysis based on homology with the target genes identified in *E. coli* (Wang and Wood, 2011) identified that the *rpoH* gene (a thermal stress response regulator) from *X. fastidiosa* contains a similar motif (AACCT(N3)CCGTT). However, this motif is located at position +39, which may indicate an alternative mechanism of regulation because the motif is located within the ORF.

Based on the analysis of the shift assay in the presence of the TA system promoter, we detected a slight shift at molar ratios of 1:2 and 1:5, and this shift may be the result of specific ligation. The promoter fragment in complex with the MqsA dimer would migrate as an approximately 200 bp DNA fragment. This shift was observed at molar ratios of 1:2 and 1:5. We also observed shifted bands at higher molar ratios, although these bands may be a result of nonspecific binding because they continued to increase in size as the molar ratio increased (Fig. 3D).

Analysis of interaction with its own 26 bp promoter was (Brown *et al*., 2013) detected a clear migratory shift. In contrast, we examined a 126 bp fragment. The lack of

shifted bands in the negative control fragment indicates that XfMqsA recognizes specific motifs and possesses the ability to self-regulate. The *E. coli* antitoxin residues involved in promoter recognition are Phe22, Arg23 and Arg61; in *X. fastidiosa,* these residues are substituted for the chemically similar residues Tyr22, Lys23 and Arg62, respectively.

It has been demonstrated by X-ray crystallography that the amino acid residues Ser43 and Met45 in the antitoxin from *E. coli* form a salt bridge with residues Val 22 and Thr25 from the toxin, thereby contributing to the protein:protein interaction (Brown *et al*., 2013; Brown *et al*., 2009). However, Val, not Ser, is conserved at position 43 of XfMqsA from *X. fastidiosa* strain 9a5c. Other secondary interactions were observed. Other residues also conserved between the *E. coli* toxin and XfMqsR, including Arg26, Asp 33 and Asp 40 from toxin; these residues correspond to Ala26, Arg33 and Asp40 in XfMqsR. These residues of MqsR interact with Glu41, Arg61 and Lys47 from the *E. coli* antitoxin; at the same positions, we identified similar residues in XfMqsA (Gln 61 and Arg47); however, a Glu residue is located at position 62. Other residues involved in the TA interaction that were identical between *X. fastidiosa* and *E. coli* included Val22, Thr25 and Leu39 of XfMqsR (Fig. 1B) (Brown *et al*., 2009).

Analysis of the apparent molecular weight of the proteins in solution resulted in the detection of approximate molecular weights for the dimer of XfMqsA (31.6 kDa) and the monomer of XfMqsR (16.9 kDa). In *E. coli*, the TA interaction was demonstrated to occur at a 1:1 ratio, consisting of the antitoxin dimer and two toxin monomers (Brown *et al*., 2009). In this study, a 1:1 molar ratio was observed for the TA interaction (Fig. 2A). The interaction between these proteins is thermodynamically favorable and forms a very stable complex, as demonstrated by thermal circular dichroism and ITC. Thermostability analysis confirmed that it was necessary to add more heat to unfold the complex than that required to denature the isolated proteins, similar to the results reported for the *E. coli* TA system (Brown *et al*., 2013).

The oscillation in protein expression was related to the growth phases. The days displaying major differences in expression (10^{th} and 15^{th}) correspond to microcolony formation (10^{th}) and the development of the biofilm architecture (15^{th}) (Caserta *et al*., 2010). The overexpression of the toxin can lead to an increase in biofilm mass (Wang *et al*., 2011), which was supported by our observations. The expression of the TA system must be well balanced to enable optimal cell growth. Free toxin inside cells can lead to the generation of persister cells, which are associated with antibiotic resistance and increased biofilm formation (Lee *et al*., 2014; Muranaka *et al*., 2012). TA systems represent a barrier to the development of antimicrobial compounds to control or abolish bacterial growth (Park *et al*., 2013; Lioy *et*

al., 2010). The mechanism underlying this hypothesis is that an antimicrobial compound that impairs antitoxin regulation would hinder growth because the toxin would act until a "point of no return", resulting in cell death (Lioy *et al*., 2010). In addition, TA systems may have other relevant uses such as in antiviral therapy, in which the toxin MazF is used to induce eukaryotic cell death (Chono *et al*., 2011).

Based on the recent discoveries that plant colonization by *X. fastidiosa* is probably modulated by OMVs (Ionescu *et al*., 2014), we analyzed the likely relationship between the TA system and OMV formation. This analysis led us to an intriguing result from MS/MS protein analysis. We found that XfMqsA does not possess a leader sequence according to SignalP 4.1 software, suggesting that it is intracellular. However, its presence in the extracellular media, which was detected by mass spectrometry, led us to hypothesize that it is secreted by vesicles; this hypothesis was confirmed by *western blotting* as seen in the figure 6. That is not the first time that a protein predicted to be intracellular was found to be associated with OMV formation. Other researchers have discovered proteins related to glycolysis and even transcription factors inside OMVs (Chen *et al*., 2014; Altindis *et al*., 2014; Choi *et al*., 2014).

The molecular mechanisms underlying vesicle formation and the mechanisms by which proteins become enveloped during vesicle formation remain unclear. Many suppositions have been made concerning OMV formation and their likely functions (i.e., modulating the microbial environment to kill competing species, signaling likely sites of nodulation for biofilm formation and modulating the immune response system in host cells (Choi *et al*., 2014, Turner *et al*., 2015; Perez-Cruz *et al*., 2015; Schwechheimer *et al*., 2014). This study is the first to report the presence of XfMqsA within OMVs. Although further studies are necessary, we hypothesize that the release of this antitoxin into the extracellular media can result in excess intracellular toxin accumulation, thereby producing favorable conditions for biofilm formation and persister cell generation, consequently inducing pathogenicity, since the biofilm formation is the mais pathogenicity mechanism for *Xylella fastidiosa* (Souza *et al*., 2004) .

X. fastidiosa is one of the most important phytopathogens investigated, and the elucidation of its mechanisms of infection is crucial for the control of disease (Mansfield *et al*., 2012). One factor that has limited our knowledge is the inability to obtain cells in which specific genes are knocked out. This work characterized a toxin and an antitoxin from *X. fastidiosa* strain 9a5c (termed XfMqsR and XfMqsA, respectively) based on heterologous expression and Western blot, which provided interesting results. We expect our results will

contribute to the understanding of proteins that participate in biofilm formation and other functions, as XfMqsA is present in OMVs.

Acknowledgments

This study was supported by grants from the Fundação de Amparo à Pesquisa do Estado de São Paulo (FAPESP, Process 2012/51580-4 and 2001/07533-7) and Coordenação de Aperfeiçoamento de Pessoal de Nível Superior (CAPES, Computational Biology Program). A.S.S. is the recipient of a Ph.D. fellowship from FAPESP (Process 2011/50268-4); CAS is the recipient of a post-doctoral fellowship and A.P.S. is the recipient of a research fellowship from the Conselho Nacional de Desenvolvimento Científico e Tecnológico (CNPq). A.A.S and A.P.S. are the recipient of a research fellowship from the Conselho Nacional de Desenvolvimento Científico e Tecnológico (CNPq). We gratefully acknowledge the Laboratório de Espectroscopia e Calorimetria (LEC) and Laboratório Nacional de Biociências – LNBio (Campinas, Brazil) for their support with the circular dichroism assays and the staff of the Life Sciences Core Facility (LaCTAD) from State University of Campinas (UNICAMP), for the isothermal calorimetry analysis".

REFERENCES

Altindis, E., Fu, Y. and Mekalanos, J. J. (2014) Proteomic analysis of *Vibrio cholerae* outer membrane vesicles. Proceedings of the National Academy of Sciences of the United States of America, **111**, 1548-1556.

Arenas, J. Cano, S., Nijland, R., van Dongen, V., Rutten, L., van der Ende, A. and Tommassen, J. (2015) The meningococcal autotransporter AutA is implicated in autoaggregation and biofilm formation. Environmental microbiology, **17**, 1321-1337.

Brantl, S. and Jahn, N. (2015) sRNAs in bacterial type I and type III toxin-antitoxin systems. FEMS Microbiology Reviews, **39**, 413-427.

Brown, B. L., Grigoriu, S., Kim, Y., Arruda, J. M., Davenport, A., Wood, T. K., Peti, W. and Page, R. (2009) Three dimensional structure of the MqsR:MqsA complex: a novel TA pair comprised of a toxin homologous to RelE and an antitoxin with unique properties. PLoS Pathogens, **5,** 1000706.

Brown, B. L., Lord, D. M., Grigoriu, S., Peti, W. and Page, R. (2013) The *Escherichia coli* toxin MqsR destabilizes the transcriptional repression complex formed between the antitoxin MqsA and the mqsRA operon promoter. The Journal of Biological Chemistry, **288**, 1286-1294.

Brown, B. L., Wood, T. K., Peti, W. and Page, R. (2011) Structure of the *Escherichia coli* antitoxin MqsA (YgiT/b3021) bound to its gene promoter reveals extensive domain rearrangements and the specificity of transcriptional regulation. The Journal of Biological Chemistry. **286**, 2285-2296.

Brzozowska, I. and Zielenkiewicz, U. (2013) Regulation of toxin-antitoxin systems by proteolysis. Plasmid, **70**, 33-41.

Caserta, R., Takita, M. A., Targon, M. L., Rosselli-Murai, L. K., de Souza, A. P., Peroni, L., Stach-Machado, D. R., Andrade, A., Labate, C. A. Kitajima, E. W., Machado, M. A. and de Souza, A. A. (2010) Expression of *Xylella fastidiosa* fimbrial and afimbrial proteins during biofilm formation. Applied and environmental microbiology, **76**, 4250-4259.

Chen, Y., Liu, L., Fu, H., Wei, C. and Jin, Q. (2014) Comparative proteomic analysis of outer membrane vesicles from *Shigella flexneri* under different culture conditions, Biochemical and biophysical research communications. **453,** 696-702.

Choi, C. W., Park, E.C., Yun, S.H., Lee, S.Y., Lee, Y.G., Hong, Y., Park, K.R., Kim, S.H., Kim, G.H. and Kim, S. I. (2014) Proteomic characterization of the outer membrane vesicle of *Pseudomonas putida* KT2440. Journal of Proteome Research, **13,** 4298-4309.

Chono, H., Matsumoto, K., Tsuda, H., Saito, N., Lee, K., Kim, S., Shibata, H., Ageyama, N., Terao, K., Yasutomi, Y., Mineno, J., Kim, S., Inouye, M. and Kato, I. (2011) Acquisition of HIV-1 resistance in T lymphocytes using an ACA-specific E. coli mRNA interferase. Human Gene Therapy, **22,** 35-43.

Chowdhury, C. and Jagannadham, M. V. (2013) Virulence factors are released in association with outer membrane vesicles of *Pseudomonas syringae* pv. tomato T1 during normal growth. Biochimica et Biophysica Acta (BBA) - Proteins and Proteomics, **1834**, 231-239.

Christensen-Dalsgaard, M., Jorgensen, M. G. and Gerdes, K. (2010) Three new RelE-homologous mRNA interferases of *Escherichia coli* differentially induced by environmental stresses. Molecular Microbiology, **75,** 333-348.

Cook, G. M., Robson, J. R., Frampton, R. A., McKenzie, J., Przybilski, R., Fineran, P. C. and Arcus, V. L. (2013) Ribonucleases in bacterial toxin-antitoxin systems. Biochimica et Biophysica Acta, **1829**, 523-531.

Domenech, M., Ruiz, S., Moscoso, M. and Garcia, E. (2015) Formation of *Streptococcus pneumoniae* choline-binding protein-DNA complexes in vitro. Implications for biofilm development. Environmental Microbiology Reports.

Ellis, T. N. and Kuehn, M. J. (2010) Virulence and immunomodulatory roles of bacterial outer membrane vesicles. Microbiology and molecular biology reviews : MMBR, **74**, 81-94.

Fasani, R. A. and Savageau, M. A. (2013) Molecular mechanisms of multiple toxin-antitoxin systems are coordinated to govern the persister phenotype. Proceedings of the National Academy of Sciences of the United States of America, **110,** 2528-2537.

Franch, T., Gultyaev, A. P. and Gerdes, K. (1997) Programmed cell death by hok/sok of plasmid R1: processing at the hok mRNA 3'-end triggers structural rearrangements that allow translation and antisense RNA binding. Journal of Molecular Biology, **273**, 38-51.

Georgiades, K. and Raoult, D. (2011) Genomes of the most dangerous epidemic bacteria have a virulence repertoire characterized by fewer genes but more toxin-antitoxin modules. PloS One, **6**, 17962.

Gerdes, K. and Maisonneuve E. (2012) Bacterial persistence and toxin-antitoxin loci. Annual Review of Microbiology, **66**, 103-123.

Gerdes, K. and Wagner, E. G. RNA antitoxins. (2007) Current Opinion in Microbiology, **10**, 117-124.

Germain, E., Roghanian, M., Gerdes, K. and Maisonneuve, E. (2015) Stochastic induction of persister cells by HipA through (p)ppGpp-mediated activation of mRNA endonucleases. Proceedings of the National Academy of Sciences of the United States of America. **112,** 5171-6

Hayes, F. and Kędzierska, B. (2014) Regulating toxin-antitoxin expression: controlled detonation of intracellular molecular timebombs. Toxins, **6**, 337-358.

Ionescu, M., Zaini, P. A., Baccari, C., Tran, S., da Silva, A. M. and Lindow, S. E. (2014) *Xylella fastidiosa* outer membrane vesicles modulate plant colonization by blocking attachment to surfaces. Proceedings of the National Academy of Sciences of the United States of America, **111,** 3910-3918.

Janissen, R., Murillo, D. M., Niza, B., Sahoo, P. K., Nobrega, M. M., Cesar, C. L., Temperini, M. L., Carvalho, H. F., de Souza, A. A. and Cotta, M. A. (2015)Spatiotemporal distribution of different extracellular polymeric substances and filamentation mediate *Xylella fastidiosa* adhesion and biofilm formation. Scientific Reports, **5**, 9856.

Kim, J. H., Lee, J., Park, J. and Gho, Y. S. Gram-negative and Gram-positive bacterial extracellular vesicles. Seminars in Cell & Developmental Biology, **40**, (2015) 97-104.

Kouzel, N., Oldewurtel, E. R. and Maier, B. (2015) Gene transfer efficiency in gonococcal biofilms: role of biofilm age, and architecture, and pilin antigenic variation. Journal of Bacteriology, **197,** 2422-31.

Kuehn, M. J. and Kesty, N. C. (2005) Bacterial outer membrane vesicles and the host-pathogen interaction. Genes & Development, **19,** 2645-2655.

Kuipers, K., Daleke-Schermerhorn, M. H., Jong, W. S., Ten Hagen-Jongman, C. M., van Opzeeland, F., Simonetti, E., Luirink, J. and de Jonge, M. I. (2015) Salmonella outer membrane vesicles displaying high densities of pneumococcal antigen at the surface offer protection against colonization. Vaccine, **33**, 2022-2029.

Kwan, B. W., Lord, D. M., Peti, W., Page, R., Benedik, M. J. and Wood, T. K. (2014) The MqsR/MqsA toxin/antitoxin system protects *Escherichia coli* during bile acid stress. Environmental Microbiology.

Lee, M. W., Tan, C. C., Rogers, E. E. and Stenger, D. C. (2014) Toxin-antitoxin systems mqsR/ygiT and dinJ/relE of *Xylella fastidiosa.* Physiological and Molecular Plant Pathology, **87**, 59-68.

Lioy, V. S., Rey, O., Balsa, D., Pellicer, T. and Alonso, J. C. (2010) A toxin-antitoxin module as a target for antimicrobial development. Plasmid, **63,** 31-39.

Lord, D. M., Uzgoren Baran, A., Soo, V. W., Wood, T. K., Peti, W. and Page, R. (2014) McbR/YncC: implications for the mechanism of ligand and DNA binding by a bacterial GntR transcriptional regulator involved in biofilm formation. Biochemistry, **53**, 7223-7231.

Mansfield, J., Genin, S., Magori, S., Citovsky, V., Sriariyanum, M., Ronald, P., Dow, M., Verdier, V., Beer, S.V., Machado, M. A., Toth, I., Salmond, G. and Foster, G. D. (2012) Top 10 plant pathogenic bacteria in molecular plant pathology. Molecular plant pathology, **13,** 614-629.

Muranaka, L. S., Takita, M.A., Olivato, J. C., Kishi, L.T. and de Souza, A. A. (2012) Global expression profile of biofilm resistance to antimicrobial compounds in the plant-pathogenic bacterium *Xylella fastidiosa* reveals evidence of persister cells. Journal of Bacteriology, **194**, 4561-4569.

O'Leary, D., McCabe, E. M., McCusker, M. P., Martins, M., Fanning, S. and Duffy, G. (2015) Acid environments affect biofilm formation and gene expression in isolates of *Salmonella enterica* Typhimurium DT104. International Journal of Food Microbiology, **206**. 7-16.

Olsen, I. and Amano, A. (2015) Outer membrane vesicles - offensive weapons or good Samaritans?, Journal of Oral Microbiology. **7,** 27468**.**

Park, S. J., Son, W. S. and Lee, B. J. (2013) Structural overview of toxin-antitoxin systems in infectious bacteria: a target for developing antimicrobial agents. Biochimica et Biophysica Acta, **1834**, 1155-1167.

Park, S. J., Son, W. S. and Lee, B. J. (2013) Structural overview of toxin-antitoxin systems in infectious bacteria: a target for developing antimicrobial agents. Biochimica et biophysica acta, **1834**, 1155-1167.

Perez-Cruz, C., Delgado, L., Lopez-Iglesias, C. and Mercade, E. (2015) Outer-inner membrane vesicles naturally secreted by gram-negative pathogenic bacteria, PloS One, **10,** 0116896.

Rodrigues, C. M., de Souza, A. A., Takita, M. A., Kishi, L. T. and Machado, M. A. (2013) RNA-Seq analysis of *Citrus reticulata* in the early stages of *Xylella fastidiosa* infection reveals auxin-related genes as a defense response. BMC Genomics, **14,** 676.

Ruhl, S., Eidt, A., Melzl, H., Reischl, U. and Cisar, J. O. (2014) Probing of microbial biofilm communities for coadhesion partners. Applied and environmental microbiology, **80**, 6583-6590.

Schertzer, J. W. and Whiteley, M. (2013) Bacterial outer membrane vesicles in trafficking, communication and the host-pathogen interaction. Journal of Molecular Microbiology and Biotechnology, **23**, 118-130.

Schwechheimer, C., Kulp, A., Kuehn, **M. J.** (2014) Modulation of bacterial outer membrane vesicle production by envelope structure and content, BMC microbiology, **14**, 324.

Simpson, A. J., Reinach, F. C., Arruda, P., Abreu, F. A., Acencio, M., Alvarenga, R., Alves, L. M., Araya, J. E., Baia, G. S., Baptista, C. S., Barros, M. H., Bonaccorsi, E. D., Bordin, S., Bové, J. M., Briones, M. R., Bueno, M. R., Camargo, A. A., Camargo, L. E., Carraro, D. M., Carrer, H., Colauto, N. B., Colombo, C., Costa, F. F., Costa, M. C., Costa-Neto, C. M., Coutinho, L. L., Cristofani, M., Dias-Neto, E., Docena, C., El-Dorry, H., Facincani, A. P., Ferreira, A. J., Ferreira, V. C., Ferro, J. A., Fraga, J. S., França, S. C., Franco, M. C., Frohme, M., Furlan, L. R., Garnier,

M., Goldman, G. H., Goldman, M. H., Gomes, S. L., Gruber, A., Ho, P. L., Hoheisel, J. D., Junqueira, M. L., Kemper, E. L., Kitajima, J. P., Krieger, J. E., Kuramae, E. E., Laigret, F., Lambais, M. R., Leite, L. C., Lemos, E. G., Lemos, M. V., Lopes, S. A., Lopes, C. R., Machado, J. A., Machado, M. A., Madeira, A. M., Madeira, H. M., Marino, C. L., Marques, M. V., Martins, E. A., Martins, E. M., Matsukuma, A. Y., Menck, C. F., Miracca, E. C., Miyaki, C. Y., Monteriro-Vitorello, C. B., Moon, D. H., Nagai, M. A, Nascimento, A. L., Netto, L. E., Nhani, A. Jr., Nobrega, F. G., Nunes, L. R., Oliveira, M. A., de Oliveira, M. C., de Oliveira, R. C., Palmieri, D. A., Paris, A., Peixoto, B. R., Pereira, G. A., Pereira, H. A. Jr., Pesquero, J. B., Quaggio, R. B., Roberto, P. G., Rodrigues, V., de M. Rosa, A. J., de Rosa, V. E. Jr., de Sá, R. G., Santelli, R. V., Sawasaki, H. E., da Silva, A. C., da Silva, A. M., da Silva, F. R., da Silva, W. A. Jr., da Silveira, J. F., Silvestri, M. L., Siqueira, W. J., de Souza, A. A., de Souza, A. P., Terenzi, M. F., Truffi, D., Tsai, S. M., Tsuhako, M. H., Vallada, H., Van Sluys, M. A., Verjovski-Almeida, S., Vettore, A. L., Zago, M. A., Zatz, M., Meidanis, J. and Setubal, J. C. (2000) The genome sequence of the plant pathogen *Xylella fastidiosa*. The *Xylella fastidiosa* Consortium of the Organization for Nucleotide Sequencing and Analysis. Nature, **406,** 151-159.

Souza, a. A.; Takita, Marco Aurélio; Coletta Filho, Helvécio Della; Caldana, Camila; Yanai, G. M; Muto, N. H; Oliveira, Regina Costa de; Nunes, Luiz R; Machado, Marcos Antonio. Gene expression profile of the plant pathogen Xylella fastidiosa during biofilm formation in vitro. FEMS Microbiology Letters, EUA, v. 237, p. 341-353, 2004.

Turner, L. Praszkier, J., Hutton, M. L., Steer, D., Ramm, G., Kaparakis-Liaskos, M. and Ferrero, R. L. (2015) Increased Outer Membrane Vesicle Formation in a Helicobacter pylori tolB Mutant. Helicobacter.

van Acker, H., Sass, A., Dhondt, I., Nelis, H. J. and Coenye, T. (2014) Involvement of toxin-antitoxin modules in *Burkholderia cenocepacia* biofilm persistence. Pathogens and Disease, **71,** 326-335.

Voegel, T. M., Warren, J. G., Matsumoto, A. Igo, M. M. and Kirkpatrick, B. C. (2010) Localization and characterization of *Xylella fastidiosa* haemagglutinin adhesins, Microbiology (Reading, England). **156,** 2172-2179.

Wang, X. and Wood, T. K. (2011) Toxin-antitoxin systems influence biofilm and persister cell formation and the general stress response. Applied and Environmental Microbiology. **77,** 5577-5583.

Wang, X., Kim, Y., Hong, S. H., Ma, Q., Brown, B. L., Pu, M., Tarone, A.M., Benedik, M. J., Peti, W., Page, R. and Wood, T. K. (2011) Antitoxin MqsA helps mediate the bacterial general stress response. Nature Chemical Biology, 7, 359-366.

Wang, X., Lord, D. M., Cheng, H. Y., Osbourne, D. O., Hong, S. H., Sanchez-Torres, V., Quiroga, C., Zheng, K., Herrmann, T., Peti, W., Benedik, M. J., Page, R. and Wood, T. K. (2012) A new type V toxin-antitoxin system where mRNA for toxin GhoT is cleaved by antitoxin GhoS. Nature chemical biology, **8**, 855-861.

Wen, Y., Behiels, E. and Devreese, B. (2014) Toxin-Antitoxin systems: their role in persistence, biofilm formation, and pathogenicity. Pathogens and Disease, **70,** 240-249.

Yamaguchi, Y., Park, J. H. and Inouye, M. (2009) MqsR, a crucial regulator for quorum sensing and biofilm formation, is a GCU-specific mRNA interferase in *Escherichia coli.* The Journal of Biological chemistry, **284**, 28746-28753.

Yamaguchi, Y., Park, J. H. and Inouye, M. (2011) Toxin-antitoxin systems in bacteria and archaea. Annual Review of Genetics, **45**, 61-79.

5 – RESULTADOS COMPLEMENTARES

Havia sido proposto inicialmente a análise de real-time RT-PCR das *orfs* em estudo para se avaliar o nível de expressão das proteínas alvos durante a formação do biofilme de *X. fastidiosa in vivo*. Contudo, não obtivemos sucesso na realização da infecção mecânica das plantas de citros com *X. fastidiosa.* Após isso, utilizamos plantas infectadas com *X.fastidiosa* estirpe 9a5c que já haviam sido diagnosticadas com CVC. Tentamos avaliar a expressão gênica das *orfs Xf1480, Xf2162* e *Xf2163*, porém não obtivemos sucesso na detecção do RNA específico das *orfs* bacterianas em estudo nas plantas infectadas. Provavelmente isso aconteceu devido ao excesso de RNA vegetal em relação aos transcritos bacteriano. Tentativas de estudo da expressão das mesmas *orfs in vitro*, com análise dos genes em bactérias coletadas de acordo com as fases de crescimento de *X. fastidiosa* foram feitas. Porém, alguns pontos de coleta correspondentes a fases específicas da formação do biofilme não produziram RNA total com rendimento satisfatório para a realização dos testes após as extrações efetuadas. Desse modo, a análise da expressão das proteínas alvo do trabalho foi baseada nos experimentos de *western blotting*, os quais tem a vantagem de representarem a quantidade de proteína produzida, e não apenas o resultado da transcrição, como é o caso de resultados obtidos por RTqPCR a partir dos quais se infere a expressão gênica.

6 -DISCUSSÃO GERAL

As proteínas alvo desta tese foram escolhidas de acordo com seu padrão de expressão reportados anteriormente (Muranaka *et al.*, 2012). Para caracterização das proteínas, as ORfs foram clonadas no vetor de expressão pET28a (Xf1480 e Xf2162) e pET29a (Xf2163). A ORF Xf2163, identificada com o XfMqsA, foi anteriormente clonada no pET28a, porém a proteína purificada apresentava baixa solubilidade. Nossa hipótese é que a Histag N-terminal impedia a conformação correta do domínio dedo de zinco. Após clonagem no pET29a, a solubilidade aumentou consideravelmente, podendo obter concentrações mais altas (120 $\mu mol.L^{-1}$), provavelmente por ter possibilitado o enovelamento correto do domínio dedo de zinco na região N-terminal.

Xf1480 apresentou 28% de similaridade com um fator de transcrição YcjZ de *E. coli*, sendo denominado XfYcjZ. Buscas feitas em bancos de dados de proteínas com estrutura conservada demonstraram que a XfYcjZ apresenta 25% de identidade com o fator de transcrição AphB de *Vibrio cholerae* que já teve sua estrutura tridimensional resolvida

(Taylor *et al*., 2012), o que permitiu a obtenção de um possível modelo tridimensional através do servidor I-TASSER. Uma característica comum às LysR é a presença do domínio HTH na extremidade N-terminal, enquanto a C-terminal apresenta os domínios reguladores, os quais estão envolvidos no reconhecimento de cofatores.

XfYcjZ foi obtida na forma solúvel e com estruturas secundárias, com predominância de α-hélices. A proteína também apresenta forma globular, pois sua razão friccional (f/f0) obtido por ultracentrifugação analítica foi igual a 1,36±0,1 e apresentou conformação oligomérica tetramérica (dados de SEC). Conformações diméricas e tetraméricas são as mais comumente encontradas na família LysR , mas formas octoméricas também já foram documentadas (Taylor *et al.*, 2012; Maddocks; Oyston, 2008).

Umas das características comum às LysR também é a capacidade de autoregulação. XfYcjZ interagiu com seu próprio promotor na análise de mobilidade eletroforética. As LysR reconhecem sequências de DNA pseudoplaindrômicos, tais como ATC-N_9-GAT e T-N_{11}-A. A promotor de XfYcjZ apresentou cinco motifs T-N_{11}-A, os quais estão nas posições : -12 to -24; -37 to -49, -59 to -71, -87 to – 99 and -102 to -114.

Análise de detecção da XfYcjZ por western blotting revelou que a proteína é diferencialmente expressa nas fases de crescimento de *X. fastidiosa* com maior expressão no décimo quinto dia nas células planctônicas e quinto e vigésimo dias nas células do biofilme. Curiosamente, a avaliação com tratamento com cobre demonstrou que somente as células planctônicas responderam ao tratamento de estresse oxidativo com cobre. Nossa hipótese a respeito da resposta no biofilme, é que a camada exopolimérica externa tenha funcionando como uma barreira ao tratamento com cobre.

Com relação às ORFs Xf2162 e Xf2163, identificadas inicialmente como proteína hipotética e regulador da transcrição do tipo HTH, respectivamente, apresentaram 61 e 42% de similaridade com a MqsR e MqsA de *E. coli*, as quais pertencem ao sistema toxina antitoxina, por isso foram denominadas XfMqsR para a toxina e XfMqsA para antitoxina. Estima-se que haja uma correlação entre a quantidade de operons toxina-antitoxina e maior patogenicidade bacteriana, pois quando foram comparadas espécies patogênicas com espécies relacionadas não patogênicas, foi encontrado um maior número de sistemas TA nas primeiras (Georgiades; Raoult, 2011)

Embora a XfMqsR apresente maior similaridade ela não possui nenhum domínio conservado e também não possui nenhum domínio relacionado com RNAses em geral. A XfMqsR reconhece motifs 5′-G▲CU and G▲CC nos mRNAs para clivagem (Wang *et al*., 2012; Christensen-Dalsgaard *et al*., 2010).

Com respeito à XfMqsA, ela possui um domínio HTH na sua extremidade C-terminal que está relacionado com o reconhecimento de regiões promotoras. Os aminoácidos relacionados com ligação ao DNA são conservados em ambas as espécies, Asn97 e Arg101 e estão relacionados com o reconhecimento do motif TAACCT(N_3)AGGTTA em *E coli*, sendo que em *X. fastidiosa,* uma sequência bem similar foi encontrada TAACCT(N_3)AAGTTA (Brown *et al*., 2011). Além do mais, a proteína heteróloga foi capaz de interagir com o fragmento de DNA contendo esse motif, mas não com o controle negativo, o qual era uma sequência mais distante do códon inicial. Baseado no teste de retardamento eletroforético em gel de agarose a proteína heteróloga foi capaz de começar a se ligar ao promotor mesmo nas relações molares mais baixas 1:2 (Brown *et al*., 2013).

A interação proteína-proteína também foi avaliada por calorimetria isotérmica e foi caracterizada por uma alta afinidade, ΔH= -8609±36.51 e ΔS=11.8 cal/mol/deg., caracterizando uma reação termodinamicamente favorável. Os resíduos envolvidos na interação proteína-proteína são conservados, destacando-se os Arg26, Asp 33 and Asp 40 na MqsR, porém na XfMqsR encontramos Ala26, Arg33 and Asp40. Na antitoxina MqsA os resíduos são Glu41, Arg61 and Lys47, porém em XfMqsA foram encontrados os resíduos Gln 61 and Arg47, entretanto o resíduo Glu foi encontrado na posição 42 (Brown *et al.*, 2009)

A detecção das XfMqsA e XfMqsR demonstrou que a expressão sofre alteração na fase planctônica. Os menores níveis de XfMqsA foram encontrados no décimo dia, corresponde ao dia que ela começa a ser detectada nas vesículas da membrana externa e no décimo quinto dia. Quanto à XfMqsR, seu menor nível de detecção foi no décimo dia. Quando comparamos as células do biofilme, o menor nível para as duas proteínas foram encontradas no décimo dia. O fato de haver mais XfMqsR no décimo e décimo quinto dia pode indicar que esteja relacionada com a formação de microcolônias, décimo dia, e desenvolvimento da arquitetura do biofilme, décimo quinto dia. A expressão do operon toxina antitoxina deve ser muito equilibrada para favorecer o crescimento bacteriano. Em caso de toxinas livres dentro da célula, a formação de células persistentes e de biofilme é favorecida (Lee *et al*., 2014; Muranaka *et al*., 2012).

Baseado em um trabalho recente sobre formação de vesículas da membrana externa (Ionescu *et al*., 2014), foi identificado que a XfMqsA também se encontra nessas vesículas. Os mecanismos moleculares pelo qual a XfMqsA é enviada para a vesícula ainda não é conhecido, uma vez que ela não possui peptídeo sinal. Nosssa hipótese é que a secreção

de XfMqsA pode acarretar em XfMqsR livre dentro da célula e favorecer a formação de biofilme.

7 - RESUMO DOS RESULTADOS

Os resultados apresentados nesta tese e resumidos a seguir demonstram que os objetivos do estudo foram alcançados.

Capítulo 1

•A utilização de ferramentas para clonagem e expressão heteróloga possibilitou o estudo de função da XfYcjZ, através de análises de presença de estrutura secundária por dicroísmo circular, juntamente com sua análise *in silico* para encontrarmos uma provável estrutura tridimensional por homologia de sequência.

- A XfYcjZ se presenta na forma tetramérica em solução, demonstrado por cromatografia por exclusão de tamanho e por ultracentrifugação analítica e, de acordo com o coeficiente e sedimentação, possui forma globular.

• Foi demonstrado que a proteína heteróloga foi capaz de interagir com o seu próprio promotor, indicando um alvo de autoregulação, o que é muito comum em fatores de transcrição do tipo LysR.

• Em condições de crescimento normal, a XfYcjZ se encontra presente em todas as fases do biofilme, mas nas células planctônicas ocorrem uma maior expressão no 15º e no 30º dia. Porém quando em condições de estresse causado por cobre, somente as células planctônicas foram capazes de responder ao tratamento. Estima-se que as células do biofilme não tenham respondido ao cobre devido à presença da matriz extracelular de substâncias poliméricas que as protege de substâncias presente no meio.

Capítulo 2

- As proteínas pertencentes ao sistema toxina antitoxina de *Xylella fastidiosa* apresentaram homologia com a MqsR e MqsA de *E. coli*, respectivamente e apresentam alguns resíduos conservados relacionado com reconhecimento de DNA e para interação proteína-proteína.

• As proteínas heterólogas apresentaram enovelamento secundário, possibilitando o ensaio de dicroísmo circular para avaliação da estabilidade do complexo. Os resultados demonstraram que o complexo XfMqsR e XfMqsA, cuja Tm foi igual a 70ºC, é mais termoestável que a XfMqsA e a XfMqsR, as quais apresentaram Tm iguais a 37ºC e 62,5ºC, respectivamente.

•As proteínas apresentaram alta afinidade de ligação como visto por calorimetria isotérmica, caracterizada por entalpia ΔH=-8609±36.51 e entropia ΔS= 11.8 cal/mol/deg.

•A interação também foi demonstrada por cromatografia por exclusão de tamanho, demonstrando total interação em condições equimolares.

• A interação está intimamente relacionada com a inibição da toxina XfMqsR pela antitoxina XfMqsA, como demonstrado com o ensaio de degradação do RNA por fluorescência.

•A avaliação da interação com o seu próprio promotor demonstrou que a XfMqsA é capaz de se ligar ao seu próprio promotor. A provável sequência de reconhecimento, TAACCT(N3)AAGTTA, foi encontrada e apresenta alta semelhança com a sequência do promotor do sistema homólogo de *E. coli*, TAACCT(N_3)AGGTTA.

• Tanto a XfMqsR quanto a XfMqsA são diferencialmente expressas durando as fases de crescimento e possuem maiores níveis nas células do biofilme.

• XfMqsA também foi encontrada no meio extracelular, como detectado por espectrometria de massas e posteriormente determinamos sua presença nas vesículas das membrana externa por western blot. Nossa hipótese é que a ocorrência dela nessas vesículas pode acarretar em XfMqsR livres dentro da célula, levando ao favorecimento da formação de biofilme.

8 - CONCLUSÕES

Embora o trabalho tenha sido feito sob uma abordagem *in vitro*, ensaios *in vivo* com *X. fastidiosa* mutante serão necessários para uma análise mais acurada para identificação dos mecanismos de regulação e das rotas metabólicas na qual essas proteínas estão envolvidas, como por exemplo o envolvimento do operon toxina antitoxina na formação de células persistentes e formação biofilme. Porém trabalhos envolvendo estirpes *knockout* de *X. fastidiosa* 9a5c ainda não são possíveis devido às limitações que essa estirpe apresenta.

Estudos funcionais de proteínas supostamente relacionadas com patogenicidade, sobrevivência e adaptação podem trazer informações importantes a respeito da biologia e genética do microrganismo em estudo. A abordagem realizada no trabalho nos permitiu identificar as *orfs* através da análise de sequência e presença de domínios com base no banco de dados do NCBI e PDB (*protein data bank*) e esperamos ter contribuído para o melhor entendimento da participação de ambas as proteínas nos mecanismos envolvidos com resposta a estresse, formação de biofilme e patogenicidade de *X. fastidiosa*.

As proteínas em questão pertencem à espécie *X. fastidiosa* estirpe 9a5c e as análises funcionais indicaram a possível participação da proteína XfYcjZ em resposta ao estresse causado pelo cobre. Com respeito ao operon toxina-antitoxina XfMqsR e XfMqsA, respectivamente, a atividade de RNAse foi detectada e avaliamos a capacidade da XfMqsA em inibir a XfMqsR e a hipótese sobre a participação delas na formação de células persistentes e biofilme também foi levantada de acordo com o levantamento bibliográfico. Outra característica importante encontrada foi a presença da XfMqsA dentro das vesículas da membrana externa, porém ainda não sabemos a ação que essa proteína poderia ter fora da célula.

9 - PERSPECTIVAS:

Com base nos resultados obtidos, novos estudos e abordagens envolvendo as proteínas alvo desta tese podem agora serem vislumbrados. Especialmente com relação ao sistema toxina-antitoxina estudado. Recentemente, a análise do secretoma de *X. fastidiosa* estirpe 9a5c efetuada por outro integrante do grupo, para identificar as proteínas por MS/MS, permitiu observar que a antitoxina é secretada, mesmo sem possuir peptídeo sinal. Foi formulada a hipótese de que esta proteína seja enviada para o meio externo através da formação de vesículas da membrana externa. Para confirmar tal hipótese, estudos futuros envolvendo a análise das vesículas produzidas por *X. fastidiosa* devem ser conduzidos. Como relatado no manuscrito presente na Parte 2 desta Tese(seção resultados e discussão), pudemos identificar a presença da antitoxina por *western blot* na fração referente às vesículas. A presença da antitoxina nas vesículas é uma informação que pode trazer novas perspectivas para descobrir o modo de funcionamento do operon toxina-antitoxina de *X. fastidiosa* 9a5c, bem como o seu envolvimento em patogenicidade bacteriana.

Novas análises de bioinformática efetuadas recentemente, permitiram a identificação do possível gene alvo da proteína XfMqsA, a *orf Xf2034*, a qual codifica uma chaperona relacionada com resposta à choque térmico identificada como o gene *cspD* (*cold shock protein*). Ensaios futuros de interação entre XfMqsA e o promotor da *orf Xf2034* podem adicionar novas informações a respeito da função do sistema toxina e antitoxina de *X. fastidiosa*.

REFERÊNCIAS

ALMEIDA, R. P. P.; NASCIMENTO, F. E.; CHAU, J.; PRADO, S. S.; TSAI, C. W.; LOPES, S. A.; LOPES, J. R. S. (2008) Genetic structure and biology of *xylella fastidiosa* strains causing disease in citrus and coffee in Brazil. Applied and Enviromental Microbiology. Vol 74, (12), 3690-3701

BOVÉ, J. M.; AYRES A. J (2007) Critical ReviewEtiology of Three Recent Diseases of Citrus in São Paulo State: SuddenDeath, Variegated Chlorosis and Huanglongbing. IUBMB Life, Vol. 59, 46-54.

BROWN, B. L.; LORD, D. M.; GRIGORIU, S.; PETI, W.; PAGE, R. (2013) The *Escherichia coli* toxin MqsR destabilizes the transcriptional repression complex formed between the antitoxin MqsA and the mqsRA operon promoter. The Journal of Biological Chemistry, 288, 1286-1294.

BROWN, B. L.; WOOD, T. K.; PETI, W.; PAGE, R. (2011) Structure of the *Escherichia coli* antitoxin MqsA (YgiT/b3021) bound to its gene promoter reveals extensive domain rearrangements and the specificity of transcriptional regulation. The Journal of Biological Chemistry. 286, 2285-2296.

CELIS, R. T. (1999) Repression and activation of arginine transport genes in *Escherichia coli* K 12 by the ArgP protein. Journal of Molecular Biology, v. 294, n. 5, p. 1087-95,

CHEN, J.; XIE, G.; HAN, S.; CHERTKOV, O.; SIMS, D.; CIVEROLO, E. L. (2010) Whole genome sequences of two *Xylella fastidiosa* strains (M12 and M23) causing almond leaf scorch disease in California. Journal of Bacteriology Vol. 192, No. 17, p 4534.

CHONO, H.; MATSUMOTO, K.; TSUDA, H.; SAITO, N.; LEE, K.; KIM, S.; SHIBATA, H.; AGEYAMA, N.; TERAO, K.; YASUTOMI, Y.; MINENO, J.; KIM, S.; INOUYE, M.; KATO, I. (2011) Acquisition of HIV-1 resistance in T lymphocytes using an ACA-specific E. coli mRNA interferase. Human Gene Therapy, 22, 35-43.

COOK, G. M.; ROBSON, J. R.; FRAMPTON, R. A.; MCKENZIE, J.; PRZYBILSKI, R.; FINERAN, P. C.; ARCUS, V. L. (2013) Ribonucleases in bacterial toxin-antitoxin systems. Biochimica et Biophysica Acta, 1829, 523-531.

CRUZ, L. F.; COBINE, P. A.; DE LA FUENTE, L. (2012) Calcium increases *Xylella fastidiosa* surface attachment, biofilm formation, and twitching motility. Appl Environ Microbiol. 78 (5):1321-31.

DODDAPANENI, H.; YAO, J.;LIN, H.;WALKER, M. A.;CIVEROLO, E. L. (2006) Analysis of the genome-wide variations among multiple strains of the plant pathogenic bacterium *Xylella fastidiosa*. BMC Genomics. Vol. 7, 225.

DRESCHER, K.; NADELL, C. D.; STONE, H. A.; WINGREEN, N. S.; BASSLER, B. L. (2014) Solutions to the public goods dilemma in bacterial biofilms. Current Biology, Vol. 24, p 50–55.

EL-SAMAD, H.; KURATA, H.; DOYLE, J. C.; GROSS, C. A.; KHAMMASH, M. (2005) Surviving heat shock: control strategies for robustness and performance. Proceedings of the National Academy of Sciences. Vol. 102, 2736–2741

ELLIS, T. N.; KUEHN, M. J. (2010) Virulence and immunomodulatory roles of bacterial outer membrane vesicles. Microbiology and Molecular Biology Reviews, 74, 81-94.

FRANCH, T., GULTYAEV, A. P.; GERDES, K. (1997) Programmed cell death by hok/sok of plasmid R1: processing at the hok mRNA 3'-end triggers structural rearrangements that allow translation and antisense RNA binding. Journal of Molecular Biology, 273, 38-51.

GERDES, K.; WAGNER, E. G. RNA antitoxins. (2007) Current Opinion in Microbiology, 10, 117-124.

GOHEEN, A. C.; NYLAND, G.; LOWE, S. K. (1973) Association of a rickettsia-like organism with Pierce's disease of grapevines and alfafa dwarf and heat therapy of the disease in grapevines. Phytopathology, v. 63, p. 5.

GOTTWALD, T. R.; GIDTTI, F. B.; SANTOS, J. M.; CARVALHO, A. C. (1993) Preliminary spatial and temporal analysis of citrus variegated chlorosis in Brazil Proc. The 12th Conf of I.O.C.V (1993), pp. 327–335 Riverside, CA

HARTUNG, J. S.; BERETTA, J.; BRLANSKY, R. H.; SPISSO, J.; LEE, R. F. (1994) Citrus variegated chlorosis bacterium: axenic culture, pathogenicity, and serological relationships with other stains of *Xylella fastidiosa*. Phytopathology v. 84, p. 7

HAURAT, M. F.; ELHENAWY, W.; FELDMAN, M. F. (2015) Prokaryotic membrane vesicles: new insights on biogenesis and biological roles. Biological Chemistry; 396(2): 95–109

HAYASHI, J.; HAMADA, N.; KURAMITSU, H. K. (2002) The autolysin of Porphyromonas gingivalis is involved inouter membrane vesicle release. FEMS Microbiology Letters, Vol. 216, p. 217-222.

HENIKOFF, S.; HAUGHN, G. W.; CALVO, J. M.; WALLACE, J. C. (1988) A large family of bacterial activator proteins. Proceedings of the National Academy of Sciences, v. 85, p. 6602-6606.

HERNANDEZ-LUCAS, I. GALLEGO-HERNÁNDEZ, A. L.; ENCARNACIÓN, S.; FERNÁNDEZ-MORA, M.; MARTÍNEZ-BATALLAR, A. G.; SALGADO, H.; OROPEZA, R.; CALVA, E. (2008) The LysR-type transcriptional regulator LeuO controls expression of several genes in *Salmonella enterica* serovar Typhi. Journal of Bacteriology, v. 190, n. 5, p. 1658-70.

HOPKINS, D. L. (1989) *Xylella fastidiosa*: Xylem-Limited Bacterial Pathogen of Plants. Annual Review of Phytopathology, v. 27, n. 1, p. 271-290.

HOPKINS, D. L.; MOLLENHAUER, H. H.; MORTENSEN, J. A. (1973) Occurrence of a Rickettsia-like Bacterium in the Xylem of Peach Trees with Phony Disease. Phytopathology, v. 63, p. 2.

IONESCU, M., ZAINI, P. A., BACCARI, C., TRAN, S., DA SILVA, A. M. LINDOW, S. E. (2014) *Xylella fastidiosa* outer membrane vesicles modulate plant colonization by blocking attachment to surfaces. Proceedings of the National Academy of Sciences of the United States of America, 111, 3910-3918.

KIM, J. H.; LEEA, J.; PARK, J.; GHO, Y. S. (2015) Gram-negative and Gram-positive bacterial extracellular vesicles. Seminars in Cell & Developmental Biology, 40, 97–104.

KIM, Y.; WANG, X.; ZHANG, X.; GRIGORIU, S.; PAGE, R.; PETI, W.; WOOD, T. K. (2010) *Escherichia coli* toxin/antitoxin pair MqsR/MqsA regulate toxin CspD. Environmental Microbiology. Vol. 12, (5), 1105-1121.

KUIPERS, K.; DALEKE-SCHERMERHORN, M. H.; JONG, W. S.; TEN HAGEN-JONGMAN, C. M.; VAN OPZEELAND, F.; SIMONETTI, E.; LUIRINK, J.; DE JONGE, M. I. (2015) Salmonella outer membrane vesicles displaying high densities of pneumococcal antigen at the surface offer protection against colonization. Vaccine, 33, 2022-2029.

KWAN, B. W., LORD, D. M., PETI, W., PAGE, R., BENEDIK, M. J. WOOD, T. K. (2014) The MqsR/MqsA toxin/antitoxin system protects *Escherichia coli* during bile acid stress. Environmental Microbiology.

KUEHN, M. J.; KESTY, N. C. (2005) Bacterial outer membrane vesicles and the host–pathogen interaction. Genes & Development. Vol 19, p. 2645–2655 ©

LEE, J. A.; HALBERT, S. E.; DAWSON, W. O.; ROBERTSON, C. J.; KEESLING, J. E.; SINGER, B. H. (2015) Asymptomatic spread of huanglongbing and implications for disease control. Proceedings of the National Academy of Sciences. Vol. 112, 24, 7605-7610.

LEE, M. W., TAN, C. C., ROGERS, E. E.; STENGER, D. C. (2014) Toxin-antitoxin systems mqsR/ygiT and dinJ/relE of *Xylella fastidiosa.* Physiological and Molecular Plant Pathology, 87, 59-68.

LI, J.; WANG, N. (2014) Foliar application of biofilm formation–inhibiting compounds enhances control of citrus canker caused by *Xanthomonas citri* subsp. *citri*. Phytopathology, Vol. 104, 2, 134-142

LIMOLI, D. H.; JONES, C. J.; WOZNIAK, D. J. (2015) Bacterial extracellular polysaccharides in biofilm formation and function. Microbiology Spectrum. Vol. 3.

LIN, H.; ISLAM, M. S.; CABRERA-LA ROSA, J. C.; CIVEROLO, E. L.; GROVES, R. L. (2015) Population structure of *Xylella fastidiosa* associated with almond leaf scorch disease in the san joaquin valley of California. Phytopathology. Vol 105 (6) p. 825-32.

LINDQUIST, S.; LINDBERG, F.; NORMARK, S. (1989) Binding of the *Citrobacter freundii* AmpR regulator to a single DNA site provides both autoregulation and activation of the inducible ampC beta-lactamase gene. Journal of Bacteriology, v. 171, n. 7, p. 3746-53.

LORD, D. M., UZGOREN BARAN, A., SOO, V. W., WOOD, T. K., PETI, W.; PAGE, R. (2014) McbR/YncC: implications for the mechanism of ligand and DNA binding by a bacterial GntR transcriptional regulator involved in biofilm formation. Biochemistry, 53, 7223-7231.

MADDOCKS, S. E.; OYSTON, P. C. (2008) Structure and function of the LysR-type transcriptional regulator (LTTR) family proteins. Microbiology, v. 154, n. Pt 12, p. 3609-23.

MASUDA H., TAN Q., AWANO N., WU K. P., INOUYE M. (2012) YeeU enhances the bundling of cytoskeletal polymers of MreB and FtsZ, antagonizing the CbtA (YeeV) toxicity in *Escherichia coli*. Molecular. Microbiology. 84, 979–989.

MIRCETICH, S. M. LOWE, S. K.; MOLLER, W. J.; NYLAND, G (1976) Etiology of almond leaf scorch disease and transmission of the causal agent. Phytopathology, v. 66, p. 8.

MURANAKA, L. S.; GIORGIANO, T. E.; TAKITA, M. A.; FORIM, M. R.; SILVA, L. F. C.; COLETTA-FILHO, H. D.; MACHADO, M. A.; SOUZA , A. A. (2012) N-

Acetylcysteine in agriculture, a novel use for an old molecule: focus on controlling the plant–pathogen *Xylella fastidiosa*. PLos ONE, 23; 8 (8).

NYLAND, G.; GOHEEN, A. C.; LOWE, S. K.; KIRKPATRICK, H. C. (1973) The ultrastructure of a rickettsia-like organism from a peach tree affected with phony disease. Phytopathology, v. 63, p. 4.

OLSEN, I.; AMANO, A. (2015) Outer membrane vesicles - offensive weapons or good Samaritans? Journal of Oral Microbiology. 7, 27468.

PARADELA FILHO, O.; SUGIMORI, M. H.; RIBEIRO, I. J. A.; GARCIA Jr., A.; BERETTA, M. J. G.; HARAKAWA, R.; MACHADO, M. A.; LARANJEIRA, F. F.; RODRIGUES NETO, J.; BERIAM, L. O. S. (1997) Constatação de *Xylella fastidiosa* em cafeeiro no Brasil. Summa Phytophatologica, v. 23, p. 4.

PARSEK, M. R. YE, R. W.; PUN, P.; CHAKRABARTY, A. M. (1994) Critical nucleotides in the interaction of a LysR-type regulator with its target promoter region. catBC promoter activation by CatR. Journal of Biological Chemistry, v. 269, n. 15, p. 11279-84.

PEREZ-RUEDA, E.; COLLADO-VIDES, J. (2001) Common history at the origin of the position-function correlation in transcriptional regulators in archaea and bacteria. Journal of Molecular Evolution, v. 53, n. 3, p. 172-9.

PICOSSI, S.; BELITSKY, B. R.; SONENSHEIN, A. L. (2007) Molecular mechanism of the regulation o*f Bacillus subtilis* gltAB expression by GltC. Journal of Molecular Biology, v. 365, n. 5, p. 1298-313.

SAUER, K.; CAMPER, A. K.; EHRLICH, G. D.; COSTERTON, J. W.; DAVIES, D. G. (2002) *Pseudomonas aeruginosa* displays multiple phenotypes during development as a biofilm. Journal of Bacteriology, 184: 1140–1154.

SCHERTZER, J. W.; WHITELEY, M. (2013) Bacterial outer membrane vesicles in trafficking, communication and the host-pathogen interaction. Journal of Molecular Microbiology and Biotechnology, 23, 118-130.

SCHUSTER C. F.; BERTRAM R. (2013) Toxin-antitoxin systems are ubiquitous and versatile modulators of prokaryotic cell fate. FEMS Microbiol Letters. 340 (2):73-85.

SIMPSON, A. J. *et al*. (2000) The genome sequence of the plant pathogen *Xylella fastidiosa*. The *Xylella fastidiosa* Consortium of the Organization for Nucleotide Sequencing and Analysis. Nature, v. 406, n. 6792, p. 151-9.

STEC, E.; WITKOWSKA-ZIMNY, M.; HRYNIEWICZ, M. M.; NEUMANN, P.; WILKINSON, A. J.; BRZOZOWSKI, A. M.; VERMA, C. S.; ZAIM, J.; WYSOCKI, S.; BUJACZ, G. D. (2006) Structural basis of the sulphate starvation response in *E. coli*: crystal structure and mutational analysis of the cofactor-binding domain of the Cbl transcriptional regulator. Journal of Molecular Biology, v. 364, n. 3, p. 309-22.

SUN, J.; KLEIN, A. (2004) A LysR-type regulator is involved in the negative regulation of genes encoding selenium-free hydrogenases in the archaeon *Methanococcus voltae.* Molecular Microbiology, v. 52, n. 2, p. 563-71.

TOYOFUKU, M.; INABA, T.; KIYOKAWA, T.; OBANAA, N.; YAWATA, Y.; NOMURAA, N. (2015) Environmental factors that shape biofilm formation. Bioscience, Biotechnology and Biochemistry.

VAN KEULEN, G.; RIDDER, A. N.; DIJKHUIZEN, L.; MEIJER, W. G. (2003) Analysis of DNA binding and transcriptional activation by the LysR-type transcriptional regulator CbbR of *Xanthobacter flavus.* Journal of Bacteriology, v. 185, n. 4, p. 1245-52.

WANG, X.; WOOD, T. K. (2011) Toxin-antitoxin systems influence biofilm and persister cell formation and the general stress response. Applied and Environmental Microbiology. 77, 5577-5583.

WANG, X.; KIM, Y.; HONG, S. H.; MA, Q.; ROWN, B. L.; PU, M.; TARONE, A.M.; BENEDIK, M. J.; PETI, W.; PAGE, R.; WOOD, T. K. (2011) Antitoxin MqsA helps mediate the bacterial general stress response. Nature Chemical Biology, 7, 359-366.

WANG, X., LORD, D. M.; CHENG, H. Y.; OSBOURNE, D. O.; HONG, S. H.; SANCHEZ-TORRES, V.; QUIROGA, C.; ZHENG, K.; HERRMANN, T.; PETI, W.; BENEDIK, M. J.; PAGE, R.; WOOD, T. K. (2012) A new type V toxin-antitoxin system where mRNA for toxin GhoT is cleaved by antitoxin GhoS. Nature Chemical Biology, 8, 855-861.

YAMAGUCHI, Y.; PARK, J. H.; INOUYE, M. (2009) MqsR, a crucial regulator for quorum sensing and biofilm formation, is a GCU-specific mRNA interferase in *Escherichia coli*. The Journal of Biological Chemistry, 284, 28746-28753.

YAMAGUCHI, Y.; PARK, J. H.; INOUYE, M. (2011) Toxin-antitoxin systems in bacteria and archaea. Annual Review of Genetics, 45, 61-79.

YONEZAWA,H.; OSAKI, T.; KAMIYA, S. (2015) Biofilm formation by *Helicobacter pylori* and its involvement for antibiotic resistance. Biomed Research International.

Anexo

Artigos publicados em colaboração

Biochimica et Biophysica Acta 1834 (2013) 697–707

Contents lists available at SciVerse ScienceDirect

Biochimica et Biophysica Acta

journal homepage: www.elsevier.com/locate/bbapap

Small-angle X-ray scattering and *in silico* modeling approaches for the accurate functional annotation of an LysR-type transcriptional regulator

M.A.S. Toledo [a,1], C.A. Santos [a,1], J.S. Mendes [a,1], A.C. Pelloso [a], L.L. Beloti [a], A. Crucello [a], M.T.P. Favaro [a], A.S. Santiago [a], D.R.S. Schneider [a], A.M. Saraiva [a,b], D.R. Stach-Machado [c], A.A. Souza [d], D.B.B. Trivella [e], R. Aparicio [e], L. Tasic [f], A.R. Azzoni [a,g], A.P. Souza [a,h,*]

[a] Centro de Biologia Molecular e Engenharia Genética, Universidade Estadual de Campinas, Campinas, SP, Brazil
[b] Instituto Nacional de Metrologia, Qualidade e Tecnologia, Rio de Janeiro, Brazil
[c] Departamento de Imunologia — Instituto de Biologia — Univerisade Estadual de Campinas, Campinas, SP, Brazil
[d] Centro APTA Citros Sylvio Moreira/IAC, Rodovia Anhanguera Km 158, Cordeirópolis, SP, Brazil
[e] Laboratório de Biologia Estrutural e Cristalografia, Instituto de Química, Universidade Estadual de Campinas, Campinas, SP, Brazil
[f] Laboratório de Química Biológica, Instituto de Química, Universidade Estadual de Campinas, Campinas, SP, Brazil
[g] Departamento de Engenharia Química, Escola Politécnica, Universidade de São Paulo, São Paulo, SP, Brazil
[h] Instituto de Biologia, Universidade Estadual de Campinas, Departamento de Biologia Vegetal, Campinas, SP, Brazil

ARTICLE INFO

Article history:
Received 23 June 2012
Received in revised form 24 December 2012
Accepted 26 December 2012
Available online 5 January 2013

Keywords:
LysR-like transcriptional regulator (LTTR)
Small-angle X-ray scattering (SAXS)
Benzoate
Muconate
Biofilm
Citrus variegated chlorosis (CVC)

ABSTRACT

Xylella fastidiosa is a xylem-limited, Gram-negative phytopathogen responsible for economically relevant crop diseases. Its genome was thus sequenced in an effort to characterize and understand its metabolism and pathogenic mechanisms. However, the assignment of the proper functions to the identified *open reading frames* (ORFs) of this pathogen was impaired due to a lack of sequence similarity in the databases. In the present work, we used small-angle X-ray scattering and *in silico* modeling approaches to characterize and assign a function to a predicted LysR-type transcriptional regulator in the *X. fastidiosa* (XfLysRL) genome. XfLysRL was predicted to be a homologue of BenM, which is a transcriptional regulator involved in the degradation pathway of aromatic compounds. Further functional assays confirmed the structural prediction because we observed that XfLysRL interacts with benzoate and *cis,cis*-muconic acid (also known as 2E,4E-hexa-2,4-dienedioic acid; hereafter named muconate), both of which are co-factors of BenM. In addition, we showed that the XfLysRL protein is differentially expressed during the different stages of *X. fastidiosa* biofilm formation and planktonic cell growth, which indicates that its expression responds to a cellular signal that is likely related to the aromatic compound degradation pathway. The assignment of the proper function to a protein is a key step toward understanding the cellular metabolic pathways and pathogenic mechanisms. In the context of *X. fastidiosa*, the characterization of the predicted ORFs may lead to a better understanding of the cellular pathways that are linked to its bacterial pathogenicity.

1. Introduction

Xylella fastidiosa is a xylem-limited, Gram-negative bacterium and the causal agent of many important crop diseases, including citrus variegated chlorosis (CVC), "phony peach" in peaches, and Pierce's disease in grapes [1–4]. Because of the economic impact of these diseases, the *X. fastidiosa* genome was sequenced [5], which allowed the identification of all of the basic genetic profiles for the survival of this bacterium, including the genes involved in metabolism, the synthesis of essential molecules (*e.g.*, amino acids, nucleotides and lipids), and mechanisms of transcription, translation and repair. However, because putative functions could be assigned to only 47% of the 2904 predicted coding regions, the functions of many *open reading frames* (ORFs) remain unknown [5–8]. Since the sequencing of the *X. fastidiosa* genome, more sophisticated experiments have been performed that have led to a better characterization and understanding of this phytopathogen and its pathogenic mechanisms [9–11]. Currently, the hypothesis for the pathogenicity of the bacterium involves the occlusion of the xylem vessels of the infected plants either through the secretion of exopolysaccharides to form biofilm structures or by mechanical occlusion, which leads to hydric stress and the appearance of disease symptoms, such as leaf marginal necrosis, leaf abscission, delayed growth, and reduced plant vigor and fruit development [12–15]. In addition, it has been reported that the gene

* Corresponding author at: Depto. de Biologia Vegetal, Universidade Estadual de Campinas, Caixa Postal 6010, CEP 13083-875, Campinas, São Paulo, Brazil. Tel.: +55 19 3521 1132.
E-mail address: anete@unicamp.br (A.P. Souza).
[1] These authors contributed equally to this work.

1570-9639/$ – see front matter © 2012 Published by Elsevier B.V.
http://dx.doi.org/10.1016/j.bbapap.2012.12.017

Anexo

expression profile of planktonic *X. fastidiosa* cells is different from that of biofilm-forming cells. The differentially regulated ORFs are likely to be involved in the cell's ability to adhere to xylem vessels and form the biofilm structure that leads to the disease onset. Therefore, investigations of these differentially expressed ORFs have been performed to understand the biofilm formation process and thus, the pathogenicity of *X. fastidiosa* [16,17].

In this study, we characterized the protein product of Xf1448 ORF, which is predicted to be a LysR-like transcriptional regulator (LTTR; http://www.xylella.lncc.br/xf-prod-bin/annotation/final/annotation.cgi?id=&gene=XF1448). Because this ORF has little amino acid sequence similarity with other LysR-type proteins, the identification of its role in the cellular metabolism was previously impaired. The LTTR family is a well-characterized group of transcriptional regulators that is ubiquitous among bacteria, has a high degree of conservation, and has functional orthologues in *archaea* and eukaryotic organisms [18–20]. These transcriptional regulators usually control their own expression, which may occur simultaneously with the regulation of a divergently transcribed target ORF or operon [21]. Based on sequence alignments, it has been shown that LTTRs have a helix-turn-helix (HTH) DNA-binding domain located 20–90 amino acids from the N-terminus, regardless of whether the transcriptional regulator acts as an activator or repressor [21]. Generally, this DNA-binding domain interacts with the promoter region of the targeted ORF or operon through a pseudo-palindromic sequence (T-N_{11}-A) that is called the LTTR box [22]. However, the LTTR box may vary in both base pair composition and length [21]. The C-terminus (amino acids 95–210) of a typical LTTR contains the co-inducer binding cleft, and the interaction between the co-inducer and LTTR modulates the activating or repressing function of the protein [23–25]. The molecules that act as co-inducers are generally by-products or metabolic intermediates of the pathways that are regulated by the LTTRs [26,27]. Considering the abundance of LTTRs within the genomes of evolutionarily distant bacteria and other organisms, LTTRs have developed regulatory functions in many different pathways, including metabolism, cell division, quorum sensing, virulence, motility, nitrogen fixation, oxidative stress response, toxin production, attachment and secretion [9,28–36]. Moreover, this class of tranSmall-angle X-ray scattering and *in silico* modeling approaches for the accurate functional annotation of an LysR-type transcriptional regulatorscription factors may act in association with other regulatory pathways that induce more complex regulatory networks inside the cell. One type of interaction is the association of the LTTR with the globally expressed histone-like nucleoid-associated regulator protein (H-NS) [37].

In the present work, we identified the structure and function of the predicted LysR-type ORF Xf1448 from *X. fastidiosa* (denoted XfLysRL for LysR-like from *X. fastidiosa* in the present work). Although the XfLysRL ORF is described as a LTTR, it does not exhibit sufficient sequence similarity with well-characterized LTTRs (functionally and/or structurally), which had previously impaired a more accurate annotation of its function. However, it does contain a conserved LTTR substrate binding domain that is involved in the catabolism of aromatic compounds. Using small-angle X-ray scattering (SAXS) and *in silico* modeling, we were able to obtain a reliable protein structure envelope, which allowed us to use structural conservation to identify putative homologues with known functions. Further functional assays confirmed the role of XfLysRL in the cell, which allowed the identification of new information and knowledge of the *X. fastidiosa* metabolism.

2. Materials and methods

2.1. Cloning, expression and purification of recombinant XfLysRL

The gene corresponding with XfLysRL was amplified by PCR using genomic DNA from *X. fastidiosa* strain *9a5c* as the template. Specific primers for the target sequence were designed such that the fragments produced could be cloned into the pET28a vector with *Nde*I and *Xho*I (forward primer: 5′ — TAATCATATGCACGACGCCGCCAGT — 3′; reverse primer: 5′ — ATCTCGAGTCACCTTGCACCAGCAC — 3′). The PCR product was cloned into pET28a and chemically transformed into competent *Escherichia coli* DH5-α cells. The positive clones were sequenced to verify the identity and presence of the cloned fragment. The competent *E. coli* BL21(DE3) strain was used for the recombinant protein expression.

E. coli BL21(DE3) cells containing the gene that encodes XfLysRL were inoculated in 3 mL of LB medium containing 30 μg/mL kanamycin. The cells were then grown at 37 °C and 300 rpm overnight. The cultures were transferred into 1 L of LB medium containing the same concentration of antibiotic and grown to an A_{600} of 0.6–0.8. The overexpression of the plasmid was induced through the addition of IPTG to a final concentration of 0.4 mM; the culture was then incubated at 25 °C and 200 rpm for 18 h. After the incubation period, the cells were centrifuged at 5000×g for 15 min (4 °C), and the pellet was resuspended in buffer A (50 mM Tris–HCl and 300 mM NaCl pH 7.5) supplemented with 1 mg/mL lysozyme and 1 mM phenylmethanesulfonyl fluoride (PMSF; Sigma Chemical, St. Louis, MO, USA). The cells were maintained under agitation conditions for 30 min (4 °C), sonicated and then centrifuged at 15,000×g for 45 min (4 °C) to obtain the protein extract. The XfLysRL protein was then purified through a single affinity chromatography step using a Ni-NTA resin (Qiagen, Hilden, Germany) equilibrated with buffer A. The purified protein was eluted using an imidazole gradient (20, 50, 75, 100, 200 and 500 mM) in buffer A. The protein yield and purity were analyzed by SDS-PAGE.

2.2. Size-exclusion chromatography

Size-exclusion chromatography was performed using a Superdex 75 10/300 GL column (GE Healthcare, USA). The column was equilibrated with 50 mM Tris–HCl pH 7.5 and 300 mM NaCl. The samples (250 μL) were injected at a flow rate of 0.6 mL/min. High molecular weight (HMW) and low molecular weight (LMW) gel filtration calibration kits (GE Healthcare) were used as the calibration standards, and the results were analyzed according to the instructions detailed in the calibration kit manuals. Conalbumin (75 kDa), ovalbumin (43 kDa), carbonic anhydrase (29 kDa), ribonuclease A (13.7 kDa), aprotinin (6.5 kDa) and blue dextran 2000 (2000 kDa) were used as the standards.

2.3. Small-angle X-ray scattering (SAXS)

The XfLysRL samples at a concentration of 1.5 mg/mL in 50 mM Tris–HCl pH 7.5, 300 mM NaCl and 500 mM imidazole buffer were subjected to SAXS data collection. The samples were centrifuged at 13,000×g and 4 °C prior to the measurements. The individual samples were carefully loaded into cells composed of two thin parallel mica windows and maintained at 25 °C throughout the measurements. The SAXS data collection was performed at the D02A-SAXS2 beamline of the Brazilian National Synchrotron Light Laboratory (LNLS, Campinas) [38] using a bi-dimensional MAR CCD 345 detector and a monochromatic X-ray beam at a wavelength of 1.488 Å. The sample-to-detector distance was adjusted to 1682.88 mm, which covers a momentum transfer interval of $0.0076<q<0.1928$ $Å^{-1}$, where $q=[(4\pi)/(\lambda)]\sin\theta$ and 2θ is the scattering angle.

The protein samples and buffer solution (used as a blank during the data analysis) were exposed to the X-ray for 10 min. Six successive frames were recorded for the protein sample. A data reduction was performed using FIT2D [39], which involved the collection of the radial integration of the images, normalization to the intensity of the transmitted beam and subtraction of the buffer scattering. To prevent artifacts caused by protein degradation during the data

Anexo

collection, only the first two frames were averaged to obtain the final curve. Guinier analysis was performed to evaluate the sample scattering linearity at very small angles [40] and estimate the radii of gyration, Rg, and the scattering at the zero angle, I(0). Further analyses were performed using the ATSAS package [41]. The indirect Fourier transform method, which was implemented in GNOM [39], was used to calculate the distance distribution function, P(r), which allowed the assessment of the maximum intramolecular distance (D_{max}) and molecular anisometry. GNOM was also used to estimate Rg and I(0). A Kratky plot [$q^2I(q)\times w$] [42,43] was used to evaluate the conformational state of the protein in solution. The molecular mass of XfLysRL was estimated using 3.3 mg/mL bovine serum albumin (BSA) as the standard. The I(0) values from the standard and sample were obtained as described above, and the equation $[Mc/I(0)]_{sample} = [Mc/I(0)]_{standard}$ (where M is the molecular mass, c is the concentration and I(0) is the scattering intensity at the zero angle) was used to estimate the molecular mass of the sample.

Ab initio dummy bead models were calculated from the experimental curves using DAMMIF [44] and imposing P2 symmetry. Forty models were averaged with DAMAVER [45]. Based on the normalized spatial discrepancy (NSD) values and a visual inspection, the 10 most similar models were selected and averaged, which resulted in the generation of the final envelope that was used in the subsequent structural comparisons. For better visualization, the envelope was presented as a mask that was built from the final averaged bead model using NCSMASK [46].

In parallel with the *ab initio* methods that were used to construct the low resolution envelope from the experimental curve, we conducted rigid-body modeling of XfLysRL based on homologous proteins. A monomeric structure of XfLysRL (model with the highest Small-angle X-ray scattering and *in silico* modeling approaches for the accurate functional annotation of an LysR-type transcriptional regulatorscore), which was predicted with I-TASSER [47–49], was utilized to compose a dimeric structure that was based on available crystallographic models using the following procedure. First, to define the most probable dimeric interface, homologous crystal structures of the LTTR family members (those automatically selected by I-TASSER) were analyzed to compose a dimer by applying different crystallographic symmetry operations and choosing the two monomers that corresponded with a known functional dimer [50–55]. The resulting models composed of two amino acid chains related by the appropriSmall-angle X-ray scattering and *in silico* modeling approaches for the accurate functional annotation of an LysR-type transcriptional regulatorate symmetry were then fitted against the experimental XfLysRL SAXS curve using CRYSOL [56]. The discrepancy (|) between the experimental data and computed theoretical scattering curve of each possible dimer was used to select the closest structural homologue. Using this model as a reference, the predicted XfLysRL monomer was superimposed onto each chain separately, and the resulting monomers were combined into a single file to represent the putative atomic model of the XfLysRL dimer, which was also assessed with CRYSOL. The structural alignments were performed with SUPCOMB [57].

2.4. Sequence alignment of XfLysRL with similar structurally characterized proteins

Protein sequence alignments were performed to identify putative homologues with known structure and function that would help in the characterization of the XfLysRL protein. An initial sequence similarity analysis was performed using the Basic Local Alignment Search Tool (BLAST, http://blast.ncbi.nlm.nih.gov/Blast.cgi), and subsequent alignments were performed using the CLUSTALW server (http://www.ebi.ac.uk/Tools/msa/clustalw2/).

2.5. Expression profile of XfLysRL during different stages of biofilm formation and in the presence of muconate and benzoate

To analyze the expression of XfLysRL during different steps of biofilm formation, a specific antibody against the purified protein was synthesized (RheaBiotech, Brazil) and used for the detection of the native XfLysRL in bacterial lysates. A *X. fastidiosa* subsp. *pauca* strain *9a5c* suspension in phosphate-buffered saline was inoculated in periwinkle wilt (PW) medium and grown at 28 °C with shaking at 130 rpm. Separated experiments were conducted in triplicate and analyzed during each day of growth, and no additional medium supplementation or changes were performed. The biofilm and planktonic cell extracts from days 3, 5, 10, 15, 20 and 30 of growth were analyzed by Western blot. Briefly, the pelleted cells were resuspended in 50 mM Tris–Cl pH 8.0, 25 mM NaCl, 5 mM EDTA, 2% Triton X-100, 1 mM PMSF and 1 mg/mL lysozyme and incubated on ice for 20 min. The cell disruption was achieved through 5 10-s sonication cycles with an output intensity setting of 5 in an Ultrasonic Homogenizer 4710 (Cole-Parmer, USA). The homogenate was centrifuged for 10 min at 10,000×g, and the resulting supernatant was collected. The total protein concentration was measured using a Micro BCA™ Protein Assay Kit (Thermo Scientific, USA), and all of the samples were normalized to the same protein concentration. After SDS-PAGE, the samples were transferred to a 0.45-μm Potran BA 85 nitrocellulose membrane (Whatman, Dassel, Germany) using a Semi-Dry Transfer Cell (BioRad, CA, USA). The transferred membrane was incubated with the specific antibody against XfLysRL at a dilution of 1:4000 for 2 h and then with a secondary antibody, which was linked to an alkaline phosphatase (goat anti-rabbit IgG-AP, Souza-Cruz, Brazil), at a dilution of 1:8000 for an additional 2 h. The Western blots were developed with the BCIP/NBT Color Development Substrate (Promega, Madison, Wisconsin, USA) following the manufacturer's instructions. Three independent blots for the biofilm and planktonic samples were performed to assess the variation in the protein transfer. The signal intensity was quantified using the Kodak Electrophoresis Documentation and Analysis System (EDAS) 290 software.

A similar approach was used to evaluate the expression of XfLysRL in biofilm *X. fastidiosa* cells in the presence of muconate and benzoate. Briefly, a *X. fastidiosa* subsp. *pauca* strain *9a5c* suspension in phosphate-buffered saline was inoculated in PW medium that was not supplemented with BSA and grown at 28 °C with shaking at 130 rpm. When indicated, a sterile muconate or benzoate solution was added to the medium to final concentrations of 0.168 mM and 0.392 mM muconate and 5 mM and 10 mM benzoate. *X. fastidiosa* was also cultivated in non-supplemented medium (no benzoate or muconate) as a control. Each experiment was performed in triplicate. The biofilm cells were harvested after 10 days, and the total protein extraction and Western blot procedures were performed as described above. Each sample was normalized to a final protein concentration of 197 ng/μL. We used a 1:2000 dilution of the specific anti-XfLysRL antibody and 1:4000 dilution of the secondary antibody as described previously.

2.6. Interaction of XfLysRL with its putative co-inducers benzoate and muconate

Based on the sequence alignments and SAXS data, we hypothesized that XfLysRL could be a transcriptional regulator induced by benzoate and muconate to activate the degradation pathway of these compounds. Clark and colleagues (2009) analyzed the interaction of benzoate and muconate with the *Acinetobacter* sp. strain ADP1 BenM, which is a LysR-type transcriptional regulator responsible for the activation of the degradation pathway of aromatic substrates [58]. Similarly, we used fluorescence emission spectroscopy to test the ability of XfLysRL to interact with benzoate and muconate

Anexo

and obtained positive results that were in agreement with our SAXS and *in silico* modeling results.

Purified XfLysRL (2.5 μM) was dialyzed against 50 mM Tris–HCl, pH 7.5, and 300 mM NaCl and then incubated with 0 to 0.7 mM muconate or 0 to 10 mM benzoate (both products were purchased from Sigma-Aldrich), and the emitted fluorescence was recorded using a Carey Eclipse spectrofluorometer (Varian, USA). The samples were excited at 295 nm and 280 nm to monitor the interactions with muconate and benzoate, respectively. The measurements were performed in triplicate, and the differences in the emissions between each spectra and the initial emission of the protein were plotted against the co-factor concentration. K_d values for benzoate and muconate interactions with the protein were calculated using OriginPro 8 SRO software (OriginLab Corporation, Version 8.0724 B724) through Stern–Volmer plots and Non Linear Least Square fitting. The equation: $Q = Q_{max} \times C/(K_d + C)$ was used, in which Q is the observed fluorescence quenching, Q_{max} is the maximum observed fluorescence quenching, K_d is the dissociation constant and C are quenchers (benzoate or muconate) concentrations.

3. Results

3.1. Sequence alignments

An initial BLAST search of the XfLysRL sequence (UniProt ID: Q9PCQ9) using the UniProt database resulted in hits that primarily included LTTR family members. The LysR transcription factors from *Xanthomonas campestris* (Q3BT83), *Acidovorax* sp. (A1W5N6), *Tolumonas auensis* (C4LAA4), *Pseudomonas aeruginosa* (B7V4X9) and *Bordetella petrii* (A9IDT1) were the top hits and exhibited a primary sequence identity that ranged from 79 to 69%. However, the structure and function of these and other hits with ~30% identity were poorly characterized at the protein level. Conversely, the hits with <30% identity, such as the LysR family members BenM and CatM from *Acinetobacter baylyi*, CbnR from *Cupriavidus necator*, CbL and CysR from *E. coli* and CysB from *Klebsiella pneumoniae*, are well characterized [48–53], and their atomic crystal structures are available in the Protein Data Bank. An alignment of the full length XfLysRL sequence deposited in the UniProt database with those of the LTTR family members is shown in Fig. 1 and colored by amino acid conservation. The alignment and structural homology parameters are displayed in Table 1 (Supplementary data). It is noteworthy that XfLysRL does not appear to have an N-terminal DNA-binding domain, which is observed in the other LysR-type transcriptional regulators.

3.2. Recombinant XfLysRL protein expression, purification and initial characterization

Recombinant XfLysRL was successfully produced in the *E. coli* BL21(DE3) strain under the conditions described in the Materials and methods section and satisfactorily purified in a single affinity chromatography step. Polyacrylamide gel electrophoresis showed a high purity level, and size exclusion chromatography revealed that the protein was found as a dimer in solution under both reducing and non-reducing conditions (Fig. 2). In addition, the oligomeric state of the protein did not change when incubated with the theoretical co-inducers muconate

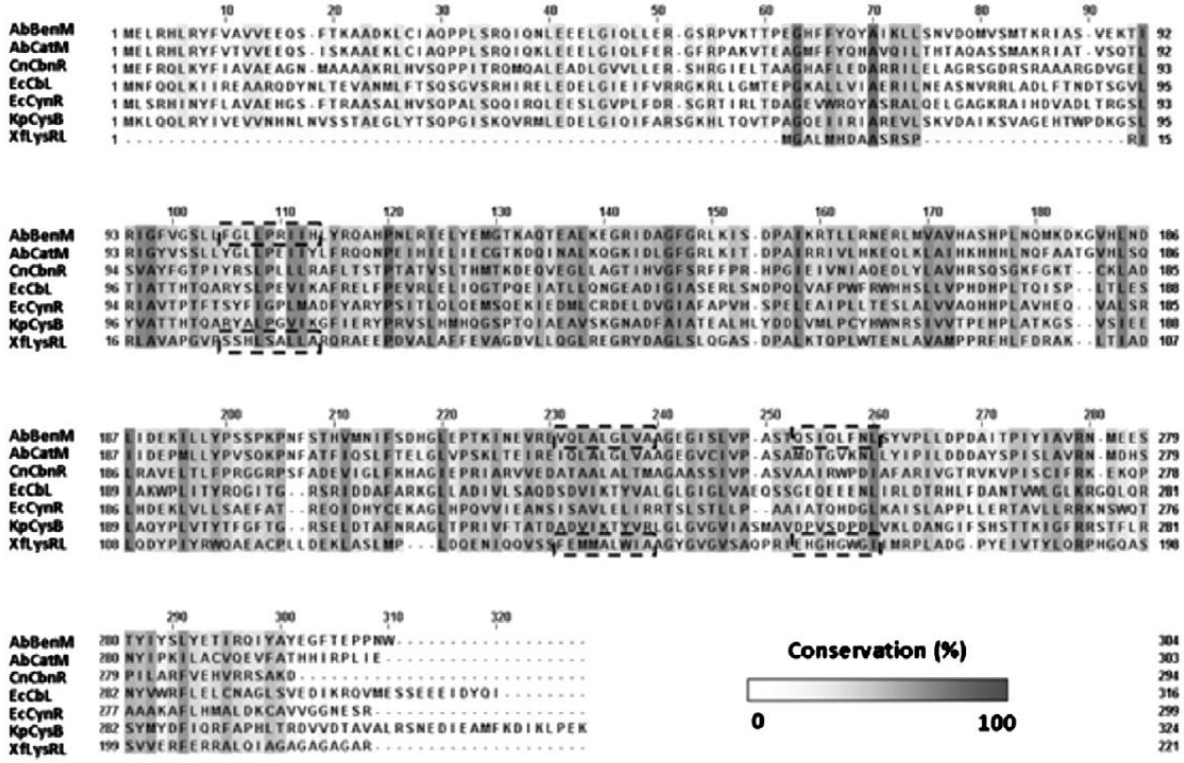

Fig. 1. Primary sequence alignment of LTTR family members. The amino acid sequences of *Acinetobacter baylyi* BenM (AbBenM) and CatM (AbCatM), *Cupriavidus necator* CbnR (CnCbnR), *Escherichia coli* CbL (EcCbL) and CynR (EcCynR), *Klebsiella pneumoniae* (KpCysB) and *Xylella fastidiosa* LysRL (XfLysRL) were aligned using multiple alignment algorithms in the ClustalW [20] software. The alignment is colored according to the conservation of the chosen LTTR sequences, which ranged from 0% (white) to 100% (dark gray). The reported AbBenM [14,15] and proposed XfLysRL dimerization interfaces are highlighted with dashed lines.

Anexo

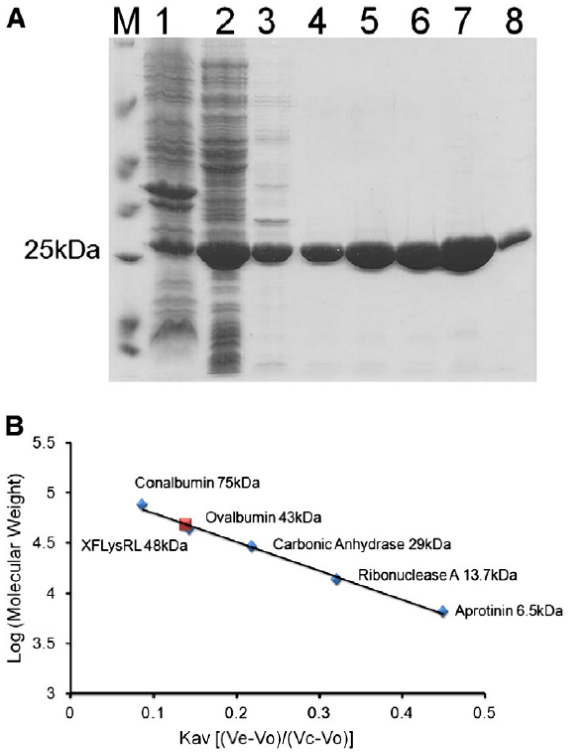

Fig. 2. Initial characterization of XfLysRL. (A) SDS-PAGE analysis of purified XfLysRL, in which M is the Fermentas Molecular Weight Marker, 1 is the insoluble fraction, 2 is the soluble fraction, and 3 through 8 are the elution imidazole gradient (20, 50, 75, 100, 200 and 500 mM). (B) Size exclusion chromatography of XfLysRL. Based on our calibration curve, XfLysRL is a dimer in solution with a molecular weight of 48 kDa.

and benzoate (data not shown). The secondary structure of the purified recombinant protein was analyzed by circular dichroism (CD) and determined to contain regular β-sheets and α-helixes (data not shown).

3.3. SAXS data analysis and modeling

Small-angle X-ray scattering (SAXS) is a technique that allows the study of the structure and interactions of a macromolecule in solution. Despite its low resolution, SAXS is considered a powerful tool for the elucidation of protein behavior in solution (which may be near physiological conditions or in the presence of different compounds, such as protein ligands or denaturing agents) and provides some key parameters, such as the molecular weight (MW), radius of gyration (Rg), and maximum intramolecular distance (D_{max}), that aid in the identification of the molecular envelope of the studied protein. In this study, it was possible to correlate the SAXS data on the XfLysRL protein (coupled with the *in silico* modeling results) to previously characterized proteins and hence speculate on the possible function of XfLysRL. The experimental SAXS curves were analyzed individually and revealed variation during the data collection process that is possibly related to radiation damage or protein degradation. Thus, the first two frames, which were essentially identical, were used to build the average scattering curve that was used in the additional analyses (Fig. 3A). The corresponding Guinier region (Fig. 3B) exhibited a linear behavior characteristic of monodisperse samples and was used to determine the radius of gyration, which was estimated to be 28.5 Å. The Kratky plot (Fig. 3C) had a well-defined maximum, as expected for well-folded, compact proteins. The distance distribution function, P(r), was calculated with GNOM [39] and found to have a symmetrical shape, with a D_{max} of 85 Å (Fig. 3D) and corresponding radius of gyration of 27.6 Å, which is similar to the less accurate value that was estimated from the Guinier analysis.

The molecular mass of XfLysRL was estimated to be 48.4 kDa based on a comparison with the scattering curve of the BSA standard. This result strongly suggests that XfLysRL is a dimer in solution, which is in agreement with available data for other members of the LTTR family that have a truncated N-terminal domain [50]. Accordingly, a P2 symmetry was imposed during the *ab initio* modeling through which the XfLysRL envelope (Fig. 4) was determined from the experimental curves.

Based on sequence and structural alignments, an atomic model for the XfLysRL monomer was predicted using I-TASSER [47–49] and the following crystal structures of homologous LTTR family members with PDB entries: 1IXC (CbnR, *C. necator*), 1IZ1 (CbnR, *C. necator*), 2F6G (BenM, *A. baylyi*), 2HXR (CynR, *E. coli*) and 2FYI (CbL, *E. coli*). For each of these known crystal structures, the respective functional dimer structures were identified and compared with the XfLysRL scattering curve. The discrepancies calculated with CRYSOL [56], which are summarized in Table 2 (supplementary data), indicate that the dimer obtained from the PDB entry 2F6G (AbBenM) exhibited the best fit to the XfLysRL experimental data, which suggests that AbBenM has the highest structural similarity to XfLysRL. Thus, a putative XfLysRL dimer was built using the XfLysRL monomer homology model generated with I-TASSER and the experimental AbBenM dimer as the template. The resulting fit of the modeled XfLysRL dimer to the experimental curve is shown in Fig. 4A. The RMSD between the residues that are structurally aligned in the predicted XfLysRL model and crystal structure of AbBenM is relatively low (1.27 Å). Not surprisingly, the | value obtained from the fit of the putative XfLysRL dimer to the experimental curve was the same as the value obtained from the AbBenM dimer (|= 3.8), even though the former corresponds with the correct protein sequence and expected electron density, which allows for a better calculation of the theoretical scattering curve.

Further attempts to improve the fit by imposing contact conditions to maintain the dimeric interface of XfLysRL were performed using SASREF [41]. However, this approach was not able to improve the fit to the experimental data. In the absence of additional information, there was no justification to modify the imposed vinculum, which allows for a greater freedom of domain movements and potentially leads to a better fit. We also note that | is a statistical parameter that is also dependent on the noise in the data. For example, because the curve tends to be nosier at higher q values, χ values as low as 1.9 could be obtained if we limit the data to a lower resolution.

An experimental envelope for XfLysRL in solution was independently obtained using the DAMMIF software [41]. This envelope was superimposed onto the putative XfLysRL dimer (Fig. 4A) and showed a remarkable fit. Altogether, these results not only support the low-resolution modeled XfLysRL dimer and demonstrate the similarity between the AbBenM and XfLysRL monomeric structures but also imply that these two proteins dimerize in a similar manner.

Finally, we analyzed whether the residues in *A. baylyi* BenM involved in muconate and benzoate binding (both molecules are well characterized co-factors of this transcription regulator) were conserved in XfLysRL. Based on the work by Ezezika and collaborators (2007) [51], sequence alignments and our XfLysRL model, we mapped the residues in our protein sequence that might be involved in co-factor binding (Supplementary data: Fig. 1 and Table 3). *A. baylyi* BenM has two binding sites for benzoate and one for muconate [51]. We observed similarities among the residues of the second benzoate binding site, which are mainly amino acids that form a hydrophobic pocket in the structure.

Anexo

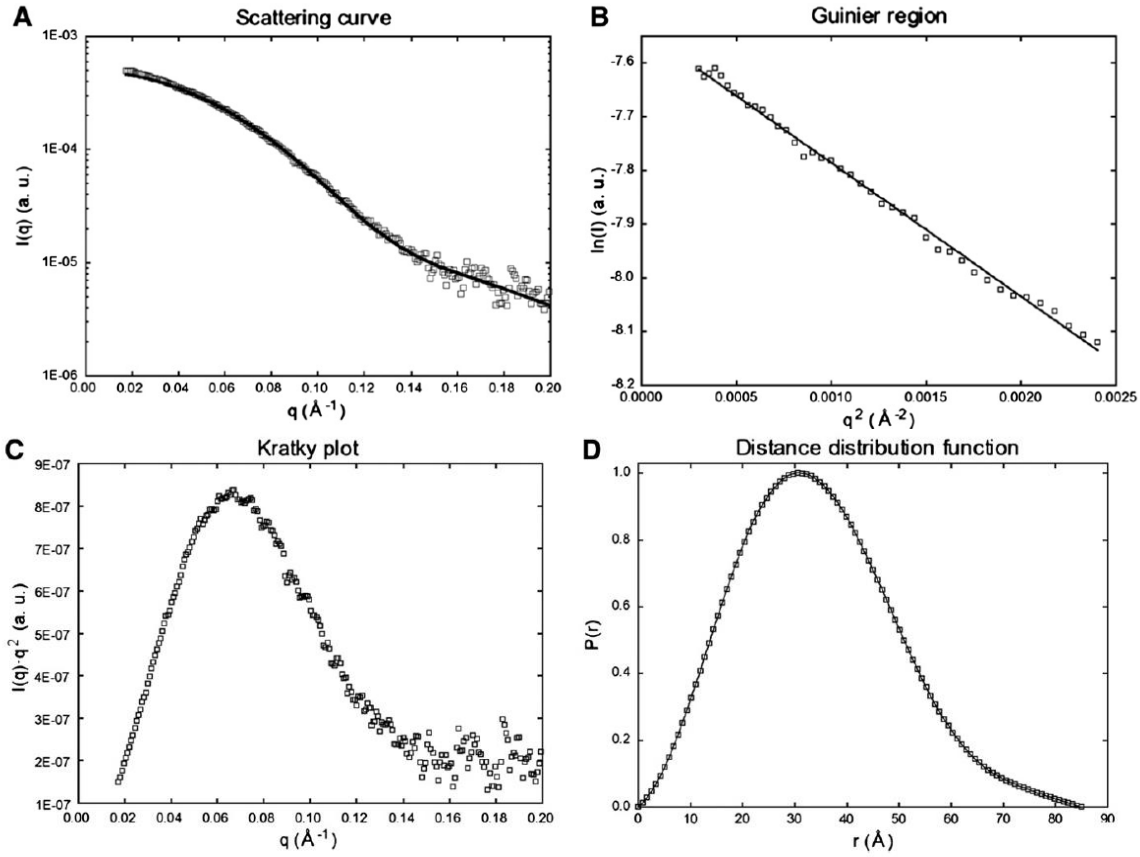

Fig. 3. XfLysRL SAXS data analysis. (A) Experimental solution scattering curve (open squares) and the resulting fitted model (solid line). (B) Guinier plot. (C) Kratky plot. (D) The distance distribution function P(r).

Moreover, two residues in the *A. baylyi* BenM those are crucial for benzoate binding (R160 and Y293) are not conserved in the XfLysRL sequence. However, we would like to stress that muconate and benzoate make 4 and 6 water mediated contacts with *A. baylyi* BenM residues respectively [51]. Additionally, it is reported that benzoate fits more loosely then muconate in the binding site and is surrounded by many more water molecules. Together, this information may suggest that despite the low conservation observed for XfLysRL co-inducer binding site residues, water mediated interactions may account for the observed interaction of the studied protein with both, muconate and benzoate.

3.4. Interactions of recombinant XfLysRL with the putative co-inducers benzoate and muconate

As revealed through the amino acid sequence alignment, XfLysRL displays 21% identity with *A. baylyi* BenM, which is a LysR family transcription factor that regulates the catabolic pathway of aromatic compounds, specifically benzoate. Additionally, based on our SAXS data and *in silico* models, it was possible to determine the molecular envelope of the XfLysRL dimer, which was shown to fit well with the BenM dimer structure. BenM, a well-characterized LysR-type transcriptional regulator, interacts with both benzoate and muconate molecules, which act as co-inducers [58].

Fluorescence emission spectroscopy clearly showed that XfLysRL is also able to interact with benzoate and muconate because we observed a co-factor concentration-dependent fluorescence quenching in both cases (Fig. 5A and B). The data fitting shows hyperbolic curves that are indicative of the absence of cooperativity in the binding of muconate and benzoate to the protein subunits (Fig. 5C and D). The observed quenching of fluorescence upon the addition of benzoate and muconate resembles the quenching observed in the incubation of *A. baylyi* BenM with both co-factors, as reported by Clark and colleagues (2004) [58]. However, no shift in the fluorescence maximum was observed for XfLysRL during the co-factor titration, which indicates that the binding does not affect the environment of the four tryptophan residues (W100, W133, W168 and W189) present in the protein sequence. In contrast, *A. baylyi* BenM showed a shift in the fluorescence maximum to higher wavelengths when incubated with benzoate, which indicates that the unique tryptophan residue (W304) of this protein was exposed to a more hydrophilic environment upon co-factor binding [58]. XfLysRL has a higher affinity for muconate than benzoate (Fig. 5C and D), which is reflected by the calculated K_d values of 0.40 ± 0.11 and 1.87 ± 0.28, respectively. These K_d values are higher but not far from the values reported for *A. baylyi* BenM (1.2 ± 0.2 for benzoate and 0.28 ± 0.05 for muconate) and for co-factor binding domain from BenM (1.1 ± 0.1 for benzoate and 0.12 ± 0.02 for muconate) [58]. This may be explained by the low level of conservation observed in the

Anexo

Fig. 4. Putative XfLysRL dimer constructed from the SAXS data. (A) Stereo view of three orthogonal orientations of an averaged SAXS envelope (gray grids), which was generated using DAMMIF and superposed with the generated XfLysRL dimer (green and magenta cartoons). The XfLysRL dimer was constructed based on the XfLysRL monomer homology models by orienting the individual subunits and comparing the resulting atomic dimeric model to the experimental scattering curve using the SASREF software. (B) The monomeric XfLysRL homology model with the two effector binding domains EBDI and EBDII, which are colored red and blue, respectively. The proposed dimerization interface is colored yellow. The figures were generated using the PyMOL software.

residues that form the co-factor binding sites in XfLysRL and *A. baylyi* BenM (Supplementary data). Additionally, these results are also in agreement with previously reported data for *A. baylyi* BenM, which showed that less amounts of muconate than benzoate were required to achieve a comparable reduction in fluorescence [58]. Taken together, these fluorescence data suggest that the recombinant XfLysRL is able to interact with both muconate and benzoate under the conditions tested.

3.5. XfLysRL expression oscillates between different stages of biofilm formation and is affected when cells are cultivated in the presence of muconate or benzoate

We used Western blot analysis to evaluate the expression profile of XfLysRL during different stages of *X. fastidiosa* biofilm formation. We analyzed both planktonic and biofilm cells because it has been reported that these distinct forms of growth have different gene expression profiles that are in turn related to the ability of planktonic cells to adhere to their host surface and form biofilm structures. Therefore, the genes that are differentially regulated by planktonic and biofilm cells are likely involved in biofilm formation and in the case of *X. fastidiosa*, pathogenicity. Biofilm is a cellular aggregate that adheres to a surface and results in many adaptive advantages, such as an increased capacity of cells to take up nutrients from the environment [59], a greater resistance to antimicrobial compounds [60,61], and a higher capacity of detoxification due to the increased expression of the efflux pump genes [62]. The stages of *X. fastidiosa* biofilm formation have been well characterized and are divided into 5 phases: reversible attachment, irreversible attachment, initial maturation process, formation of mature biofilm, and dispersion [16,63]. In *X. fastidiosa* strain *9a5c*, the maturation phase occurs between days 15 and 20 *in vitro*, whereas the dispersion stage occurs between days 25 and 30. The biofilm formation in the xylem vessels is considered the primary mechanism of *X. fastidiosa* pathogenicity because it leads to hydric stress and the development of symptoms in the plant [15]. In the present work, we observed differences in the expression level of XfLysRL throughout the stages of biofilm formation and between biofilm and planktonic cells (Fig. 6A). The most significant difference was the lack of XfLysRL expression in planktonic cells at the early stages of biofilm formation (days 3 and 5) compared with its expression in biofilm cells at the same time points (Fig. 6B). In addition, we observed a decrease in the expression level of XfLysRL in the last stage of biofilm formation (day 30), which may be explained by the fact that biofilm cells dissociate from the biofilm structure and turn into planktonic cells during this stage. However, the XfLysRL protein expression is increased in planktonic cells at the same stage; this increase may be correlated with the accumulation of aromatic metabolites in the medium and the need of an additional carbon source because the depletion of the growth medium may occur at this stage. As mentioned above, proteomic investigations have shown that sessile cells present in a biofilm structure diverge from planktonic cells in their expression of central metabolism genes, including genes that are involved in amino acid metabolism, co-factor biosynthesis and carbon metabolism [64]. Therefore, because our data indicate that XfLysRL is a BenM homologue, the observed expression profile differences between planktonic and biofilm *X. fastidiosa* can be explained in light of a XfLysRL role as a transcriptional regulator that activates genes that are involved in the aromatic compound and carbon metabolism pathways. In addition, genes related to the aromatic compound metabolism pathway are directly involved in the defense against plant chemicals, which are produced through the systemic acquired resistance process [65]. In the context of *X. fastidiosa* pathogenicity, the expression of XfLysRL, which is a putative homologue of BenM, in biofilm cells could also be related to resistance to plant chemicals that are produced during the colonization process. However, further investigations are needed to draw solid conclusions regarding the role and relevance of this protein in biofilm formation and carbon metabolism.

Finally, we analyzed whether the growth of *X. fastidiosa* in the presence of muconate and benzoate would lead to an alteration in XfLysRL expression. In the presence of benzoate (10 mM), we observed a clear decrease in the expression of XfLysRL in biofilm cells compared to our control ($p = 0.048$), whereas the XfLysRL expression was increased in the presence of 0.392 mM muconate ($p = 0.033$; Fig. 7A and B). No significant differences were observed

Anexo

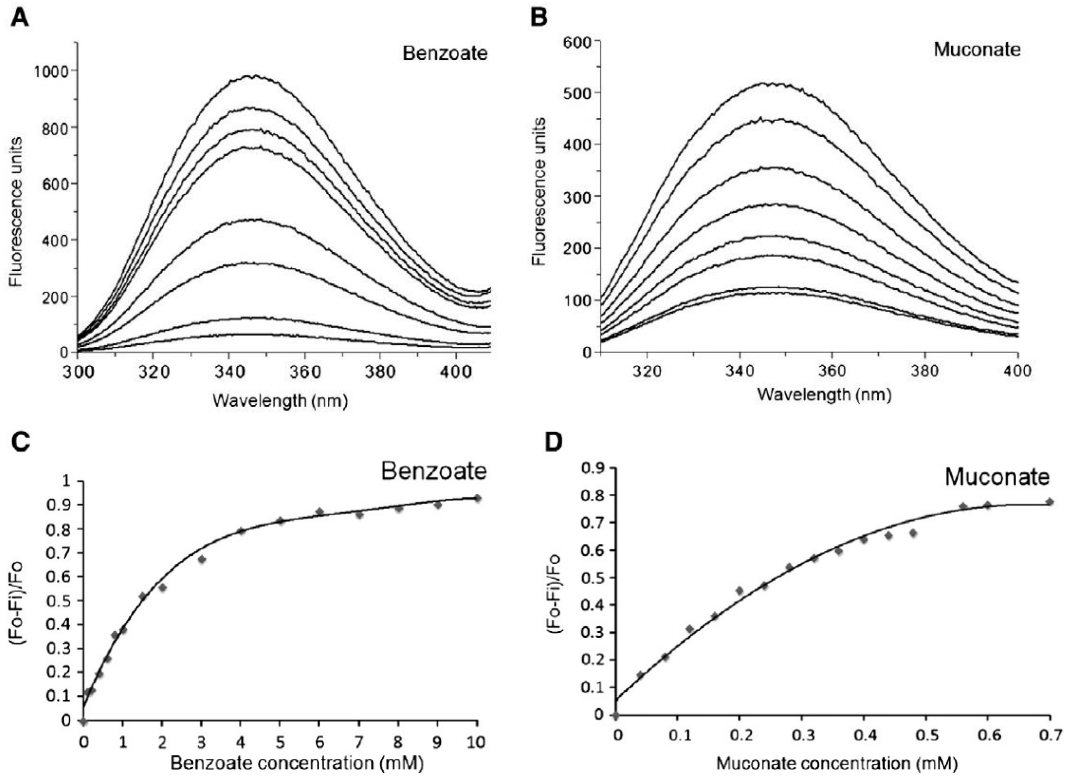

Fig. 5. (A) and (B) Fluorescence curves for XfLysRL in the presence of benzoate and muconate, respectively. From top to bottom, the following concentrations were used: 0, 0.1, 0.4, 0.6, 1.5, 6, and 10 mM benzoate and 0, 0.04, 0.12, 0.2, 0.32, 0.4, 0.56, and 0.7 mM muconate. (C) and (D) Change at $\Lambda_{max} = 347$ nm intensity after the addition of benzoate and muconate, respectively. This change is expressed as the initial fluorescence (F_0) minus the fluorescence at a specific concentration (I) of the co-factor (F_i) divided by the intensity of the initial fluorescence (F_0). Both plots were fitted to a hyperbolic curve, which indicates a lack of cooperativity in the interaction between the XfLysRL monomers and co-factors.

when the cells were cultivated in the presence of lower concentrations of muconate (0.168 mM) and benzoate (5 mM). Our data suggest that although XfLysRL exhibits structural homology with *A. baylyi* BenM, it does not have its expression induced by benzoate, which is conflicting with its speculated role as a BenM homologue.

4. Discussion

4.1. SAXS envelope and the atomic model of XfLysRL are similar to the structure of A. baylyi BenM

We used recombinant protein expression, sequence alignments and SAXS approaches to assign a possible function to a predicted LysR-type transcriptional regulator that is present in the *X. fastidiosa* genome. Full-length LTTR family members have been identified as tetramers in solution [66,67]. However, members with a truncated N-terminal domain (containing only the effector-binding domains, EBDs) assemble as dimers in solution [50,51,53], most likely because the tetramer interface is formed through the interaction of the DNA-binding domain (DBD, N-terminal region) and the hinge that connects the EBD to the DBD [52].

In agreement with this information, size exclusion chromatography showed that the target protein XfLysRL forms a dimer in solution. An amino acid sequence alignment with other full-length LysR-type transcriptional regulators indicated that XfLysRL lacks the N-terminal binding domain. The crystal structures of diverse LTTR family members revealed similar compact dimers that are formed by their EBDs [50,53]. However, further inspection of the LTTR dimer interface showed that the residues that participate in the monomer–monomer contacts could be drastically different between the LTTR members [52]. For example, the dimer interface in the CysB EBD crystal structure is mediated by 11 β–β main chain contacts [53], whereas the dimer interfaces of the CbnR [52] and BenM [50] crystal structures are mediated by a hydrophobic cluster that is surrounded by an H-bond network.

In this work, we report a low-resolution XfLysRL EBD structure in solution. Our data strongly suggest that XfLysRL is a dimer in solution and is similar to the *A. baylyi* BenM EBD dimer [49,50]. The putative XfLysRL dimer is formed by two monomers that are oriented anti-parallel to each other to form a compact structure. The two XfLysRL EBDs are easily identified (Fig. 4B) and have the same structure topology as the LTTR members that have been previously characterized experimentally [48,50,52,53]. The suggested XfLysRL dimer interface is composed of helices α1 and α3 and a connecting loop that contains residues 21–29, 140–154, and 163–170 (highlighted as dashed lines in Fig. 1). According to the constructed XfLysRL atomic homology model, the monomer–monomer contacts are mediated mainly through hydrophobic residues, which possibly form a hydrophobic cluster that includes helix α3 and the loop from one of the monomers and helix α1 from the other monomer. Polar amino acids are also found at the putative interface and possibly surround the hydrophobic cluster, further stabilizing the XfLysRL dimer. Similar observations were made with the *A. baylyi* BenM crystal structures [49,50], which indicates that the dimer formed by XfLysRL is similar to that of its homologue, *A. baylyi* BenM.

Anexo

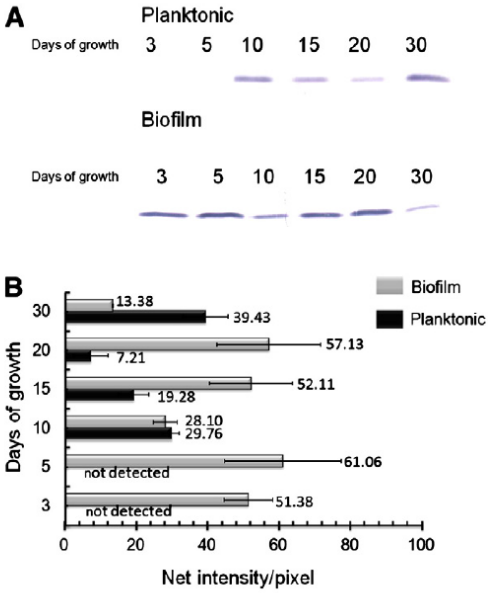

Fig. 6. (A) Western blot analysis of XfLysRL expression during different stages of *X. fastidiosa* biofilm formation and planktonic cell growth. (B) Total pixel intensity values of XfLysRL in biofilm and planktonic cells at each day of growth. The values represent the mean of the results obtained from three independent experiments.

4.2. XfLysRL interacts with benzoate and muconate, which are co-inducers of A. baylyi BenM

Although it lacks an N-terminal DNA-binding domain, we showed that the recombinant XfLysRL was able to interact with muconate and benzoate, which are both co-inducers of *A. baylyi* BenM. We observed that XfLysRL and *A. baylyi* BenM exhibited similar interaction behavior; for example, both proteins had a greater affinity for muconate than benzoate and lacked a fluorescence maximum shift upon interaction with muconate. However, benzoate caused a shift in the maximum fluorescence of *A. baylyi* BenM, which indicates that its sole tryptophan residue was exposed to a more hydrophilic environment. This shift was not observed with XfLysRL, which has four tryptophan residues in its sequence. Therefore, the observed fluorescence data for XfLysRL is a combination of the emission of four tryptophan residues, which may justify the difference from the *A. baylyi* BenM fluorescence data. Interestingly, XfLysRL exhibited reduced conservation with the *A. baylyi* BenM residues that have been found to be involved in muconate and benzoate binding. Bearing this in mind, we must consider that the observed quenching in fluorescence emission spectroscopy might be the result of unspecific binding; thus, further investigation is necessary to draw solid conclusions on the roles of muconate and benzoate as co-factors of XfLysRL.

4.3. XfLysRL is differentially expressed during different stages of biofilm formation and planktonic cell growth and is differentially induced by muconate and benzoate

Western blot analysis showed that XfLysRL is differentially expressed during different stages of biofilm formation and planktonic cell growth. Differences in expression were also observed between biofilm and planktonic growth, which indicates that XfLysRL is included in the pool of proteins that may contribute to the ability of *X. fastidiosa* cells to form and maintain biofilm structures. However, additional investigations are necessary to properly address this question. When *X. fastidiosa* is cultivated in the presence of benzoate and muconate, we also observed oscillations in the XfLysRL protein level in the total cellular extracts. Benzoate induced a clear reduction, whereas muconate generated a slight increase in the XfLysRL expression level that is not in agreement with the reported behavior of *A. baylyi* BenM because its expression is induced by both co-factors. Therefore, in light of our structural and functional data, we provide evidence that supports the hypothesis that XfLysRL is involved in carbon metabolism, specifically in the aromatic compound detoxification pathway.

We believe that further investigations are necessary to elucidate whether benzoate and muconate are indeed co-factors of XfLysRL, which might be achieved by the structural analysis of the XfLysRL protein in the presence of both molecules. The observed effects of muconate and benzoate on the XfLysRL expression must be confirmed by additional approaches. RT-PCR analysis of the XF1448 ORF could provide valuable information of its expression in planktonic and biofilm *X. fastidiosa* cells in the presence of muconate, benzoate or other organic compounds. Finally, the ability of XfLysRL to bind to DNA must be tested because this protein does not have an N-terminal HTH-DNA binding motif, which is common to LTTRs. Gel shift assays with promoter regions of the *X. fastidiosa* ORFs that are predicted to be involved in the carbon metabolism pathway and the promoter of XF1448 itself might indicate whether XfLysRL is able to specifically bind to DNA. Together with the presented data, these

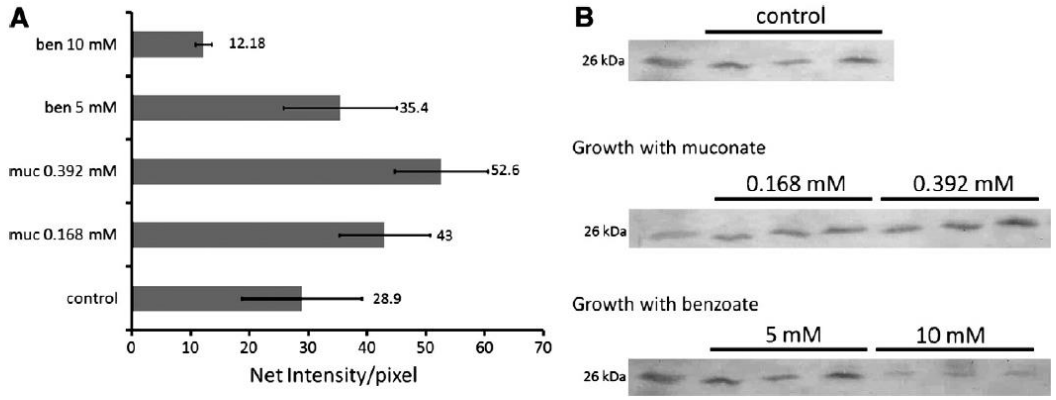

Fig. 7. (A) Quantification (net intensity/pixel) of XfLysRL Western blot bands obtained during *X. fastidiosa* growth in the presence of muconate and benzoate. Significant differences were obtained in the presence of 10 mM benzoate ($p = 0.048$) and 0.392 mM muconate ($p = 0.033$) compared with the control. (B) Western blots were performed for each experiment. All of the experiments with the tested concentrations of muconate and benzoate, as well as the control experiment, were performed in triplicate.

Anexo

approaches might confirm the function of XfLysRL as a transcriptional regulator and determine its relevance in the *X. fastidiosa* metabolism and biofilm formation.

Supplementary data to this article can be found online at http://dx.doi.org/10.1016/j.bbapap.2012.12.017.

Acknowledgements

This work was supported in part by the Fundação de Amparo à Pesquisa do Estado de São Paulo (FAPESP Process 01/07533-7). M.A.S. Toledo, C.A. Santos, A.C. Pelloso, L. L. Beloti, A. Crucello and M.T.P Favaro were supported by fellowships from FAPESP; D.R.S. Schneider received a PhD fellowship from the Conselho Nacional de Desenvolvimento Científico e Tecnológico (CNPq), and A.S. Santiago and J.S. Mendes received PhD fellowships from Coordenação de Aperfeiçoamento de Pessoal de Nível Superior (CAPES). The authors gratefully acknowledge the Laboratório Nacional de Luz Síncrotron (LNLS) for the beamline time and Professor Nilson Zanchin for providing CD spectropolarimeter facilities.

References

[1] C.J. Chang, M. Garnier, L. Zreik, V. Rossetti, J.M. Bové, Culture and serological detection of the xylem limited bacterium causing citrus variegated chlorosis and its identification as a strain of *Xylella fastidiosa*, Curr. Microbiol. 27 (1993) 137–142.
[2] J.S. Hartung, J. Beretta, R.H. Brlansky, J. Spisso, R.F. Lee, Citrus variegated chlorosis bacterium: axenic culture, pathogenicity, and serological relationships with other stains of *Xylella fastidiosa*, Phytopathology 84 (1994) 591–597.
[3] M.J. Davis, A.H. Purcell, S.V. Thomson, Pierce's disease of grapevines: isolation of the causal bacterium, Science 199 (1978) 75–77.
[4] J.M. Wells, B.C. Raju, G. Nyland, Isolation, culture and pathogenicity of the bacterium causing phony peach disease, Phytopathology 73 (1983) 859–862.
[5] A.J. Simpson, F.C. Reinach, P. Arruda, F.A. Abreu, M. Acencio, R. Alvarenga, L.M. Alves, J.E. Araya, G.S. Baia, C.S. Baptista, M.H. Barros, E.D. Bonaccorsi, S. Bordin, J.M. Bové, M.R. Briones, M.R. Bueno, A.A. Camargo, L.E. Camargo, D.M. Carraro, H. Carrer, N.B. Colauto, C. Colombo, F.F. Costa, M.C. Costa, C.M. Costa-Neto, L.L. Coutinho, M. Cristofani, E. Dias-Neto, C. Docena, H. El-Dorry, A.P. Facincani, A.J. Ferreira, V.C. Ferreira, J.A. Ferro, J.S. Fraga, S.C. França, M.C. Franco, M. Frohme, L.R. Furlan, M. Garnier, G.H. Goldman, M.H. Goldman, S.L. Gomes, A. Gruber, P.L. Ho, J.D. Hoheisel, M.L. Junqueira, E.L. Kemper, J.P. Kitajima, J.E. Krieger, E.E. Kuramae, F. Laigret, M.R. Lambais, L.C. Leite, E.G. Lemos, M.V. Lemos, S.A. Lopes, C.R. Lopes, J.A. Machado, M.A. Machado, A.M. Madeira, H.M. Madeira, C.L. Marino, M.V. Marques, E.A. Martins, E.M. Martins, A.Y. Matsukuma, C.F. Menck, E.C. Miracca, C.Y. Miyaki, C.B. Monteiro-Vitorello, D.H. Moon, M.A. Nagai, A.L. Nascimento, L.E. Netto, A. Nhani Jr., F.G. Nobrega, L.R. Nunes, M.A. Oliveira, M.C. de Oliveira, R.C. de Oliveira, D.A. Palmieri, A. Paris, B.R. Peixoto, G.A. Pereira, H.A. Pereira Jr., J.B. Pesquero, R.B. Quaggio, P.G. Roberto, V. Rodrigues, A.J. de M Rosa, V.E. de Rosa Jr., R.G. de Sá, R.V. Santelli, H.E. Sawasaki, A.C. da Silva, A.M. da Silva, F.R. da Silva, W.A. da Silva Jr., J.F. da Silveira, M.L. Silvestri, W.J. Siqueira, A.A. de Souza, A.P. de Souza, M.F. Terenzi, D. Truffi, S.M. Tsai, M.H. Tsuhako, H. Vallada, M.A. van Sluys, S. Verjovski-Almeida, A.L. Vettore, M.A. Zago, M. Zatz, J. Meidanis, J.C. Setubal, The genome sequence of the plant pathogen *Xylella fastidiosa*, Nature 406 (2000) 151–159.
[6] J.M. Dow, M.J. Daniels, *Xylella* genomics and bacterial pathogenicity to plants, Yeast 17 (2000) 263–271.
[7] N.T. Keen, C.K. Dumenyo, C.H. Yang, D.A. Cooksey, From rags to riches: Insights from the first genomic sequence of a plant pathogenic bacterium, Genome Biol. 1 (2000) 10191–10194.
[8] F.R. Silva, A.L. Vettore, E.L. Kemper, A. Leite, Fastidiam gum: the *Xylella fastidiosa* exopolysaccharide possibly involved in bacterial pathogenicity, FEMS Microbiol. Lett. 203 (2001) 165–171.
[9] M.A.S. Toledo, D.R. Schneider, A.R. Azzoni, M.T.P. Favaro, A.C. Pelloso, C.A. Santos, A.M. Saraiva, A.P. Souza, Characterization of an oxidative stress response regulator, homologous to *Escherichia coli* OxyR, from the phytopathogen *Xylella fastidiosa*, Protein Expr. Purif. 75 (2011) 204–210.
[10] C.A. Santos, L.L. Beloti, M.A.S. Toledo, A. Crucello, M.T.P. Favaro, J.S. Mendes, A.S. Santiago, A.R. Azzoni, A.P. Souza, A novel protein refolding protocol for the solubilization and purification of recombinant peptidoglycan-associated lipoprotein from *Xylella fastidiosa* overexpressed in *Escherichia coli*, Protein Expr. Purif. 82 (2012) 284–289.
[11] A.M. Saraiva, M.A. Reis, S.F. Tada, L.K. Rosselli-Murai, D.R.S. Schneider, A.C. Pelloso, M.A.S. Toledo, C. Giles, R. Aparicio, A.P. Souza, Functional and small-angle X-ray scattering studies of a new stationary phase survival protein E (SurE) from *Xylella fastidiosa* — evidence of allosteric behavior, FEBS J. 276 (2009) 6751–6762.
[12] D.L. Hopkins, *Xylella fastidiosa* — xylem-limited bacterial pathogen of plants, Annu. Rev. Phytopathol. 27 (1989) 271–290.
[13] D.L. Hopkins, A.H. Purcell, *Xylella fastidiosa*: cause of Pierce's disease of grapevine and other emergent diseases, Plant Dis. 86 (2002) 1056–1066.
[14] S.M. Mircetich, S.K. Lowe, W.J. Moller, G. Nyland, Etiology of almond leaf scorch disease and transmission of causal agent, Phytopathology 66 (1976) 17–24.
[15] D. Osiro, L.A. Colnago, A.M.M.B. Otoboni, E.G.M. Lemos, A.A. de Souza, H.D.C. Filho, M.A. Machado, A kinetic model for *Xylella fastidiosa* adhesion, biofilm formation, and virulence, FEMS Microbiol. Lett. 236 (2004) 313–318.
[16] A.A. de Souza, M.A. Takita, H.D. Coletta-Filho, C. Caldana, G.M. Yanai, N.H. Muto, R.C. Oliveira, L.R. Nunes, M.A. Machado, Gene expression profile of the plant pathogen *Xylella fastidiosa* during biofilm formation *in vitro*, FEMS Microbiol. Lett. 237 (2004) 341–353.
[17] A.A. de Souza, M.A. Takita, E.O. Pereira, H.D. Coletta-Filho, M.A. Machado, Expression of pathogenicity-related genes of *Xylella fastidiosa in vitro* and in planta, Curr. Microbiol. 50 (2005) 223–228.
[18] E. Pérez-Rueda, J. Collado-Vides, Common history at the origin of the position–function correlation in transcriptional regulators in archaea and bacteria, J. Mol. Evol. 53 (2001) 172–179.
[19] J. Sun, A. Klein, A LysR-type regulator is involved in the negative regulation of genes encoding selenium-free hydrogenases in the archaeon *Methanococcus voltae*, Mol. Microbiol. 52 (2004) 563–571.
[20] E. Stec, M. Witkowska-Zimny, M.M. Hryniewicz, P. Neumann, A.J. Wilkinson, A.M. Brzozowski, C.S. Verma, J. Zaim, S. Wysocki, G.D. Bujacz, Structural basis of the sulphate starvation response in *E. coli*: crystal structure and mutational analysis of the cofactor-binding domain of the Cbl transcriptional regulator, J. Mol. Biol. 364 (2006) 309–322.
[21] S.E. Maddocks, P.C. Oyston, Structure and function of the LysR-type transcriptional regulator (LTTR) family proteins, Microbiology 154 (2008) 3609–3623.
[22] M.R. Parsek, R.W. Ye, P. Pun, A.M. Chakrabarty, Critical nucleotides in the interaction of a LysR-type regulator with its target promoter region. *catBC* promoter activation by CatR, J. Biol. Chem. 269 (1994) 11279–11284.
[23] J.E. Burn, W.D. Hamilton, J.C. Wooton, A.W. Johnston, Single and multiple mutations affecting properties of the regulatory gene *nodD* of Rhizobium, Mol. Microbiol. 3 (1989) 1567–1577.
[24] A. Cebolla, C. Sousa, V. de Lorenzo, Effector specificity mutants of the transcriptional activator NahR of naphthalene degrading *Pseudomonas* define protein sites involved in binding of aromatic inducers, J. Biol. Chem. 272 (1997) 3986–3992.
[25] C. Jørgensen, G. Dandanell, Isolation and characterization of mutations in the *Escherichia coli* regulatory protein XapR, J. Bacteriol. 181 (1999) 4397–4403.
[26] R.T. Celis, Repression and activation of arginine transport genes in *Escherichia coli* K 12 by the ArgP protein, J. Mol. Biol. 294 (1999) 1087–1095.
[27] G. van Keulen, A.N. Ridder, L. Dijkhuizen, W.G. Meijer, Analysis of DNA binding and transcriptional activation by the LysR type transcriptional regulator CbbR of *Xanthobacter flavus*, J. Bacteriol. 185 (2003) 1245–1252.
[28] G. Kovacikova, K. Skorupski, A *Vibrio cholerae* LysR homolog, AphB, cooperates with AphA at the *tcpPH* promoter to activate expression of the ToxR virulence cascade, J. Bacteriol. 181 (1999) 4250–4256.
[29] A.E. Deghmane, S. Petit, A. Topilko, Y. Pereira, D. Giorgini, M. Larribe, M.K. Taha, Intimate adhesion of *Neisseria meningitidis* to human epithelial cells is under the control of the *crag* gene, a novel LysR-type transcriptional regulator, EMBO J. 19 (2000) 1068–1078.
[30] A.E. Deghmane, D. Giorgini, M. Larribe, J.M. Alonso, M.K. Taha, Down-regulation of pili and capsule of *Neisseria meningitides* upon contact with epithelial cells is mediated by CrgA regulatory protein, Mol. Microbiol. 43 (2002) 1555–1564.
[31] H. Cao, G. Krishnan, B. Goumnerov, J. Tsongalis, R. Tompkins, L.G. Rahme, A quorum sensing-associated virulence gene of *Pseudomonas aeruginosa* encodes a LysR-like transcription regulator with a unique self-regulatory mechanism, Proc. Natl. Acad. Sci. U. S. A. 98 (2001) 14613–14618.
[32] J. Kim, J.G. Kim, Y. Kang, J.Y. Jang, G.J. Jog, J.Y. Lim, S. Kim, H. Suga, T. Nagamatsu, I. Hwang, Quorum sensing and the LysR-type transcriptional activator ToxR regulate toxoflavin biosynthesis and transport in *Burkholderia glumae*, Mol. Microbiol. 54 (2004) 921–934.
[33] D.A. Russell, G.A. Byrne, E.P. O'Connell, C.A. Boland, W.G. Meijer, The LysR-type transcriptional regulator VirR is required for expression of the virulence gene *vapA* of *Rhodococcus equi* ATCC 33701, J. Bacteriol. 186 (2004) 5576–5584.
[34] G.A. Byrne, D.A. Russell, X. Chen, W.G. Meijer, Transcriptional regulation of the *virR* operon of the intracellular pathogen *Rhodococcus equi*, J. Bacteriol. 189 (2007) 5082–5089.
[35] Z. Lu, M. Takeuchi, T. Sato, The LysR-type transcriptional regulator YofA controls cell division through the regulation of expression of ftsW in *Bacillus subtilis*, J. Bacteriol. 189 (2007) 5642–5651.
[36] V. Sperandio, C.C. Li, J.B. Kaper, Quorum-sensing *Escherichia coli* regulator A: a regulator of the LysR family involved in the regulation of the locus of enterocyte effacement pathogenicity island in enterohemorrhagic *E. coli*, Infect. Immun. 70 (2002) 3085–3093.
[37] M. Ko, C. Park, H-NS-dependent regulation of flagellar synthesis is mediated by a LysR family protein, J. Bacteriol. 182 (2000) 4670–4672.
[38] G. Kellermann, F. Vicentin, E. Tamura, M. Rocha, H. Tolentino, A. Barbosa, A. Craievich, I. Torriani, The small-angle X-ray scattering beamline of the Brazilian Synchrotron Light Laboratory, J. Appl. Crystallogr. 30 (1997) 880–883.
[39] A.P. Hammersley, S.O. Svensson, M. Hanfland, A.N. Fitch, D. Hausermann, Two dimensional detector software: from real detector to idealised image or two-theta scan, High Pressure Res. 14 (1996) 235–248.
[40] O. Glatter, O. Kratky, Small Angle X-ray Scattering, Academic Press Inc. Ltd., London, 1982.
[41] P.V. Konarev, M.V. Petoukhov, V.V. Volkov, D.I. Svergun, ATSAS 2.1, a program package for small-angle scattering data analysis, J. Appl. Crystallogr. 39 (2006) 277–286.
[42] S. Doniach, Changes in biomolecular conformation seen by small angle X-ray scattering, Chem. Rev. 101 (2001) 1763–1778.
[43] G.V. Semisotnov, H. Kihara, N.V. Kotova, K. Kimura, Y. Amemiya, K. Wakabayashi, I.N. Serdyuk, A.A. Timchenko, K. Chiba, K. Nikaido, T. Ikura, K. Kuwajima, Protein

Anexo

globularization during folding, a study by synchrotron small-angle X-ray scattering, J. Mol. Biol. 262 (1996) 559–574.
[44] D. Franke, D.I. Svergun, DAMMIF, a program for rapid ab-initio shape determination in small-angle scattering, J. Appl. Crystallogr. 42 (2009) 342–346.
[45] V.V. Volkov, D.I. Svergun, Uniqueness of *ab initio* shape determination in small-angle scattering, J. Appl. Crystallogr. 36 (2003) 860–864.
[46] The CCP4 suite: programs for protein crystallography, Acta Crystallogr. D: Biol. Crystallogr. 50 (1994) 760–763.
[47] A. Roy, A. Kucukural, Y. Zhang, I-TASSER: a unified platform for automated protein structure and function prediction, Nat. Protoc. 5 (2010) 725–738.
[48] Y. Zhang, I-TASSER server for protein 3D structure prediction, BMC Bioinforma. 9 (2008) 40.
[49] Y. Zhang, I-TASSER: fully automated protein structure prediction in CASP8, Proteins Struct. Funct. Bioinforma. 77 (2009) 100–113.
[50] T. Clark, S. Haddad, E. Neidle, C. Momany, Crystallization of the effector-binding domains of BenM and CatM, LysR-type transcriptional regulators from *Acinetobacter* sp. ADP1, Acta Crystallogr. D: Biol. Crystallogr. 60 (2004) 105–108.
[51] O.C. Ezezika, S. Haddad, T.J. Clark, E.L. Neidle, C. Momany, Distinct effector-binding sites enable synergistic transcriptional activation by BenM, a LysR-type regulator, J. Mol. Biol. 367 (2007) 616–629.
[52] O.C. Ezezika, S. Haddad, E.L. Neidle, C. Momany, Oligomerization of BenM, a LysR-type transcriptional regulator: structural basis for the aggregation of proteins in this family, Acta Crystallogr., Sect. F: Struct. Biol. Cryst. Commun. 63 (2007) 361–368.
[53] A. Lochowska, R. Iwanicka-Nowicka, D. Plochocka, M.M. Hryniewicz, Functional dissection of the LysR-type CysB transcriptional regulator — regions important for DNA binding, inducer response, oligomerization, and positive control, J. Biol. Chem. 276 (2001) 2098–2107.
[54] S. Muraoka, R. Okumura, N. Ogawa, T. Nonaka, K. Miyashita, T. Senda, Crystal structure of a full-length LysR-type transcriptional regulator, CbnR: Unusual combination of two subunit forms and molecular bases for causing and changing DNA bend, J. Mol. Biol. 328 (2003) 555–566.
[55] R. Tyrrell, K.H.G. Verschueren, E.J. Dodson, G.N. Murshudov, C. Addy, A.J. Wilkinson, The structure of the cofactor-binding fragment of the LysR family member, CysB: a familiar fold with a surprising subunit arrangement, Structure 5 (1997) 1017–1032.
[56] D.I. Svergun, C. Barberato, M.H.J. Koch, CRYSOL — a program to evaluate X-ray solution scattering of biological macromolecules from atomic coordinates, J. Appl. Crystallogr. 28 (1995) 768–773.
[57] M.B. Kozin, D.I. Svergun, Automated matching of high- and low-resolution structural models, J. Appl. Crystallogr. 34 (2001) 33–41.
[58] T.J. Clark, R.S. Phillips, B.M. Bundy, C. Momany, E.L. Neidle, Benzoate decreases the binding of cis, cis-muconate to the BenM regulator despite the synergistic effect of both compounds on transcriptional activation, J. Bacteriol. 186 (2004) 1200–1204.
[59] P.A. Zaini, A.C. Fogaça, F.G.N. Lupo, H.I. Nakaya, R.Z.N. Vêncio, A.M. da Silva, The iron stimulon of *Xylella fastidiosa* includes genes for type IV pilus and colicin V-like bacteriocins, J. Bacteriol. 190 (2008) 2368–2378.
[60] P.S. Stewart, J.W. Costerton, Antibiotic resistance of bacteria in biofilms, Lancet 358 (2001) 135–138.
[61] T.F. Mah, B. Pitts, B. Pellock, G.C. Walker, P.S. Stewart, G.A. O'Toole, A genetic basis for *Pseudomonas aeruginosa* biofilm antibiotic resistance, Nature 426 (2003) 306–310.
[62] K. Nishino, E. Nikaido, A. Yamaguchi, Regulation of multidrug efflux systems involved in multidrug and metal resistance of *Salmonella enterica* serovar *Typhimurium*, J. Bacteriol. 189 (2007) 9066–9075.
[63] K. Sauer, A.K. Camper, G.D. Ehrlich, J.W. Costerton, D.G. Davies, *Pseudomonas aeruginosa* displays multiple phenotypes during development as a biofilm, J. Bacteriol. 184 (2002) 1140–1154.
[64] M.S. Silva, A.A. de Souza, M.A. Takita, C.A. Labate, M.A. Machado, Analysis of the biofilm proteome of *Xylella fastidiosa*, Proteome Sci. 9 (2011) 58.
[65] L.M. Moreira, R.F. de Souza, L.A. Digiampietri, A.C. da Silva, J.C. Setubal, Comparative analyses of *Xanthomonas* and *Xylella* complete genomes, OMICS 9 (2005) 43–76.
[66] B.E. Miller, N.M. Kredich, Purification of the Cysb protein from *Salmonella–Typhimurium*, J. Biol. Chem. 262 (1987) 6006–6009.
[67] M.A. Schell, P.H. Brown, S. Raju, Use of saturation mutagenesis to localize probable functional domains in the NahR protein, a LysR-type transcription activator, J. Biol. Chem. 265 (1990) 3844–3850.

Anexo

Cidade Universitária "Zeferino Vaz",
17 de agosto de 2015.

CIBio: 03/2015

Identificação:
Doutorado: André da Silva Santiago, CPG-GBM UNICAMP

Projeto: Caracterização de duas proteínas pertencentes ao operon toxina-antitoxina e de um fator de transcrição do tipo LysR de Xylella fastidiosa.

Parecer:
Projeto aprovado pela CIBio/CBMEG sob número 15/2003
Coordenador: Profa. Dra. Anete Pereira de Souza

Profa. Dra. Edi Lúcia Sartorato
Presidente da CIBio/CBMEG - UNICAMP

UNIVERSIDADE ESTADUAL DE CAMPINAS - CENTRO DE BIOLOGIA MOLECULAR E ENGENHARIA GENÉTICA
CIDADE UNIVERSITÁRIA "ZEFERINO VAZ" - BARÃO GERALDO, CX.P.: 6010 - CEP 13083-875 - CAMPINAS - SP - BRASIL
FONE: (55-0xx19) 3521.1147, 3521.1130 ou 3521.1131 - FAX: (55-0xx19) 3788.1089

Anexo

Profa. Dra. Rachel Meneguello
Presidente
Comissão Central de Pós-Graduação
Declaração

As cópias de artigos de minha autoria ou de minha co-autoria, já publicados ou submetidos para publicação em revistas científicas ou anais de congressos sujeitos a arbitragem, que constam da minha Dissertação/Tese de Mestrado/Doutorado, intitulada **Caracterização de duas proteínas pertencentes ao operon toxina-antitoxina e de um fator de transcrição do tipo Lysr de Xylella fastidiosa**, não infringem os dispositivos da Lei n.° 9.610/98, nem o direito autoral de qualquer editora.

Campinas, 01 de setembro de 2015

Assinatura : _____
Nome do(a) autor(a): **André da Silva Santiago**
RG n.° 0996234047

Assinatura : _____
Nome do(a) orientador(a): **Anete Pereira de Souza**
RG n.° 8680325